IHSM La Mayora
Instituto de Hortofruticultura Subtropical y Mediterránea

UNIVERSIDAD DE MÁLAGA

CSIC
Consejo Superior de Investigaciones Científicas

Tesis Doctoral por compendio de publicaciones

Optical properties and location of phenolic compounds in plant cuticles

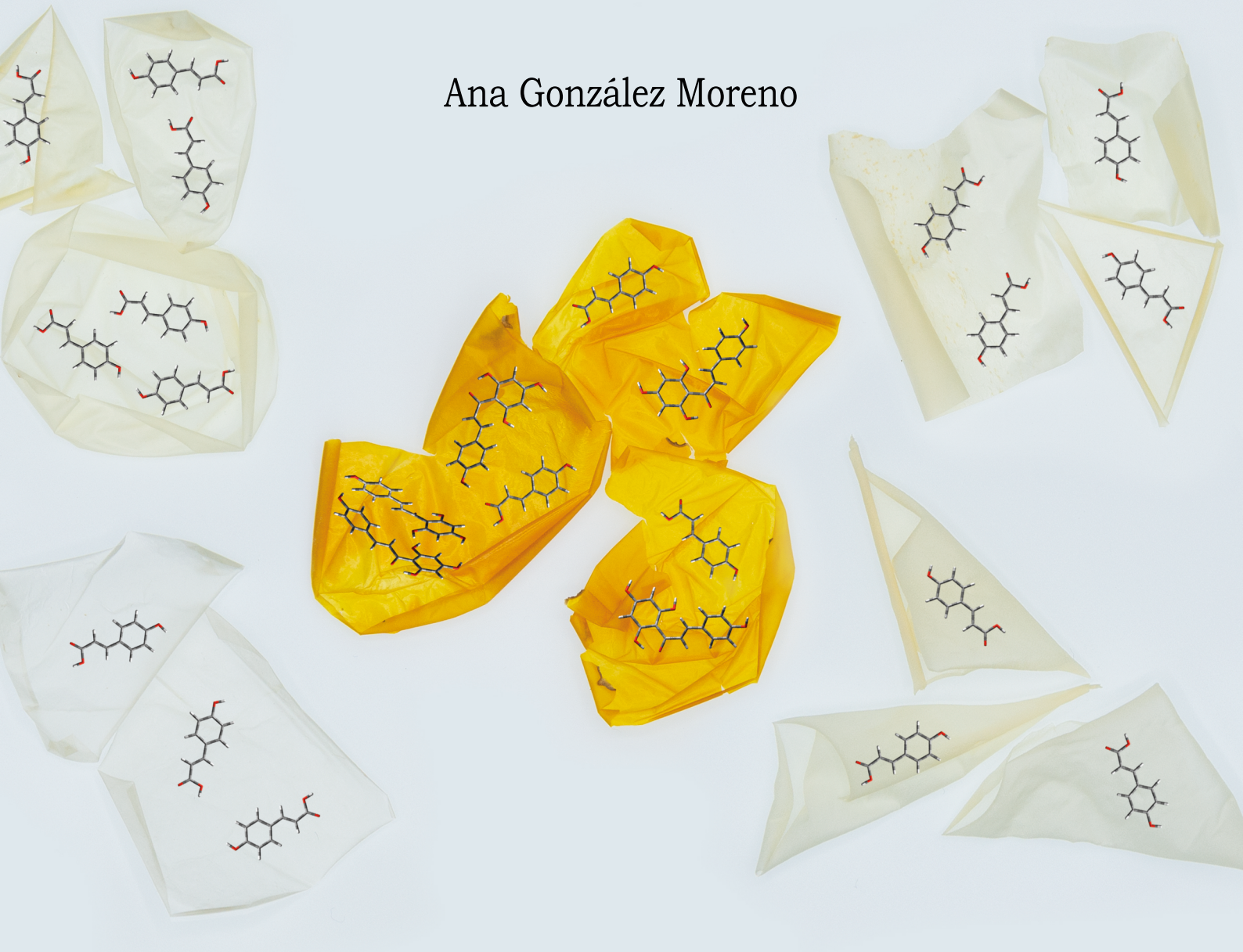

Ana González Moreno

Directores de Tesis: Antonio Heredia Bayona y Eva María Domínguez Carmona

Programa de Doctorado
Química y Tecnologías Químicas,
Materiales y Nanotecnología

Departamento de
Biología Molecular
y Bioquímica

Facultad de Ciencias
Universidad de Málaga

Málaga 2023

AUTORA: Ana González Moreno

https://orcid.org/0000-0001-9843-1244

EDITA: Publicaciones y Divulgación Científica. Universidad de Málaga

Departamento de Biología Molecular y Bioquímica
Facultad de Ciencias
Universidad de Málaga
Programa de Doctorado:
Química y Tecnologías Químicas, Materiales y Nanotecnología

Tesis Doctoral por compendio de publicaciones

Optical properties and location of phenolic compounds in plant cuticles

Propiedades ópticas y localización de compuestos fenólicos en cutículas vegetales

Memoria de la tesis doctoral presentada por

Ana González Moreno

para optar al grado de

Doctora

Con Mención **"Doctorado Internacional"**

Directores de tesis:

Antonio Heredia Bayona
Eva María Domínguez Carmona

Instituto de Hortofruticultura Subtropical y Mediterránea
"La Mayora" (IHSM-CSIC-UMA)

Málaga, 31 de mayo de 2023

DECLARACIÓN DE AUTORÍA Y ORIGINALIDAD DE LA TESIS PRESENTADA PARA OBTENER EL TÍTULO DE DOCTOR

D./Dña ANA GONZÁLEZ MORENO
Estudiante del programa de doctorado QUÍMICA Y TECNOLOGÍAS QUÍMICAS, MATERIALES Y NANOTECNOLOGÍA de la Universidad de Málaga, autor/a de la tesis, presentada para la obtención del título de doctor por la Universidad de Málaga, titulada: OPTICAL PROPERTIES AND LOCATION OF PHENOLIC COMPOUNDS IN PLANT CUTICLES

Realizada bajo la tutorización de MARÍA DEL CARMEN RUIZ DELGADO y dirección de ANTONIO HEREDIA BAYONA Y EVA MARÍA DOMÍNGUEZ CARMONA (si tuviera varios directores deberá hacer constar el nombre de todos)

DECLARO QUE:

La tesis presentada es una obra original que no infringe los derechos de propiedad intelectual ni los derechos de propiedad industrial u otros, conforme al ordenamiento jurídico vigente (Real Decreto Legislativo 1/1996, de 12 de abril, por el que se aprueba el texto refundido de la Ley de Propiedad Intelectual, regularizando, aclarando y armonizando las disposiciones legales vigentes sobre la materia), modificado por la Ley 2/2019, de 1 de marzo.

Igualmente asumo, ante a la Universidad de Málaga y ante cualquier otra instancia, la responsabilidad que pudiera derivarse en caso de plagio de contenidos en la tesis presentada, conforme al ordenamiento jurídico vigente.

En Málaga, a 31 de MAYO de 2023

Fdo.: ANA GONZÁLEZ MORENO Doctorando/a	Fdo.: MARÍA DEL CARMEN RUIZ DELGADO Tutor/a
Fdo.: ANTONIO HEREDIA BAYONA Director/es de tesis	EVA MARÍA DOMÍNGUEZ CARMONA

Edificio Pabellón de Gobierno. Campus El Ejido. 29071
Tel.: 952 13 10 28 / 952 13 14 61 / 952 13 71 10
E-mail: doctorado@uma.es

Departamento de Biología Molecular y Bioquímica

Programa de Doctorado: Química y Tecnologías Químicas, Materiales y Nanotecnología

Antonio Heredia Bayona, Catedrático de Bioquímica y Biología Molecular de la Universidad de Málaga.

Eva Domínguez Carmona, Científica Titular del Instituto de Hortofruticultura Subtropical y Mediterránea La Mayora, UMA-CSIC.

INFORMAN QUE:

Doña Ana González Moreno ha realizado, bajo la dirección de ambos y supervisión de la Dra. María del Carmen Ruiz Delgado como tutora, el trabajo de investigación que con el título "Optical properties and location of phenolic compounds in plant cuticles" constituye su Tesis Doctoral para aspirar a la obtención del grado de Doctora con Mención Internacional.

La Tesis Doctoral está presentada como compendio de cuatro publicaciones que versan sobre distintos aspectos de la interacción de la luz con la cutícula vegetal, temática directamente relacionada con el objetivo de esta Tesis, por lo que queda avalada la idoneidad de su presentación por compendio de publicaciones. Las cuatro publicaciones, en las que la doctoranda es primera o segunda autora, se encuentran en revistas indexadas en el *Journal of Citation Reports* (JCR), en el cuartil 1 (Q1) de su área y no han sido utilizadas en Tesis Doctorales anteriores. Además, la Tesis Doctoral presentada cumple con el formato indicado en el apartado 2 del artículo 21 del Reglamento de los Estudios de Doctorado de la Universidad de Málaga (última modificación aprobada el 25 de octubre de 2019).

En Málaga, a 31 de mayo de 2023.

Fdo. Antonio Heredia Bayona

Eva María Domínguez Carmona

Departamento de Química Física, Facultad de Ciencias, Universidad de Málaga.

M. Carmen Ruiz Delgado, Profesora Titular del Departamento de Química Física de la Universidad de Málaga.

INFORMA QUE: Doña Ana González Moreno ha realizado, bajo mi supervisión como tutora y bajo la dirección de D. Antonio Heredia Bayona y Doña Eva Domínguez Carmona como directores, el trabajo de investigación que con el título "Optical properties and location of phenolic compounds in plant cuticles" constituye su Tesis Doctoral para aspirar a la obtención del grado de Doctora con Mención Internacional. La Tesis Doctoral está presentada como compendio de cuatro publicaciones que versan sobre distintos aspectos de la interacción de la luz con la cutícula vegetal, temática directamente relacionada con el objetivo de esta Tesis, por lo que queda avalada la idoneidad de su presentación por compendio de publicaciones. Las cuatro publicaciones, en las que la doctoranda es primera o segunda autora, se encuentran en revistas indexadas en el Journal of Citation Reports (JCR), en el cuartil 1 (Q1) de su área y no han sido utilizadas en Tesis Doctorales anteriores. Además, la Tesis Doctoral presentada cumple con el formato indicado en el apartado 2 del artículo 21 del Reglamento de los Estudios de Doctorado de la Universidad de Málaga (última modificación aprobada el 25 de octubre de 2019). En Málaga, a 31 de mayo de 2023.

Prof. M. Carmen Ruiz Delgado

TESIS DOCTORAL POR COMPENDIO DE PUBLICACIONES

Para la realización de la presente tesis doctoral he sido beneficiaria de un contrato predoctoral de Formación de Profesorado Universitario (FPU) entre los años 2018-2023 (Ref: FPU17/01771).

La presente tesis doctoral se presenta en formato compendio de publicaciones, cumpliendo los requisitos recogidos del Reglamento del programa de doctorado de la Universidad de Málaga, para la obtención del título de Doctor con mención internacional, cumpliendo así mismo los requisitos exigidos para dicha mención. A continuación, se recogen en orden cronológico los artículos que avalan la presente Tesis Doctoral, siendo el aspirante a título de doctor primer o segundo autor de dichas publicaciones:

1 A. González Moreno, A. de Cózar; P. Prieto; M.C. Ruiz Delgado; E. Domínguez; A. Heredia. (2021). Structure, isomerization and dimerization processes of naringenin flavonoids, *Physical Chemistry Chemical Physics*, 23, 18068-18077. https://doi.org/10.1039/D1CP01161H

2 J.J. Benítez; A. González Moreno; S. Guzman-Puyol; J.A. Heredia-Guerrero; A. Heredia; E. Domínguez. (2022). The response of tomato fruit cuticle membranes against heat and light, *Frontiers in Plant Science*, 12, 807723-807723. https://doi.org/10.3389/fpls.2021.807723

3 A. González Moreno; A. de Cózar; P. Prieto; E. Domínguez; A. Heredia. (2022). Radiationless mechanism of UV deactivation by cuticle phenolics in plants, *Nature Communications*, 13, 1786. https://doi.org/10.1038/s41467-022-29460-9

4 A. González Moreno; E. Domínguez; K. Mayer; N. Xiao; P. Bock; A. Heredia; N. Gierlinger. (2023). 3D (x-y-t) Raman imaging of tomato fruit cuticle: microchemistry during development, *Plant Physiology*, 191, 219-232. https://doi.org/10.1093/plphys/kiac369

Además, se incluye un capítulo adicional:

A. González Moreno; J.M. Woolley; E. Domínguez; A. de Cózar; A. Heredia; V.G. Stavros. (2023). Synergic photoprotection of phenolic compounds present in tomato

fruit cuticle: a spectroscopic investigation in solution, *Physical Chemistry Chemical Physics*, 25, 12791-12799. https://doi.org/10.1039/D3CP00630A

Agradecimientos

Parece mentira que sea el momento de escribir estas palabras, parece mentira que haya pasado tanto tiempo desde aquel mes de Julio en el que recibí ese mensaje de que mi solicitud para hacer el doctorado había sido aceptada. Pero a la vez, han pasado tantas cosas... Que sin duda esa Ana no es la misma que termina hoy su tesis doctoral. Como en todos los periodos han pasado cosas positivas y otras no tan positivas, pero hoy puedo decir que aunque las cosas no sucedieron tal y como yo esperaba, ha merecido la pena llegar hasta aquí.

Sin duda este día no hubiera llegado nunca sin la ayuda y el apoyo de muchísimas personas. Quiero comenzar como no puede ser de otra manera agradeciendo a mis directores Antonio y Eva. Antonio, gracias por confiar en mí desde el primer minuto, gracias por guiarme durante todos estos años, no sólo en lo profesional sino también en lo personal, gracias por retarme a superarme día a día y por tratarme siempre con ese cariño tan especial. Eva, muchas gracias por enseñarme tanto, por escucharme de forma tan paciente a cualquier hora y cualquier día de la semana, por tranquilizarme en los muchos momentos malos que he tenido. Gracias a los dos porque soy consciente que no he sido siempre fácil de comprender.

Quiero agradecer también a Mari Carmen por ser mi tutora de tesis y estar ahí siempre que la necesitaba. También me gustaría agradecer de forma especial a Abel, el hombre que me descubrió el mundo de los cálculos, gracias por enseñarme tantas cosas. Lo que comenzó con un par de correos de dudas ha terminado en Skype de horas hablando de ciencia y de más allá de la ciencia. Mil gracias, sin ti esta tesis no hubiera sido lo mismo. Gracias por las muchas charlas y consejos. Gracias también a Pilar por tu ayuda en mis primeros pasos en los cálculos. Gracias Fali por siempre estar ahí para cualquier papeleo, para escucharme, aconsejarme y para recordarme entre otras cosas que me siente bien; gracias Jesús por acogerme en Sevilla para hacer medidas y también por enseñarme tantas cosas; gracias Ale y Susana por hacerme los inicios más fáciles. En realidad, quiero mandar un gracias enorme a todas y cada una de las personas que están o han estado en el laboratorio, no me atrevo a mencionar nombres porque con mi mala cabeza me olvidaría de alguno, pero gracias desde los primeros

que estabais hasta los que seguís por aquí. Gracias y gracias por las charlas infinitas en el laboratorio, por las comidas, por escucharme, por los consejos, por las aventuras y a algunos incluso por limpiarme las lágrimas en momentos difíciles. Gracias por hacer más fáciles todos estos años. Gracias a mis compis del IHSM Rocío, Laura, Pablo, Pedro, Ana Luna, Patri y Paolo que me han hecho más alegres y agradable sobre todos estos últimos meses en el laboratorio.

¿Y qué decir de mis estancias? Yo que nunca había salido de casa… La verdad que he tenido mucha suerte con ambas estancias. Me gustaría agradecer a todas las personas que me ayudaron en esos meses; pero por supuesto agradecer especialmente a Burgi que aunque probablemente nunca leerá estas palabras, confió mucho en mí y me hizo tener más confianza en mí misma. Gracias también por darme las facilidades para volver a completar la estancia en medio de una pandemia mundial. Por otra parte, quiero agradecer de forma especial a Stavros, una de las personas más inteligentes que he conocido nunca. Admiración sería la palabra que mejor define lo que pienso sobre él; pero además quiero agradecer la comprensión y confianza que me mostró durante la estancia incluso cuando lo más fácil hubiera sido dejarme volver. Gracias Vas. Sumo a Jack en este agradecimiento por su inmensa paciencia conmigo esos meses. Y aquí ¿cómo no acordarme de Jagoba e Itziar? Mi familia vasca. Los que me hicieron crecer tanto, los que me aceptaron como una más de su familia en su casa de Viena. Gracias a los dos porque no sabía que se podía conocer a personas tan maravillosas, no sabía que se podía crear tanto vínculo en tan poco tiempo. Sin vosotros sin duda no sería la Ana que soy ahora. Gracias también a Batir por tratarme tan bien durante mi estancia y acogerme con tanto cariño. No me olvido tampoco de Seda, mi gran compañía y apoyo en Inglaterra, muchas gracias por cuidarme tanto. Gracias en general a todas aquellas personas que conocí durante mis estancias y me ayudaron de una u otra forma.

Quiero agradecer también al Ministerio de Universidades por concederme la ayuda para la formación de profesorado universitario (FPU17/01771) que ha permitido la realización de esta tesis doctoral; así como a la Universidad de Málaga (UMA) que ha financiado parte de mis estancias en el extranjero y ha permitido que esta tesis sea posible. Gracias también al Servicio de Supercomputación y

Bioinformática (SCBI) de la UMA y al SCAI por su apoyo y soporte técnico durante estos años, especialmente a Jessica, Zafra, Cristina Capel, José María, David, Goyo, Cristina y Ana Lucena. Gracias por vuestra ayuda estos años. Agradecer también la financiación proporcionada por los proyectos del Plan Nacional: “Aspectos genéticos y biofísicos de la formación de la cutícula del fruto de tomate (RTI2018-094277-B-C21”) y “Genética y biofísica de la cutícula del fruto de tomate (PID2021-126604OB-C22)”.

Después de todo esto y no por eso menos importante quiero dar las gracias por su infinita paciencia, apoyo y cariño a mi familia. Mamá, no tengo palabras para agradecer todo el soporte que me has dado y me sigues dando cada día. Gracias por escucharme cada día, por aprender a ponerte en mi lugar, por hacer el esfuerzo de comprender lo que pasa por mi cabeza, por confiar en mí más que yo misma, por empujarme día a día, por respetarme y por mostrarme cada día que estás y estarás orgullosa de mí pase lo que pase. Papá, gracias por mostrarme siempre las soluciones y nunca los problemas, por ser un gran ejemplo en mi vida, por animarme a seguir, por confiar en mí, por llevarme siempre de tu mano porque como tú dices la familia unida jamás será vencida, gracias por mostrarme que existe la generosidad desinteresada, te quiero y te admiro. Carmen, mi hermana del alma, mi medio limón. Gracias por ser una segunda madre para mí, por enseñarme a darle importancia a lo importante, gracias por animarme cada día y por mostrarme tanto amor siempre. ¿Y mi Miguelito? Es tan mágico cuando estoy con él, gracias mi bebé por llegar a nuestras vidas para hacernos desconectar del día a día y por hacerme sonreír incluso en momentos en los que no sabía que podía sonreír. Por desgracia hay personas que ya no están con nosotros desde hace mucho tiempo pero que me acompañan día a día, abuelos os echo de menos. Os dedico con gran cariño esta tesis.

Especiales gracias también a Juan Carlos. Desde que nos conocimos en aquella noche de los investigadores te has convertido en una pieza fundamental en mi día a día, ya lo sabes. Gracias por aguantarme día a día en el trabajo y en casa, gracias por escucharme una y mil veces la misma historia, por no juzgar lo que pienso, por hacerme salir de mi burbuja de agobio tantas veces, por valorar cada cosa que hago y por repetirme una y mil veces que yo puedo. Gracias de verdad

por convertirte en mi gran compañero de vida. Te quiero mucho. Gracias también a mis niñas, las de siempre, las que me hacen desconectar del trabajo y me sacan carcajadas. Gracias por darme siempre esas bonitas palabras y por haber construido juntas el equipo perfecto. Gracias también a las que no son de siempre, pero que han llegado a mi vida con tanta fuerza que ya son parte de mí. Gracias también a Javi Zamudio, por haber estado de una u otra forma durante todos estos años. Gracias a Nieves y Noelia, por guiarme estos años, hacerme crecer como persona y enseñarme a comprenderme y respetarme.

En resumen, soy muy afortunada de tener en mi vida personas tan maravillas, porque el término familia puede englobar a tantas personas… Gracias por formar parte de mi gran familia, y por tanto, gracias por hacer posible esta tesis doctoral.

A mis abuelos

A mi(s) familia(s)

TABLE OF CONTENTS

RESUMEN

La conquista del medio terrestre por las plantas hace 470 millones de años implicó el desarrollo de mecanismos de aclimatación ante nuevos desafíos. Una de las principales adaptaciones fue el recubrimiento de las partes aéreas de hojas, frutos y tallos no lignificados con una capa lipídica e hidrofóbica denominada cutícula vegetal. Como primera barrera entre la planta y el medio ambiente, la cutícula se encarga de la protección de los tejidos vegetales ante la pérdida excesiva de agua, cambios de temperatura, sobreexposición a radiación, infecciones por patógenos y daños mecánicos, entre otros. El componente principal de la mayoría de las cutículas vegetales es el poliéster amorfo cutina, aunque algunas especies también incluyen cután. Los polisacáridos, ceras y compuestos fenólicos completan normalmente la restante composición de la cutícula vegetal. A pesar de su proporción minoritaria en la cutícula vegetal, los compuestos fenólicos participan en funciones esenciales para la supervivencia de la planta. De hecho, han sido unánimemente aceptados como los principales responsables de la fotoprotección en plantas, entre otras funciones esenciales adscritas a estos metabolitos secundarios.

El término cutícula vegetal ha sufrido profundas transformaciones desde que fue mencionado por primera vez para definir la piel de las plantas. Actualmente, la cutícula vegetal se define como una pared celular cutinizada. A pesar de los notables avances alcanzados sobre la composición, biogénesis y propiedades biomecánicas (térmicas, hidrodinámicas y mecánicas) de la cutícula vegetal, se necesita más investigación para completar algunas brechas de conocimiento que permanecen aún inciertas. De esta forma, esta tesis se ha enfocado principalmente en comprender el papel protector de los compuestos fenólicos, con especial énfasis en sus propiedades ópticas. El tema ha sido abordado desde diferentes perspectivas para obtener una visión transversal. Aunque en esta investigación se han utilizado distintos tejidos y especies vegetales, el fruto de tomate ha sido un modelo recurrente.

La presente tesis doctoral está estructurada en cinco partes: Introducción General, Objetivos, Capítulos, Resumen Global de Resultados y Discusión y Conclusiones.

El Capítulo 1 ha sido dedicado a estudiar la interconversión entre flavonoides presentes en la cutícula de fruto de tomate en diferentes entornos, así como a explorar la potencial agregación molecular que pudiera existir entre ellos. Aunque la chalconaringenina ha sido el flavonoide detectado en cutícula de fruto de tomate maduro, la presencia de su isómero estructural naringenina fue sugerida en algunas investigaciones anteriores. La distinción selectiva entre ambos compuestos ha sido desafiante debido a que su aislamiento requiere condiciones drásticas de pH y temperatura que podrían alterar sus conformaciones, pudiendo causar incluso su isomerización. En plantas, la CHALCONA ISOMERASA (CHI) ha sido identificada como enzima responsable de la conversión estereoespecífica entre chalconaringenina y *(2S)*-naringenina. Sin embargo, no se ha registrado actividad de la CHI en tomates durante la maduración, periodo en el que se acumula la chalconaringenina. Una isomerización espontánea lenta y no estereoespecífica entre la chalconaringenina y la naringenina se ha detectado *in vitro* y podría ser la responsable de la acumulación de naringenina en cutículas de fruto maduro de tomate. Resultados computacionales revelaron que la interconversión entre chalconaringenina y naringenina no era energéticamente viable en *n*-octanol, entorno seleccionado para mimetizar el escenario de la cutícula vegetal. El estudio en agua, simulando un entorno citoplasmático, desveló la importancia de las redes de puentes de H para hacer factible la conversión. El proceso de isomerización puede resumirse del siguiente modo: primero, la chalconaringenina se desprotona; a continuación, el intermedio alcóxido solvatado resultante cicla, siendo éste el paso limitante de la velocidad de reacción; y finalmente, la protonación del intermedio formado (fuerza motriz de la reacción) da lugar a la naringenina solvatada (ver Figura 4.1 en la página 94). Estos datos descartaron la posibilidad de conversión *in situ* del flavonoide en la cutícula vegetal y apuntaron hacia otro escenario, una isomerización previa en el citoplasma y un posterior transporte hacia la pared celular epidérmica externa, como explicación más verosímil de la putativa presencia de naringenina en la cutícula de fruto de tomate.

La formación de agregados de flavonoides en la cutícula de fruto de tomate ha sido sugerida anteriormente. Sin embargo, hasta la fecha, no se ha realizado ningún estudio adicional para explorar la viabilidad energética de esta agregación, así como para establecer las fuerzas estabilizadoras de estos agregados. En el Capítulo 1, se modelaron homodímeros y heterodímeros de chalconaringenina y naringenina en *n*-octanol para vislumbrar si su agregación en la cutícula vegetal podría ser posible. Los resultados indicaron que apilamientos de tipo π-π fueron las principales interacciones estabilizadoras entre estos flavonoides (ver Figura 4.2 en la página 96). Un homodímero de chalconaringenina fue el dímero más favorecido termodinámicamente. La tendencia de agregación de la naringenina fue baja, solo uno de los confórmeros de sus homodímeros mostró una energía de enlace libre de Gibbs ligeramente negativa. La formación de heterodímeros estuvo aún menos favorecida energéticamente.

La falta de resolución espacial de las técnicas tradicionales, así como la falta de disponibilidad de anticuerpos y colorantes específicos para algunos componentes cuticulares han limitado el esclarecimiento de la conformación *in vivo* de los compuestos de la cutícula y el patrón de microdistribución dentro de la cutícula. En el Capítulo 2, se ha empleado la combinación de microscopía confocal Raman y análisis de datos multivariante para superar esta limitación. El patrón de distribución de componentes a lo largo de la cutícula de fruto de tomate fue revelado, incluyendo incluso cambios durante el desarrollo del fruto. En primer lugar, se empleó *Non-negative Matrix Factorization* (NMF) para separar selectivamente regiones que compartían características Raman (*basis*). Un espectro prácticamente puro de compuestos fenólicos carente de flavonoides, así como un espectro prácticamente puro de cutina, con contribución de polisacáridos y ceras, fueron extraídos de diferentes estadios de desarrollo. Por el contrario, solo se logró un espectro enriquecido en flavonoides, incluyendo características de fenoles y cutina (ver Figura 4.3 en la página 99). La naturaleza química de estos tres *basis* computados fue verificada a través del algoritmo *Orthogonal Matching Pursuit* (OMP) y una librería de referencia que incluyó agua, cutina de una línea endogámica recombinante carente de compuestos fenólicos, y un amplio grupo de compuestos aromáticos, lípidos, minerales y carbohidratos. El espectro del *basis*

de cutina se ajustó a la cutina de la librería, mostrando únicamente una pequeña contribución de polisacáridos. El espectro del *basis* de compuestos fenólicos coincidió con ácido *p*-hidroxibenzoico y un éster del ácido *p*-cumárico, mientras que el espectro del *basis* de flavonoides fue asignado a modificaciones metoxiladas y glicosiladas del flavonoide chalconaringenina. Por consiguiente, los compuestos fenólicos podrían ser hipotetizados como unión entre los dominios hidrofóbicos de la cutina y la fracción hidrofílica de polisacáridos.

La localización espacial de los espectros de estos *basis* a lo largo de la cutícula mediante *basis analysis* reveló una visión preliminar de la distribución de sus principales componentes, incluyendo cambios durante el desarrollo del fruto. Sin embargo, un mayor esclarecimiento fue logrado mediante la aplicación del algoritmo OMP en combinación con la librería de referencias al conjunto de datos hiperespectrales de los diferentes estadios de desarrollo del fruto de tomate.

Tres patrones de microdistribución fueron distinguidos a lo largo del desarrollo del fruto (ver Figura 4.4 en la página 100). En los estadios de desarrollo más tempranos, la procutícula era un matriz enriquecida en fenoles, colocalizando compuestos fenólicos y cutina a lo largo de toda la cutícula vegetal. En los siguientes estadios, durante la mayor parte del periodo de crecimiento, la cutina mantuvo su distribución homogénea a lo largo de la cutícula. Los compuestos fenólicos se acumularon principalmente en forma de una capa superficial cercana a la superficie externa y en el área central de los *pegs* (pared anticlinal cutinizada de la célula epidérmica). Estos compuestos fenólicos fueron identificados principalmente como una mezcla de ácido *p*-hidroxibenzoico libre y ácido *p*-cumárico esterificado. En los estadios maduros, se observó un aumento notable de compuestos fenólicos, principalmente debido a la incorporación de flavonoides en la cutícula. Sorprendentemente, los espectros de cutículas maduras se ajustaron mejor a chalconas metoxiladas y glicosiladas que a la chalconaringenina en forma libre. Merece la pena mencionar que se observó un mayor error en el ajuste en los estadios maduros. La interacción entre flavonoides y otros componentes, así como cambios en el entorno de la cutícula durante la maduración podrían explicar este mayor desajuste. En estadios maduros, la cutina continuó siendo una matriz homogénea dentro de la cutícula vegetal. Por el contrario, la distribución de los

compuestos fenólicos se vio alterada durante la maduración. Mientras que el ácido *p*-hidroxibenzoico preservó su localización previa (capa superficial y en el centro de los *pegs*), el éster del ácido *p*-cumárico fue localizado a lo largo de toda la cutícula y *pegs*. La mayor acumulación de flavonoides fue detectada en la parte interna de la cutícula hacia la pared celular epidérmica. Una capa de ceras muy delgada se evidenció también a partir de la etapa de crecimiento. La distribución de polisacáridos a lo largo de la cutícula necesita más investigación, aunque algunos resultados preliminares sugirieron que su localización en estadios tempranos coincide con la potencial localización de flavonoides en estadios maduros.

Su localización externa en la cutícula de fruto de tomate desde estadios tempranos del desarrollo respaldó el papel fundamental de los compuestos fenólicos de la cutícula en la fotoprotección de las plantas, tema escasamente estudiado en la literatura. En el Capítulo 3, se han inspeccionado las propiedades ópticas de cutículas de fruto de tomate en diferentes estadios de desarrollo. El máximo de transmitancia fue localizado en la región visible para todos los estadios, permitiendo que la luz visible alcance los tejidos fotosintéticos. Se evidenció un fuerte descenso en la región ultravioleta A (UV-A) en los estadios de fruto verde, el cual se desplazó progresivamente hacia mayores longitudes de onda durante la maduración. La transmitancia UV-B fue extremadamente baja para todos los estadios (ver Figura 4.5b en la página 102). Por tanto, la cutícula de fruto de tomate filtró eficazmente esta radiación energética desde estadios muy tempranos de desarrollo. En relación a la región UV-C, un pico de transmitancia débil alrededor de 260 nm se observó en los espectros. Este pico decreció durante el crecimiento hasta que se extinguió prácticamente por completo a partir de los 45 días después de antesis (daa). La transmitancia decreció de forma general durante el crecimiento y maduración del fruto. La transmitancia en el visible disminuyó desde un 70% en un estadio muy temprano (15 daa) hasta un 53% en rojo maduro, mientras que solo se detectaron pequeñas variaciones en la transmitancia UV-B a lo largo del desarrollo (ver Figura 4.5b en la página 102). En general, la reflectancia de cutículas de fruto de tomate fue baja alcanzando su máximo, entre el 20 y el 45%, en el visible; aunque sin mostrar ninguna tendencia clara a lo largo del desarrollo del fruto (ver Figura 4.5c en la página 102). La reflectancia combinada de las regiones UV-

A y UV-B fue mayor (alrededor del 10%) antes de la maduración. Los espectros de absorbancia mostraron tres bandas principales alrededor de 235, 310 y 380 nm, las cuales aumentaron durante el crecimiento y maduración del fruto.

El bloqueo de la luz UV por las cutículas de fruto de tomate se asignó a la absorción de esta radiación por los compuestos fenólicos, derivado de la baja reflectancia UV de todos los estadios de desarrollo. Sin embargo, el bloqueo fue altamente efectivo en la región UV-B, pero limitado en la UV-A. El bloqueo UV-A aumentó desde 15 hasta 30 daa, periodo en el cual la cantidad de fenoles es prácticamente constante. Se encontró una relación entre el bloqueo UV-A y el espesor de la cutícula en estadios tempranos con bajo contenido de fenoles; mientras que, durante la maduración, el mayor bloqueo de la radiación UV-A fue atribuido a la incorporación de chalconaringenina en la cutícula. El análisis comparativo con cutículas sin ceras reveló que las ceras tienen un efecto prácticamente nulo en el filtrado de la radiación UV-B y una influencia muy baja (5%) en la reflectancia UV-A, lo cual disminuyó durante el crecimiento y maduración del fruto. Por el contrario, las ceras participan significativamente en la reflectancia de la radiación visible.

Adicionalmente, se estudiaron las propiedades térmicas de la cutícula de fruto de tomate a lo largo del desarrollo. En los estadios de fruto verde se evidenció una clara transición vítrea (T_g), por debajo de los 0ºC. A temperaturas inferiores a la T_g la cutícula vegetal se comportaba como un material vítreo rígido; mientras que por encima de la T_g se convertía en un polímero gomoso. Por el contrario, la T_g durante la maduración no fue tan evidente y se desplazó hacia mayores temperaturas, alcanzando valores dentro del rango de las condiciones ambientales (20-35ºC) (ver Figura 4.5a en la página 102). Esto implica que la cutícula del fruto pudiera estar cambiando desde un comportamiento vítreo a uno gomoso en función de la estación del año o incluso de la hora del día. Se sugirió que la presencia de ceras intracuticulares y fenoles podían aumentar la T_g, actuando como fases de relleno dentro de la cutícula. Además, la capacidad calorífica específica reversible (Cp_{rev}) de la cutícula de todos los estadios de desarrollo estudiados fue mayor que la del aire; por tanto, las plantas podrían aclimatarse a fluctuaciones de temperatura sin experimentar cambios bruscos en la temperatura de los tejidos de la planta.

El estudio de propiedades ópticas se extendió a hojas y frutos de diversas especies vegetales. Cutículas aisladas de hojas de *Brassica oleracea* L., *Beta vulgaris* L., *Hedera helix* L., *Iris germanica* L., *Agave americana* L. y *Clivia miniata* (Lindl.) Regel así como de frutos de *Capsicum annuum* L. y *Vitis vinifera* L. fueron empleadas en el Capítulo 4 para obtener una amplia perspectiva sobre la interacción luz-cutícula vegetal. Esta investigación se dirigió a dilucidar si hay un mecanismo de fotoprotección común para las plantas. En general, las cutículas vegetales mostraron una transmitancia UV-B y UV-C muy baja (0.3-12%), con la excepción de *I. germanica*, *B. vulgaris* y *B.oleracea* que filtraron esta radicación en menor medida. La transmitancia UV-A fue más dependiente de la especie, aunque todas tuvieron en común un aumento brusco de transmitancia en este rango, hasta alcanzar su máximo (60-90%) en el visible. Se detectó una muy pequeña reflectancia de la radiación UV para todas las especies; mientras que la reflectancia alcanzó su máximo (10-35%) en el visible. Dos bandas principales centradas alrededor de 220-240 y 280-310 nm respectivamente, definieron el espectro de absorbancia de la mayoría de las cutículas. De forma excepcional, los espectros de absorbancia de *B.oleracea*, *B. vulgaris* e *I. germanica* mostraron una banda ancha alrededor de 200 nm y un hombro en 280-300 nm. Los espectros de absorbancia de todas las especies estudiadas fueron prácticamente nulos a partir de 500 nm.

Todas las especies estudiadas tuvieron en común la presencia de ácido *p*-cumárico en su fracción fenólica. La acumulación de compuestos fenólicos en los tejidos vegetales ha sido relacionada con la prevención de fotodaños en las plantas. Además, la isomerización de algunos compuestos fenólicos ha sido presentado como mecanismo de fotoprotección en diferentes formulaciones de protectores solares. Sin embargo, el mecanismo por el cual la cutícula vegetal lleva a cabo esta fotoprotección de las plantas no ha sido determinado previamente. La espectroscopía de absorción transitoria (TAS) es una técnica bomba-sonda que permite recopilar información sobre las vías de relajación de las moléculas en estado excitado. El examen de los mapas de TAS junto con un análisis de decaimiento cinético permitió revelar información sobre los procesos dinámicos ultrarrápidos.

En primer lugar, para explorar el efecto del entorno en los procesos dinámicos se registraron los mapas de TAS de una disolución de ácido *p*-cumárico en metanol, así como de dos muestras sólidas, ácido *p*-cumárico en polvo y un oligómero de alquilcumarato, tras excitación a 300 nm (ver Figuras 4.6a-c en la página 106). Estas conformaciones pretenden servir de aproximación a las localizaciones del ácido *p*-cumárico en el interior de la cutícula, como moléculas libres atrapadas en la cutícula o esterificados a otros componentes cuticulares. El mapa TAS de la disolución de ácido *p*-cumárico en metanol (ver Figura 4.6a en la página 106) mostró una fuerte absorción en estado excitado (ESA) alrededor de los 340-450 nm y una emisión estimulada (SE) débil en torno a los 400-500 nm. Sin embargo, las muestras sólidas (ver Figuras 4.6b-c en la página 106) presentaron una única banda ancha entre 350-550 nm. Tres tiempos de vida (τ_2, τ_3 y τ_4) fueron calculados para las tres muestras a partir del análisis de decaimiento cinético (ver Tabla 4.1 en la página 107). Se supuso que un tiempo de vida adicional muy rápido (τ_1), asignable a la relajación asociada al principio de Franck-Condon, podría caer en el rango de la función de respuesta del instrumento. τ_2 y τ_3 fueron los tiempos de vida implicados en la potencial isomerización y τ_4 se asignó a la formación de especies de vida larga que persistían más allá de la ventana de medida. A modo comparativo, los dos tiempos de vida involucrados en la isomerización fueron mucho más largos para los sólidos, especialmente para el oligómero, que para el ácido *p*-cumárico solvatado (ver Tabla 4.1 en la página 107). Para descifrar estas diferencias, el camino de isomerización *trans-cis* del ácido *p*-cumárico fue computado mediante cálculos computacionales en metanol y un modelo minimalista de estado sólido. Se revelaron dos escenarios de relajación distintos desde el estado excitado (S_1). En la disolución de metanol, el isómero *trans* es promocionado al S_1 tras irradiación UV, preservando la geometría del estado fundamental (S_0). Esta geometría se relaja inicialmente siguiendo el principio de Franck-Condon (τ_1). A continuación, a lo largo de τ_2 esta molécula evoluciona en S_1 cambiando su estructura hacia la intersección cónica (CI), geometrías moleculares donde las superficies de energía potencial de S_0 y S_1 se cruzan. Finalmente, la molécula atravesaba la CI, la cual era muy cercana al estado de transición (TS) en S_0. En consecuencia, la molécula podía regresar al S_0 recuperando el isómero *trans* o isomerizando a *cis* (ver Figura 4.7a en la página

109). La presencia del isómero *cis* en disolución se demostró mediante ^{1}H-RMN. El mecanismo en fase sólida mostró diferencias significativas. Aunque τ_1 y τ_2 se definieron de forma análoga a lo explicado anteriormente, la posición de la CI cambió significativamente. Se detectó una CI "temprana" lejos del TS, impidiendo la isomerización *trans-cis* del ácido *p*-cumárico. Consecuentemente, en estado sólido el τ_3 se definió como la recuperación del isómero *trans* tras atravesar la CI (ver Figura 4.7b en la página 109).

Los mapas de TAS de cutículas vegetales tras excitación a 300 nm (ver Figuras 4.6d-k en la página 106) mostraron características similares a los TAS del ácido *p*-cumárico en entornos sólidos. La mayoría de las especies mostraron una única banda ancha alrededor de 340-450 nm. Solo se observaron pequeñas modificaciones para *B. vulgaris* e *I. germanica*. El análisis de decaimiento cinético de los mapas TAS de las cutículas se ajustó a tres tiempos de vida para todas las especies (ver Tabla 4.1 en la página 107). Los τ_2 fueron por lo general similares o menores que el calculado para el polvo de ácido *p*-cumárico excepto en el caso de *B. vulgaris* que mostró valores similares al oligómero; así como *I. germanica* y *C. miniata* cuyos τ_2 estuvieron comprendidos entre los valores calculados para el polvo y el oligómero. En general, los τ_3 de las cutículas fueron del rango de cientos de picosegundos, similares al valor computado para el polvo. De nuevo, un tiempo de vida más largo fue calculado para *B. vulgaris*. La presencia del polímero rígido cután como principal componente de la cutícula de *B. vulgaris* podría explicar sus tiempos de vida más largos. Se obtuvieron resultados análogos a partir de mapas de TAS de hojas de *Adiantum raddianum*, *Cycas revoluta* y *Araucaria bidwilli*, lo cual demostró la naturaleza superficial de las medidas de TAS.

A modo de resumen, la cutícula vegetal podría prevenir fotodaños en la planta a través de un mecanismo no radiativo, común para múltiples especies vegetales. El ácido *p*-cumárico tras excitación UV atraviesa una CI "temprana" para regresar al isómero *trans*, permitiendo así la disipación de energía. Este mecanismo podría ser complementado por reflexión de la luz o fluorescencia de la cutícula (ver Figura 4.8 en la página 110). Los fenoles presentes en las paredes celulares y/o los fenoles acumulados en las células epidérmicas podrían aportar una fotoprotección

adicional que contribuyera a prevenir fotodaños en especies cuyas cutículas mostraron alta transmitancia.

Finalmente, en el Capítulo 5 se han explorado los efectos sinérgicos entre diferentes compuestos fenólicos que coexisten en la cutícula de fruto de tomate maduro. Los perfiles de fotodegradación de ácido *p*-cumárico y chalconaringenina en etanol mostraron que mientras que la principal banda de absorbancia del ácido *p*-cumárico (centrada en 312 nm) disminuyó aproximadamente un 29% tras dos horas de irradiación solar, la chalconaringenina solo experimentó un descenso muy ligero de su principal banda (a 365 nm). La formación del isómero *cis* se observó únicamente en la disolución post-irradiada de ácido *p*-cumárico, en concordancia con la desactivación no radiativa discutida anteriormente. La disolución de ácido *p*-cumárico mostró una emisión baja alrededor de 380 nm. Se detectó un *quenching* asimétrico de esta fluorescencia al aumentar la concentración de chalconaringenina. La transferencia de energía de resonancia de Förster, un tipo de *quenching* dinámico, podría explicar esta atenuación sugiriendo la formación de interacciones dipolo-dipolo entre estas moléculas. El perfil de fotodegradación de una mezcla equimolar de ambos compuestos resultó esencialmente en la suma de las contribuciones individuales.

Explorar los eventos que ocurren a nivel molecular inmediatamente después de irradiación con luz UV fue crucial para entender la sinergia entre ambos compuestos fenólicos. El mapa TAS de una disolución de ácido *p*-cumárico en etanol después de excitación a 312 nm mostró una fuerte ESA alrededor de 375 nm y algunas absorciones débiles alrededor de 330, 390 y 600 nm asignables a la formación de especies de vida larga, concretamente al isómero *cis*, radicales fenoxi y electrones solvatados (ver Figura 4.9a en la página 114). El análisis de decaimiento cinético ajustó a tres tiempos de vida las características del TAS: un primer τ_1 muy rápido de relajación de la molécula en S_1 hacia la CI (cercana al TS), el τ_2 asignado al cruce de la CI y su posterior relajación no radiativa hacia los isómeros *cis* y *trans*, y un τ_3 muy largo relacionado con las especies de vida larga mencionadas arriba. El mapa TAS de una disolución de chalconaringenina en etanol después de excitación a 312 nm mostró una fuerte ESA a 420 nm así como un *bleaching* del estado fundamental (GSB) alrededor de 360 nm (ver Figura 4.9b

en la página 114). La falta de isomerización *trans-cis* de chalconaringenina fue demostrada por ^{1}H-RMN y por la ausencia de señales del isómero *cis* en su perfil de fotodegradación. La exploración teórica del perfil de isomerización *trans-cis* evidenció una CI “temprana” que pudo explicar la atenuación de la radiación UV incidente a través de un mecanismo no radiativo, sin experimentar isomerización. Brevemente, en la disolución de chalconaringenina un rápido τ_1 fue asignado al tiempo de relajación de la molécula en S_1 mientras se aproxima a la CI, el τ_2 correspondió al cruce de la CI y la recuperación del isómero *trans* y el τ_3 largo apuntó hacia la presencia de algunas moléculas atrapadas en estados excitados. El mapa de TAS de una mezcla equimolar de ácido *p*-cumárico y chalconaringenina tras ser excitada a 312 nm (ver Figura 4.9c en la página 114) no resultó en la suma de los componentes individuales. Por el contrario, se pareció mucho al TAS de la chalconaringenina. Mientras que el τ_1 fue comparable para chalconaringenina y la mezcla; τ_2 y τ_3 fueron más largos en la mezcla. Esto podría ser debido a las arriba mencionadas interacciones dipolo-dipolo entre ambos compuestos fenólicos.

Considerando todo lo anterior y extrapolando los datos obtenidos en disolución al escenario de cutícula vegetal, las potenciales interacciones entre compuestos fenólicos que colocalizan dentro de la cutícula implica una sinergia en fotoprotección. Esto fue probado por la alteración de las dinámicas del ácido *p*-cumárico en presencia de chalconaringenina. Adicionalmente, esta investigación proporciona nuevos conocimientos sobre la modulación de la fotoprotección en relación con los cambios de composición de la cutícula de fruto de tomate durante el desarrollo del fruto.

SUMMARY

The conquest of land by plants 470 million years ago entailed the development of mechanisms to acclimatize to new challenges. One of the main adaptations was the covering of aerial parts of leaves, fruits and non-lignified stems with a hydrophobic lipid layer named plant cuticle. As the first barrier between the plant and the environment, the cuticle deals with the protection of plant tissues against excessive water loss, changes in temperature, overexposure to radiation, infections by pathogens and mechanic injuries, among others. The main component of most of plant cuticles is the amorphous polyester cutin, although some species also include cutan. Polysaccharides, waxes and phenolic compounds usually complete the remaining composition of the plant cuticle. Despite of their minor proportion in plant cuticle, phenolic compounds participate in essential functions for the survival of plants. Indeed, phenolic compounds have been unanimously agreed as being responsible for plant photoprotection, among other pivotal roles ascribed to these secondary metabolites.

The term plant cuticle has suffered deep transformations since it was firstly mentioned to define the skin in plants. Currently, the plant cuticle is defined as a cutinized cell wall. Despite the notable advance on the knowledge about composition, biogenesis and biomechanical (thermal, hydrodynamical and mechanical) properties of the plant cuticle, further research is needed to fill some knowledge gaps which still remain unclear. In this way, this thesis has been mainly focused on understanding the protective role of cuticle phenolic compounds, with special stress on their optical properties. The topic has been approached from different perspectives to obtain a transversal view. Although different plant tissues and species have been employed in this research, tomato fruit has been a recurrent model.

The present doctoral thesis is structured in five parts: General Introduction, Objectives, Chapters, Overall Summary of Results and Discussion and Conclusions.

Chapter 1 was devoted to study the interconversion between flavonoids present in tomato fruit cuticle in different environments, as well as to explore the potential molecular aggregation among them. Although naringenin chalcone has been the flavonoid detected in ripe tomato fruit cuticle, the presence of its structural isomer naringenin was suggested in some earlier reports. The selective distinction of both compounds has been challenging since their isolation require drastic conditions of pH and temperature which may alter their conformation, even enabling its isomerisation. In plants, CHALCONE ISOMERASE (CHI) has been identified as the enzyme responsible of the stereospecific conversion of naringenin chalcone to *(2S)*-naringenin. However, no CHI activity has been registered in tomatoes during ripening, the period where naringenin chalcone is accumulated. A slow non-stereospecific spontaneous isomerization between naringenin chalcone and naringenin has been detected *in vitro* and it could be responsible for the accumulation of some naringenin in ripe tomato fruit cuticle. Computational results revealed that the interconversion between naringenin chalcone and naringenin was not energetically feasible in *n*-octanol, the selected environment to mimic the plant cuticle scenario. The exploration in water, simulating a cytoplasm environment, unveiled the importance of the H bonding network to make the conversion plausible. The isomerization process could be summarized as follow: firstly, naringenin chalcone is deprotonated; subsequently, the resulting solvated alkoxy intermediate is cycled, being this the rate-determining step of the process; and finally, the protonation of the forming intermediate (driving force of the reaction) results in solvated naringenin (see Figure 4.1 on page 94). These data discarded the possibility of the *in situ* flavonoid interconversion within the plant cuticle and pointed towards another scenario, previous isomerisation within the cytoplasm and a later transport to the outer epidermal cell wall, as the most plausible explanation for the putative presence of naringenin in the tomato fruit cuticle.

The formation of flavonoid *clusters* within tomato fruit cuticle has been previously suggested. Nevertheless, to date, no additional study has been carried out to explore the energetic viability of this aggregation as well as to stablish the stabiliser interactions of those aggregates. In Chapter 1, homodimers and heterodimers of naringenin chalcone and naringenin were modelled in *n*-octanol to

glimpse if they could aggregate within the plant cuticle. Results indicated that π-π stacking were the main stabilizer interactions among flavonoids (see Figure 4.2 on page 96). A naringenin chalcone homodimer was the most thermodynamically favoured dimer. The tendency of naringenin to aggregate was low, only one conformer of its homodimers displayed a slightly negative Gibbs free binding energy. Even less energetically favoured was the formation of heterodimers.

The lack of spatial resolution of traditional techniques as well as the non-availability of antibodies or specific stains for some cuticle components has limited the elucidation of the *in vivo* conformation of cuticle compounds and the microdistribution pattern within the plant cuticle. In Chapter 2, confocal Raman microscopy in combination with multivariate data analysis has been employed to overcome this limitation. The distribution pattern throughout the tomato fruit cuticle has been revealed, even including changes along fruit development. Firstly, non-negative matrix factorization (NMF) was employed to selectively separate regions which shared Raman signatures (basis). An almost pure spectrum of phenolic compounds devoid of flavonoids, as well as an almost pure spectrum of cutin, with contribution of polysaccharides and waxes, were extracted from different stages of development. Contrary, only an enriched spectrum in flavonoids with signals from phenolics and cutin could be achieved (see Figure 4.3 on page 99). The chemical nature of these three computed basis were verified by the orthogonal matching pursuit (OMP) algorithm and a reference library which included water, cutin from a recombinant inbred line devoid of phenolics and a large set of aromatic compounds, lipids, minerals and carbohydrates. The cutin basis spectrum fitted with cutin from the library, only showing a small contribution of polysaccharides. The phenolic basis spectrum matched with *p*-hydroxybenzoic acid and an ester of *p*-coumaric acid, while the flavonoid spectrum was assigned to methoxylated and glycosylated modifications of the flavonoid naringenin chalcone. Consequently, phenolics could be hypothesized as linkers between hydrophobic cutin domains and the hydrophilic polysaccharide fraction.

The spatial location of these basis spectra throughout the plant cuticle by *basis analysis* unveiled a preliminary view of the distribution of the main cuticle components, including changes along fruit development. Nevertheless, further

elucidation was achieved by running the OMP algorithm in combination with the reference library to the hyperspectral dataset of different stages of development of tomato fruit. This analysis enabled to locate specific compounds throughout the whole cuticle of different stages of development of tomato fruit.

Three microdistribution patterns were distinguished along fruit development (see Figure 4.4 on page 100). At very early stages of development, the procuticle was a phenolic enriched matrix, co-locating phenolic compounds and cutin throughout the plant cuticle. In next stages, during most of the growing period, the cutin maintained its homogenous distribution along the cuticle. Phenolics were mainly accumulated as a superficial layer close to the outer surface and in the middle area of the pegs (cutinized anticlinal epidermal wall). These phenolics were mainly identified as a mixture of free *p*-hydroxybenzoic acid and esterified *p*-coumaric acid. During the ripe stages a notable increase in phenolic compounds was observed, mainly due to the incorporation of flavonoids into the cuticle. Surprisingly, the spectra of ripe cuticles fitted better with methoxylated and glycosylated chalcones than with free naringenin chalcone. It is worth mentioning that a higher spectral misfit was observed in ripe stages. The interaction of flavonoids with other cuticle components as well as changes in the cuticle environment during ripening might explain this larger mismatch. In ripe stages, cutin continued to be a homogenous matrix within the plant cuticle. Contrary, phenolic compounds altered their distribution during ripening. While *p*-hydroxybenzoic acid remained its previous location (superficial layer and middle of the pegs), the ester of *p*-coumaric acid was located throughout the whole cuticle and pegs. The main accumulation of flavonoids was detected in the inner side of the cuticle towards the epidermal cell wall. A very thin waxy layer was also evidenced from the growing stage. Polysaccharide distribution within the cuticle needs further research, although some preliminary results suggested that their location in early stages coincided with the potential location of flavonoids in ripe stages.

Their outer location within the tomato fruit cuticle from the earliest stages of development supported the key role of cuticle phenolic compounds in plant photoprotection, topic barely studied in the literature. In Chapter 3, the optical properties of tomato fruit cuticles from different stages of development have been

inspected. The maximum of transmittance was located in the visible region for all the stages, enabling visible light to reach the photosynthetic tissues. A strong decrease was evidenced within the ultraviolet A (UV-A) for green fruit stages and was progressively shifted toward higher wavelength during ripening. The UV-B transmittance was extremely low for all the stages (see Figure 4.5b on page 102). Thus, the tomato fruit cuticle effectively screens this energetic radiation from very early stages of development. Regarding UV-C region, a low peak of transmittance around 260 nm was observed in the spectra. This peak decreased during growth until being almost extinguished from 45 days after anthesis (daa). The overall transmittance decreased along fruit growth and ripening. The visible transmittance decreased from 70% in a very early stage (15 daa) to 53 % in red ripe, while only slight variations were detected in the UV-B transmittance along development (see Figure 4.5b on page 102). Generally, the reflectance of tomato fruit cuticles was low reaching its maximum, between 20 and 45%, in the visible; yet without a clear tendency along fruit development (see Figure 4.5c on page 102). The combined reflectance of the UV-B and UV-A was higher (around 10%) before ripening. The absorbance spectra showed three main bands around 235, 310 and 380 nm which increased during fruit growth and ripening.

The UV blockage of tomato fruit cuticle was assigned to the absorption of this radiation by phenolic compounds, stemmed from the low UV reflectance of all the stages of development. Nevertheless, the blockage was strongly effective in the UV-B region, but limited in the UV-A. The UV-A blockage increased from 15 to 30 daa, period in which the amount of phenolics was almost constant. A relationship between UV-A blockage and cuticle thickness was found in early stages with low content of phenolics; whereas during ripening, the higher UV-A blockage was ascribed to the incorporation of naringenin chalcone into the cuticle. The comparative analysis with dewaxed cuticles revealed that waxes had an almost null effect on UV-B screening and a very low (5%) influence on UV-A reflectance, which decreased along growth and ripening. Contrary, waxes significatively participated in the reflectance of visible radiation.

Additionally, thermal properties of tomato fruit cuticle along fruit development were also studied. A clear glass transition (T_g), below 0ºC, was evidenced in green

fruit stages. Below T_g the plant cuticle behaved as a rigid glassy material; while over T_g it turned into a rubbery polymer. Contrary, the T_g during ripening was not as evident and it was shifted towards higher temperatures, reaching values within environmental conditions (20-35ºC) (see Figure 4.5a on page 102). It implied that the fruit cuticle could be changing from a glassy to a rubbery behaviour depending on the season or even the time of the day. The presence of intracuticular waxes as well as phenolics was suggested to increase the T_g, acting as fillers within the cuticle. Moreover, the reversible specific heat capacity (Cp_{rev}) of the plant cuticle for all the studied stages of development were higher than the one of atmospheric air; thus, plants could acclimatize to fluctuations in temperatures without experimenting drastic changes in the temperature of their plant tissues.

The study of optical properties was extended to leaves and fruits from multiple plant species. Isolated cuticles from *Brassica oleracea* L., *Beta vulgaris* L., *Hedera helix* L., *Iris germanica* L., *Agave americana* L. and *Clivia miniata* (Lindl.) Regel leaves as well as from *Capsicum annuum* L. and *Vitis vinifera* L. fruits were employed in Chapter 4 to gain a wide overview about the light-plant cuticle interaction. This research intended to elucidate whether there is a common photoprotection mechanism in plants. Generally, plant cuticles displayed a very low UV-B and UV-C transmittance (0.3-12%), with the exception of *I. germanica*, *B. vulgaris* and *B. oleracea* which screened this radiation to a lesser extent. UV-A transmittance was more dependent on the species, although all had in common a sharp increase in transmittance within this range until reaching its maximum (60-90 %) in the visible. A very little UV radiation reflectance was detected in all the species; whereas reflectance reached its maximum (10-35%) in the visible. Two main bands centred around 220-240 and 280-310 nm respectively, defined the absorbance spectra of most of cuticles. Exceptionally, the absorbance spectra of *B. oleracea*, *B. vulgaris* and *I. germanica* showed a broad band around 200 nm and a shoulder at 280-300 nm. Absorbance spectra of all the studied species were almost negligible from 500 nm.

All the studied species had in common the presence of *p*-coumaric acid within their cuticle phenolic fraction. The accumulation of phenolic compounds in plant tissues has been related to prevent plants from photodamage. Also, the

isomerization of some phenolics has been reported as a photoprotection mechanism in different solar formulations. Nevertheless, the mechanism by which the plant cuticle carries out plant photoprotection has not been previously resolved. Transient absorption spectroscopy (TAS) is a pump-probe technique which enables to gather knowledge about relaxation pathways of excited-state molecules. The inspection of TAS maps in combination with a kinetic decay analysis allowed to reveal findings about ultrafast dynamics.

Firstly, TAS maps of a methanolic solution of *p*-coumaric acid as well as of two solid samples, *p*-coumaric acid powder and an alkylcoumarate oligomer, were registered after 300 nm excitation (see Figures 4.6a-c on page 106) to explore the effect of the environment on dynamics. These conformations intended to serve as approaches to *p*-coumaric acid locations within the plant cuticle, as free molecules trapped into the cuticle or esterified to other cuticle components. TAS map of the methanolic solution (see Figure 4.6a on page 106) displayed a strong excited state absorption (ESA) around 340-450 nm and a weak stimulated emission (SE) around 400-500 nm. Nevertheless, solid samples (see Figures 4.6b-c on page 106) showed only a broad band between 350-550 nm. Three lifetimes (τ_2, τ_3 and τ_4) were computed from the kinetic decay analysis for the three samples (see Table 4.1 on page 107). An additional very fast lifetime (τ_1), assigned to the relaxation associated to the Franck Condon principle, was supposed to fall within the instrument response function. τ_2 and τ_3 were the lifetimes implied in the potential isomerization and τ_4 was attributed to the formation of long-lived species, which persisted beyond the measurement window. Comparatively, the two lifetimes implied on the isomerization were much longer for solids, especially for the oligomer, than for the solvated *p*-coumaric acid (see Table 4.1 on page 107). To unravel these differences, the *trans-cis* isomerization pathway of *p*-coumaric acid was computed by quantum calculations in both, a methanolic environment and a minimalistic solid-state model. Two distinct relaxation scenarios from the excited state (S_1) were revealed. In the methanolic solution, the *trans* isomer was promoted to S_1 under UV irradiation, preserving its geometry from the ground state (S_0). This geometry initially relaxed following the Franck–Condon principle (τ_1). Then, along τ_2 this molecule evolved in S_1 changing its structure towards a conical intersection (CI), molecular geometries

where S_0 and S_1 potential energy surfaces crossed. Finally, the molecule traversed the CI, which were very close to the transition state (TS) in S_0. Consequently, the molecule could return the S_0 recovering the *trans* isomer or isomerizing to *cis* (see Figure 4.7a on page 109). The presence of the *cis* isomer in the solution was proved by ^{1}H-NMR. The mechanism in solid phase unveiled significant differences. Although τ_1 and τ_2 were analogously defined to the above explained for solution, the location of the CI significatively differed. An “early" CI far from the TS was detected, impeding the *trans-cis* isomerization of the *p*-coumaric acid. Consequently, τ_3 in solid environment was defined as the recovering of the *trans* isomer after traversing the CI (see Figure 4.7b on page 109).

TAS maps of plant cuticles after 300 nm excitation (see Figures 4.6d-k on page 106) showed similar features than TAS from *p*-coumaric in solid environment. Most of species showed a unique broad band around 340-450 nm. Only minor modifications were observed for *B. vulgaris* and *I. germanica*. The kinetic decay analysis of the cuticle TAS maps fitted to three lifetimes for all the species (see Table 4.1 on page 107). The τ_2 were in general similar or lower than that computed for the powder of *p*-coumaric acid except for *B. vulgaris* which displayed values akin to the oligomer; as well as *I. germanica* and *C. miniata* whose τ_2 were in between powder and oligomer computed values. In general, the τ_3 of the cuticles were in the range of hundreds of picoseconds, similar to that computed for the powder. Again, a longer lifetime was calculated for *B. vulgaris*. The presence of the rigid cutan polymer as the main component of the *B. vulgaris* cuticle could explain their longer calculated lifetimes. Analogous results were obtained from TAS analysis of *Adiantum raddianum*, *Cycas revoluta* and *Araucaria bidwilli* fresh leaves, which proved the superficial nature of TAS measurements.

To summarize, the plant cuticle could prevent photodamage *via* a non-radiative mechanism, common to multiple plant species. The *p*-coumaric acid after UV excitation traversed an “early” CI to return to the *trans* isomer, enabling energy dissipation. This mechanism could be complemented by cuticle light reflection or fluorescence (see Figure 4.8 on page 110). Additional photoprotection provided by the phenolics present in the cell walls and/or phenolics accumulated within

epidermal cells could contribute to prevent photodamage in species whose cuticles showed high transmittance.

Finally, in Chapter 5 the synergic effects between different phenolic compounds co-existing in ripe tomato fruit cuticle have been explored. Photodegradation profiles of *p*-coumaric acid and naringenin chalcone in ethanol unveiled that while *p*-coumaric acid decreased around 29% its main absorbance band (centred at 312 nm) after two hours of solar irradiation, naringenin chalcone only experimented a very slight decrease in its main band (at 365 nm). The formation of the *cis* isomer was only evidenced in the post-irradiated *p*-coumaric acid solution, in agreement with the non-radiative deactivation above discussed. The *p*-coumaric acid solution showed a weak emission around 380 nm. An asymmetrical quenching of this fluorescence by increasing amount of naringenin chalcone was detected. Förster resonance energy transfer, a type of dynamic quenching, might explain this attenuation suggesting dipole-dipole interactions among these phenolics. The photodegradation profile of an equimolar mixture of both compounds essentially resulted in the sum of individual contributions.

Exploring the events at the molecular level which occur immediately after UV irradiation was crucial to understand the synergism between phenolics. TAS map of an ethanolic solution of *p*-coumaric acid after 312 nm excitation showed a strong ESA around 375 nm and some lower absorptions around 330, 390 and 600 nm assigned to the formation of long-lived species, concretely the *cis* isomer, phenoxyl radicals and solvated electrons (see Figure 4.9a on page 114). The kinetic decay analysis fitted TAS features to three lifetimes: a first very fast τ_1 as the relaxation of the molecule in S_1 towards a CI (close to the TS), the τ_2 assigned to the cross of the CI and the subsequent non-radiative relaxation to *trans* and *cis* isomers, and a very long τ_3 related to the above mentioned long-lived species. TAS map of an ethanolic solution of naringenin chalcone after 312 nm excitation showed a strong ESA at 420 nm as well as a ground state bleaching (GSB) around 360 nm (see Figure 4.9b on page 114). The lack of *trans-cis* isomerization of naringenin chalcone was proved by ^{1}H-NMR and the absence of signals from the *cis* isomer in its photodegradation profile. The theoretical exploration of its *trans-cis* isomerization profile evidenced an “early” CI which could explain the attenuation of the incident

UV radiation through a non-radiative mechanism, lacking isomerization. Briefly, in naringenin chalcone solution a fast τ_1 was assigned to the relaxation time of the molecule in S_1 while approaching to the CI, the τ_2 corresponded to the traversing of the CI and the recovering of the *trans* isomer and the long τ_3 pointed towards the presence of some molecules trapped in excited states. TAS map from an equimolar mixture of *p*-coumaric acid and naringenin chalcone after excitation at 312 nm nm (see Figure 4.9c on page 114) did not return in the sum of features from the individual compounds. Contrary, it strongly resembled to TAS from naringenin chalcone. While τ_1 for naringenin chalcone and the mixture were comparable; τ_2 and τ_3 were longer for the mixture. It might be due to the above-mentioned dipole-dipole interactions between both phenolics.

From above and extrapolating data obtained in solution to the plant cuticle, potential interaction among phenolic compounds collocating within the cuticle implied a synergism in photoprotection. It was proved by the alteration of *p*-coumaric acid dynamics on the presence of the flavonoid naringenin chalcone. Additionally, this research provided new insights into the modulation of photoprotection with the changing composition of the tomato fruit cuticle along fruit development.

1. GENERAL INTRODUCTION

The plant cuticle: a continuously evolving term

The transition of plants from water to land, around 470 million years ago, was accompanied by the development and modification of some biological structures and mechanisms. One of the most remarkable adjustments of plants to battle against radiation, temperature changes, drought, wind, etc., was covering their aerial parts of leaves, fruits and non-lignified stems with a hydrophobic lipid layer, the plant cuticle (Bhanot et al., 2021). Recently, a cuticle has been detected in the root cap during early stages of development (Berhin et al., 2019).

In the fourth century BC Theophrastus, a Greek botanist, introduced for the first time the concept of skin in plants, similar to the skin of animals (Domínguez et al., 2011). The outer part of plant organs was labelled cuticle by Grew (1672) and Malpighi (1675). Later on, Ludwig observed the presence of a subtle membrane overlaying this “cuticle” (Domínguez et al., 2011), which was originally isolated from cabbage leaves and its lipid nature identified after staining with Sudan dyes (Brongniart, 1830; Brongniart, 1834). Brongniart (1830) and Henslow (1831) defined the cuticle as a continuous and homogenous layer covering the epidermal cells. The plant cuticle was originally interpreted as an independent layer not linked to the cell wall (CW) (Martens, 1933), although some years later the junction between both the epidermal CW and the cuticle was evidenced (Meyer, 1938). The distinction of different layers within the plant cuticle was attributed to von Mohl (1847). He distinguished a cuticle proper (CP), the first layer in contact with the CW through a pectic layer developed after ontogeny, and a cuticle layer (CL), which appears along development of the CW and it has been supposed to be the only layer with polysaccharides. An outermost layer, the epicuticular wax (EW) layer, was later included in this model (Jeffree, 2006).

Changes in cuticle composition and structure along plant development have been detected, from a simple and thin lipid layer in early stages to a more detailed and sophisticated architecture in mature stage organs (Sargent, 1976). The term cuticle is currently defined as a heterogeneous and anisotropic biocomposite which covers the aerial organs of plants (Jeffree, 2006; Riederer, 2006). Notwithstanding,

some aspects of the generally accepted definition of cuticle have recently been questioned, which will be discussed hereinafter.

The plant cuticle composition

The plant cuticle is present in plants since very early stages of development, it has even been documented in zygotes (Bruck and Walker, 1985; Yang et al., 2008) and seed covers (Molina et al., 2008; De Giorgi et al., 2015). Its thickness is highly variable among species, organs and stages of development; for instance, fruits usually have thicker cuticles than leaves. Additionally, the cuticle is not always uniform along the surface, it can thicken towards the anticlinal walls (Jeffree, 2006). Cuticle thicknesses from 0.03 to more than 10 μm and cuticle weight from 20 to 3000 μg/cm² have been reported (Heredia, 2003). A complete chemical analysis of the cuticle has only been developed in a limited number of plant species. Figure 1.1 shows some of the compounds identified in plant cuticles (Lara et al., 2019).

Cutin is the main component of the plant cuticle constituting between 40-80% of its total weight. It is an insoluble, amorphous polyester formed by bonding of C_{16} and/or C_{18} long chain polyhydroxy fatty acids. Different monomers are present in C_{16} cutin (Figure 1.1) being 10,16-dihydroxyhexadecanoic acid and 9,16-dihydroxyhexadecanoic acid the most widespread among plant species. C_{18} cutin monomers are more varied, being 9,10-epoxy-18-hydroxyoctadecanoic acid, 9,10,18-trihydroxyoctadecanoic acid and their monounsaturated homologues the most abundant (Domínguez et al., 2011) (Figure 1.1). Notable amounts of glycerol has been detected in the cutin of some plant species (Graça et al., 2002; Yang et al., 2016). Despite *Arabidopsis thaliana* L. has been considered a plant model, its cuticle has an uncommon composition, with α,ω-dicarboxylic acids as the main cutin components (Franke et al., 2005). Another aliphatic polymer composed of polyunsaturated fatty acids linked by ether bond, cutan, has been identified in some plant species (Villena et al., 1999). This polymer, extremely resistant to chemical degradation, has usually been present in combination with cutin (Nip et al., 1986a), although in some species such as *Beta vulgaris* L. it can be found as the only polymer present in the cuticle scaffold (Nip et al., 1986b).

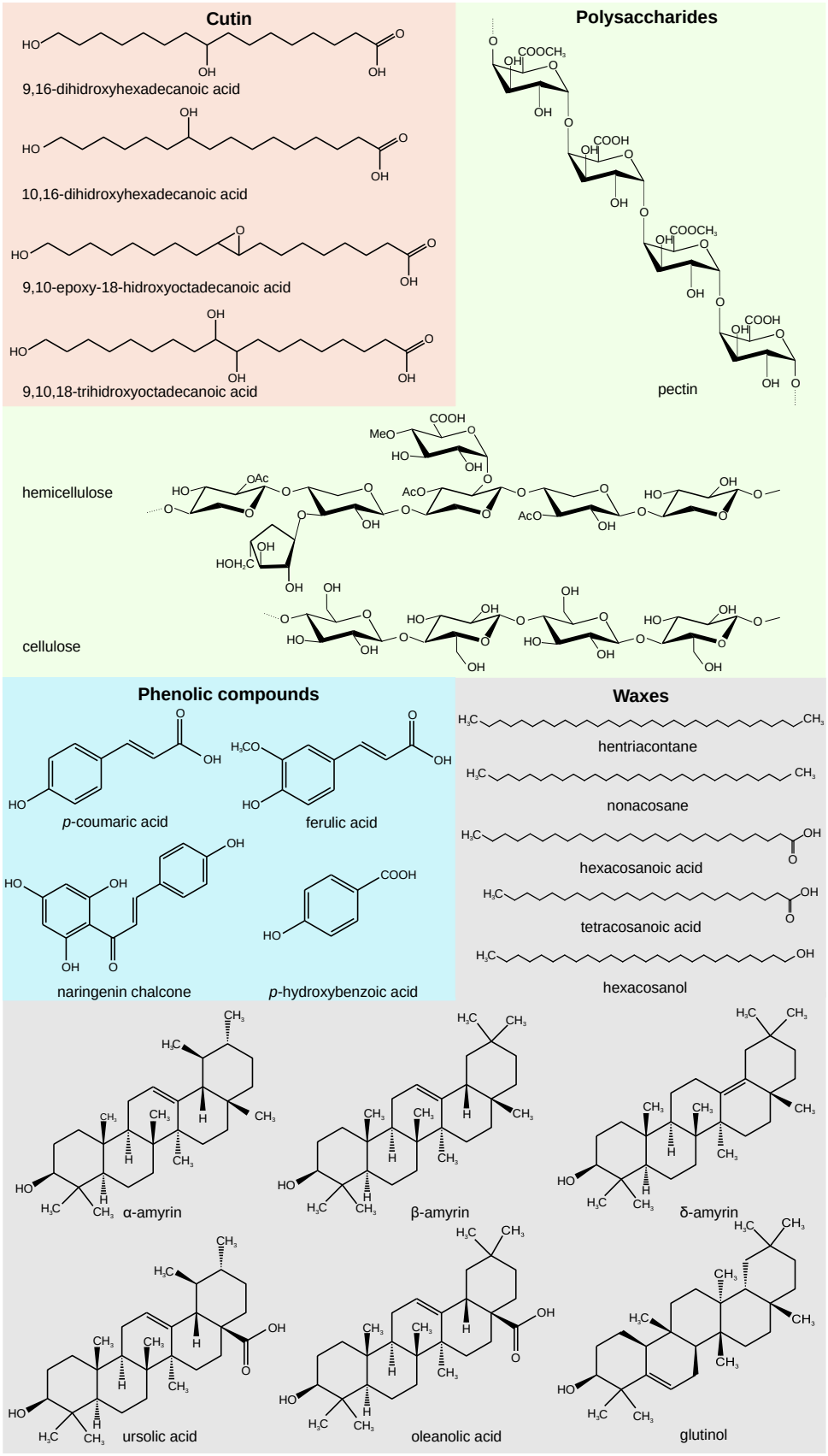

Figure 1.1. Main compounds identified in plant cuticles. Adapted with permission from (Lara et al., 2019). Copyright 2019 *Frontiers in Plant Science* ©.

Much effort has been devoted to elucidating cutin monomer biosynthesis, transport to the outer epidermal wall and later polymerization (Kolattukudy, 2001; Kolattukudy, 2002; Li and Beisson, 2009; Domínguez et al., 2015a). Figure 1.2 details current knowledge on cutin and wax biosynthesis. Several enzymes putatively involved in cutin polymerization have been identified in different plant species (Croteau and Kolattukudy, 1974; Panikashvili et al., 2009; Molina and Kosma, 2015). Additionally, a non-enzymatic polymerization based on self-assembling of cutin monomers has also been postulated (Heredia-Guerrero et al., 2008). Despite the notable advances in the identification of genes involved in cutin and wax biosynthesis and deposition, further research is required to fully unravel cuticle biosynthesis and deposition.

Waxes can be located either on the surface of the cuticle or embedded within the cuticle (Jeffree, 2006). They are a heterogeneous mixture of long chain primary and secondary alcohols, fatty acids, aldehydes, ketones, hydrocarbons, esters, terpenes, steroids and triterpenoids, such as amyrins, ursolic and oleanolic acids (Bianchi, 1995; Buschhaus and Jetter, 2011; Lara et al., 2019) (Figure 1.1). They can represent from 1 to 40 % of the total cuticle weight and their composition can also vary among plant species (Casado and Heredia, 1999; Tsubaki et al., 2013; Diarte et al., 2019). Numerous genes involved in wax biosynthesis have been identified, nevertheless, although some transporters have been suggested, transport mechanisms from the cytoplasm to the cuticle are still unclear and further research is needed (Kunst and Samuels, 2003; Yeats and Rose, 2013; Thimmappa et al., 2014; Bhanot et al., 2021).

Another component of the plant cuticle that has traditionally received little attention is the polysaccharide fraction derived from the plant CW. Cellulose, hemicellulose and pectin are the main constituents of the polysaccharide fraction of plant cuticles (López-Casado et al., 2007; Guzmán et al., 2014; Benítez et al., 2021). Therefore, and strictly speaking, the plant cuticle can be considered as a cutinized cell wall (Domínguez et al., 2011; Guzmán et al., 2014).

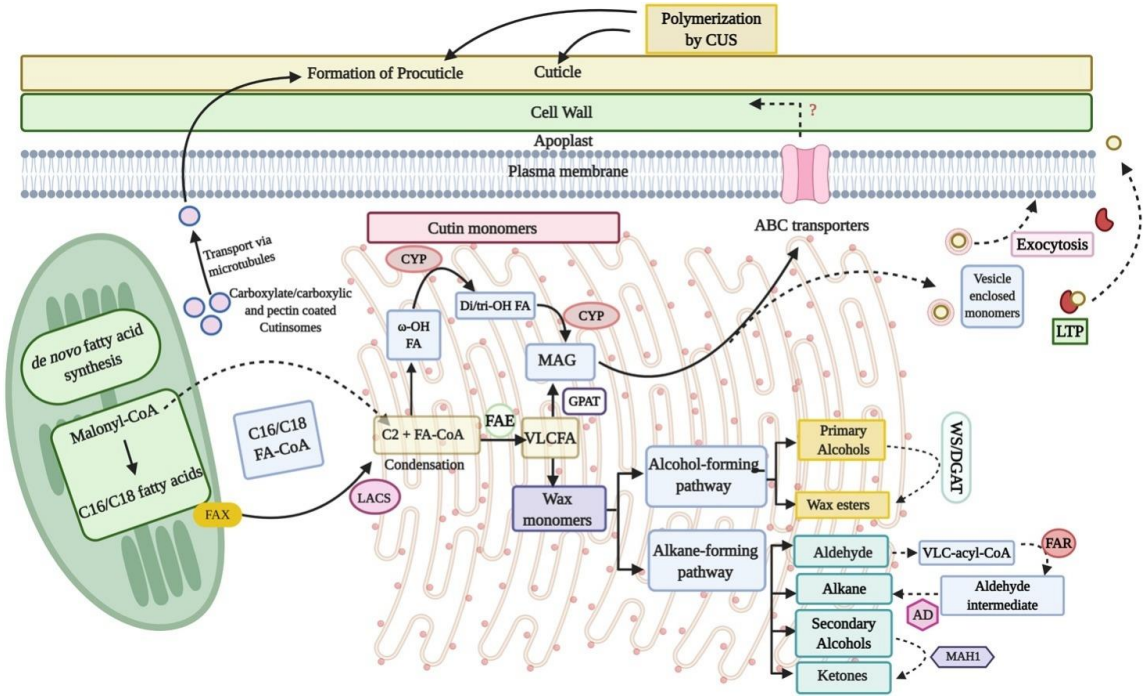

Figure 1.2. Schematic representation of the biosynthesis and transport of cutin and wax monomers in plants. CUS: cutin synthase; ABC transporters: ATP binding cassette transporters; FA-CoA: Fatty acyl CoA; CYP: cytochrome P450 monooxygenases family; LACS: long chain acyl-CoA synthetases; MAG: monoacylglycerol; GPAT: glycerol-3-phosphate: acyl-CoA acyltransferases; VLCFA: very long chain fatty acid; FAE: fatty acid elongase; LTP: lipid transfer protein; WS/DGAT: wax synthase/acyl–CoA: diacylglycerol acyltransferase; VLC-acyl-CoA: very long chain-acyl-CoA; FAR: fatty acyl–CoA reductase; AD: aldehyde decarbonylase; MAH1: midchain alkane hydroxylase 1. Reprinted with permission from (Bhanot et al., 2021). Copyright 2021 *Environmental and Experimental Botany* ©.

Finally, phenolic compounds, plant secondary metabolites with a phenol group in their structure, are also present in the plant cuticle. Although this fraction has not been thoroughly studied in most species, *p*-hydroxybenzoic acid, cinnamic acid derivatives such as *p*-coumaric acid, ferulic acid and flavonoids have been reported in several plant species. The fluorescence emitted by some plant cuticles has been ascribed to these aromatic compounds (Fernández et al., 2011). The phenolic composition of the cuticle has been shown to differ among species and stages of development (Hunt and Baker, 1980; Ju and Bramlage, 1999; España et

al., 2014b). Moreover, a significant lignin domain has been detected in the cuticle of some gymnosperms (Kögel-Knabner et al., 1994; Reina et al., 2001).

Although the chemical conformation, modifications and location of phenolic compounds within the cuticle is still unclear, it has been postulated that cinnamic acids derivatives could be esterified to the cutin framework; while flavonoids could be aggregated as *clusters* (Domínguez et al., 2009a; Leide et al., 2018). A schematic representation of the prevailing model of the distribution of the main components in a cross section of the plant cuticle is shown in Figure 1.3.

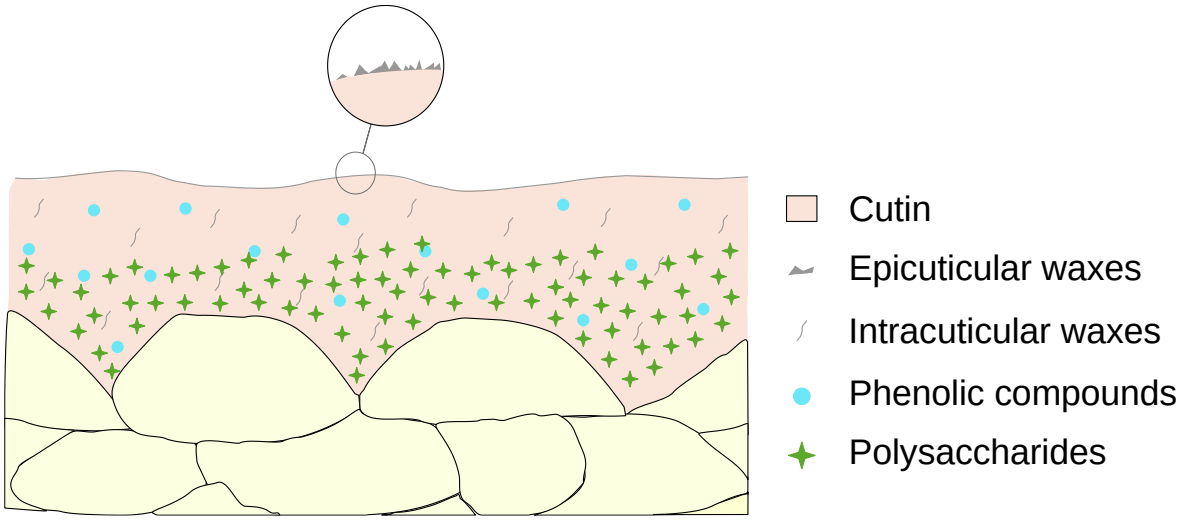

Figure 1.3. Schematic representation of the prevailing structure of a cross section of the plant cuticle.

Tomato fruit cuticle: a model plant for research

Worldwide, tomato (*Solanum lycopersicum* L.) fruit is one of the most consumed horticultural species. According to data from FAOSTAT (Food and Agriculture Organization Corporate Statistical Database) (FAOSTAT, 2020), the tomato world production in 2020 (Figure 1.4a) amounted to 186,821,216 tonnes, being China the main producer (64,768,158 tonnes) followed by India (20,573,000 tonnes). In trade terms, 7,773,934 tonnes of tomatoes were worldwide exported in

2020. Mexico was the world's largest exporter of tomato regarding both quantity and value (Figure 1.4b) (FAOSTAT, 2020).

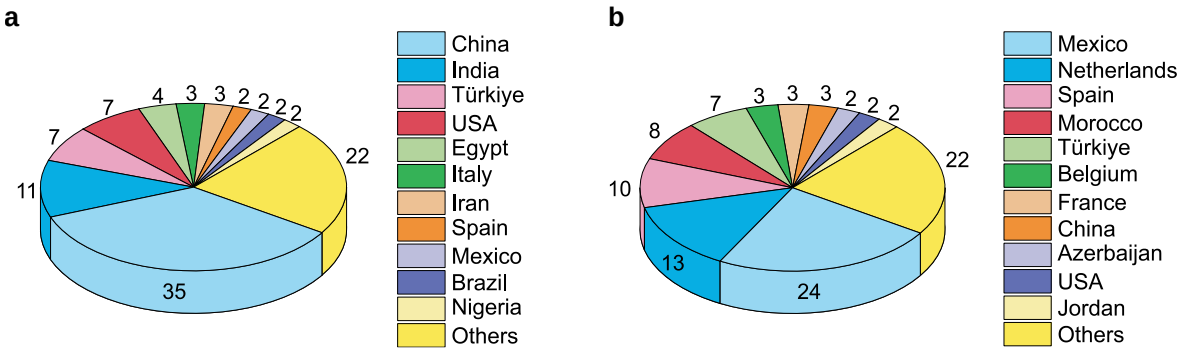

Figure 1.4. (a) World's leading tomato fruit producers ranked by produced tonnes. (b) World's leading tomato fruit exporters ranked by exported tonnes. Numbers in graphs represent percentages (%) (FAOSTAT, 2020).

Spain occupied the eighth position within the ranking of tomato producers (4,312,900 tonnes) and the third one related to exported tonnes (734,223 tonnes) and export value (1,073,643 thousand US$). Tomato was the sixth crop in Spain among agricultural production based on its gross production value (1,371,071 current thousand Standard Local Currency) (FAOSTAT, 2020).

Tomato has been used as model plant in research due to its relatively short life cycle, and its flowering is insensitivity to photoperiod, allowing seed production under variable light conditions. Additionally, it tolerates a wide range of environmental conditions, facilitating the study of the influence of various abiotic stresses. Since it is an autogamous plant, recessive mutations can be easily detected and its hybridization under controlled conditions is feasible. The tomato genome is fairly small around 783 megabases, with scarce gene duplication (The tomato Genome Consortium, 2012; Hosmani et al., 2019). Moreover, there are multiple germplasm banks with a large number of tomato entries besides an available wide collection of mutants useful for plant breeding (Petit et al., 2021). Regarding the tomato fruit cuticle, it displays a number of advantages in comparison

with cuticles from other plant species. Its absence of stomata, thickness and amount of cuticle per surface unit, and its relatively easy isolation allows the study of biomechanical and permeability properties (Martin and Rose, 2014).

The main tomato fruit cutin monomers are the dihydroxy-C_{16}-fatty acids 10,16-dihydroxyhexadecanoic acid and 9,16-dihydroxyhexadecanoic acid. Waxes are a minor component of tomato fruit cuticle representing around 3-5% of its total weight (Domínguez et al., 2009b). Long chain alkanes such as hentriacontane or nanocosane together with some triterpenoids such as α, β and δ-amyrin have been detected in tomato fruit cuticle (Vogg et al., 2004; Kosma et al., 2010). In contrast to other species where waxes are mainly accumulated in first stages of development (Peschel et al., 2007), tomato increase its wax amount along fruit development until reaching its maximum at the ripe stage (Kosma et al., 2010). This increase has been appreciated as a general increase in all types of waxes, except branched alkanes (Kosma et al., 2010). Similar proportions of cellulose, hemicellulose and pectin have been identified in both, mature green and red ripe tomato fruit cuticles (López-Casado et al., 2007; Benítez et al., 2021).

Hydroxycinnamic acid derivatives and flavonoids have been detected in tomato fruit cuticles. The amount of phenolics changed during fruit development starting with a small amount in the first stages of development and experimenting a dramatic increase during ripening (España et al., 2014b). The analysis of this phenolic fraction has revealed the presence of *p*-coumaric acid and *p*-hydroxybenzoic acid in the fruit cuticle during the whole growth and ripening period. The amount of *p*-coumaric acid in tomato fruit cuticle has been reported to be practically constant during growth and only a mild increase was observed during ripening. The content of *p*-hydroxybenzoic acid, also remained constant during development but with an important increase during ripening (España et al., 2014b). Flavonoids, specifically naringenin chalcone, only accumulated during ripening (España et al., 2014b). Naringenin chalcone is responsible for the yellow-orange colour of the tomato fruit cuticle. Although naringenin, the structural isomer of naringenin chalcone, was reported in ripe tomato cuticles (Baker et al., 1982), its identification has remained elusive.

Despite the well-known composition of tomato fruit cuticle (Hunt and Baker, 1980; Vogg et al., 2004), the lack of resolution of conventional techniques has limited the study of the distribution pattern of each compound (Fernández et al., 2016). Domínguez et al. (2009a) studied for the first time the interaction of flavonoids within the tomato fruit cuticle. Results (see Figure 1.5) showed that at low concentrations of the flavonoid, the dominant interactions were between naringenin and cutin and only weak interactions were detected among flavonoids. However, at high concentrations, flavonoids aggregated forming *clusters* (Domínguez et al., 2009a). Apart from this work, no additional research has been carried out into the *in vivo* interaction, location and conformation of phenolic compounds within tomato fruit cuticle. This information would be highly valuable to better understand its biophysical properties as well as to shed some light into the potential transport of phenolic compounds within the plant cuticle.

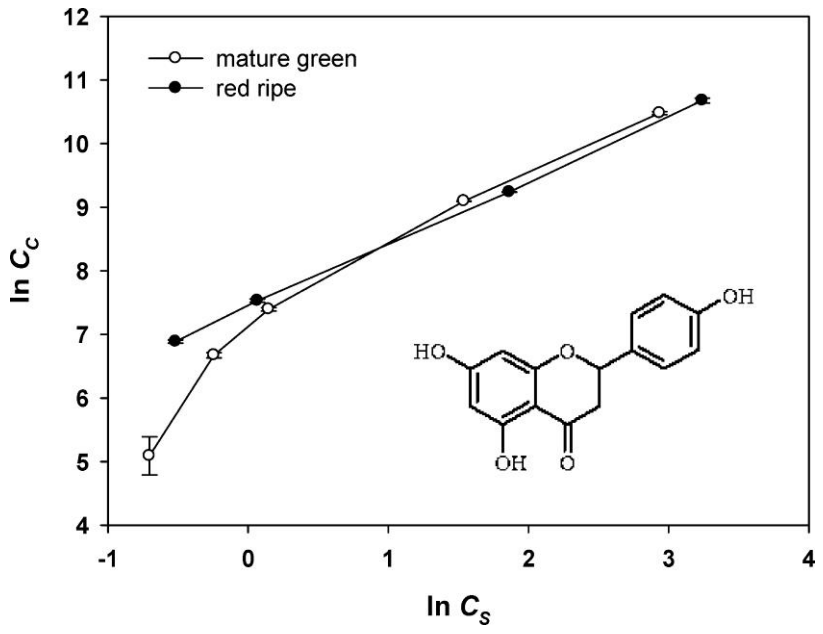

Figure 1.5. Sorption isotherms (at 25 ºC) of naringenin solution to mature green (○) and red ripe (●) tomato fruit cuticles. C_c: flavonoid concentration (g/kg) in the cuticle; *Cs* flavonoid concentration (g/kg) in the water solution at equilibrium. Reprinted with permission from (Domínguez et al., 2009a). Copyright 2009 *American Chemical Society* ©.

Biological functions of the plant cuticle

The plant cuticle represents the first barrier between the plant and the environment; consequently, it modulates and performs key functions for plants which are summarised below.

The cuticle protects plants against uncontrolled water loss and regulates plant water uptake from the environment. The cuticle is also responsible for controlling the exchange of CO_2 and solutes with the atmosphere (Schreiber and Schönherr, 2009; Lara et al., 2019). The cuticle provides remarkable mechanical support to plants, maintaining the integrity of their organs (Matas et al., 2004a; Martin and Rose, 2014), contributing to the defence against pathogens attacks, such as fungi or bacteria (Riederer, 2006; Bhanot et al., 2021), as well as against external agents including heavy rain or wind (Domínguez et al., 2017). Furthermore, the cuticle acts as a thermal regulator, reducing the impact of drastic environmental temperature on the plant (Casado and Heredia, 2001).

Epicuticular waxes can create highly slippery surfaces or with variable adherence properties, which can act as traps for insects (Eigenbrode and Jetter, 2002; Gorb et al., 2004). This layer gives the plant surface a high hydrophobicity which ascribes to the cuticle the feature of being a self-cleaning surface via the "lotus-effect" (Neinhuis and Barthlott, 1997; Bhanot et al., 2021). Epicuticular waxes have been reported to reflect and scatter ultraviolet radiation (UVR), attenuating this potentially harmful radiation (Steinmüller and Tevini, 1985; Steinmüller and Tevini, 1986; Grant et al., 1995; Tafolla-Arellano et al., 2018). On the other hand, the presence of phenolic compounds with UV absorption properties in the cuticle has been postulated as an effective photoprotection procedure, mainly filtering UVR without affecting the penetration of photosynthetically active radiation (Solovchenko and Merzlyak, 2003). The cuticle has also been shown to prevent organ fusion during plant development (Lolle et al., 1997; Tanaka et al., 2004; Leide et al., 2007; Tafolla-Arellano et al., 2018). Additionally, it has been suggested that some lipid compounds present in the plant cuticle are involved in signalling processes related to cell division and expansion and some defence mechanisms (Qin et al., 2007; Raffaele et al., 2009; Roudier et al., 2010; Nobusawa et al., 2013).

The fruit cuticle has been shown to play a role in fruit colour, brightness and firmness (Lara et al., 2019). Thus, red ripe tomatoes have an orange cuticle due to the accumulation of naringenin chalcone, whereas in pink tomatoes the cuticle is colourless due to the absence of this flavonoid (Adato et al., 2009). On the other hand, epicuticular waxes and cutin have been reported to participate in tomato fruit glossiness (Ward and Nussinovitch, 1996; Petit et al., 2014; Lara et al., 2019). Moreover, the cuticle has been shown to contribute to fruit and vegetable post-harvest and shelf-life (Lara et al., 2019).

Biophysical properties of the plant cuticle

The plant cuticle has some biophysical properties that can be modified in response to environmental conditions such as temperature, humidity or radiation.

Hydrodynamical properties

The study of the cuticle's interaction with water has been an extensively explored topic (Kannan, 1986; Fernandez and Eichert, 2009; Fernández et al., 2016). Foliar water uptake has recently gained further consideration (Dawson and Goldsmith, 2018; Berry et al., 2019; Schreel and Steppe, 2020), especially geared towards the development of foliar sprays for crop nutrition. Stomata (Burkhardt, 2010), cuticle (Fernández et al., 2021) and other specialized structures such as trichomes (Berry et al., 2019) has been reported to participate in water exchange between plant and environment. Cuticle water sorption, permeability and transpiration implied a bidirectional flux of water molecules within the plant cuticle.

Chamel et al. (1991) found similar water sorption for cuticles and dewaxed cuticles isolated from different plant species whereas their cutin presented significantly lower values. Luque et al. (1995a) by the study of water isotherms from isolated tomato fruit cuticle poposed a model to explain water permeability which included water clustering and water molecules variedly interacting with the biopolymer. Polysaccharides were suggested as main responsible for cuticle water

sorption. Besides, water clustering were corroborated (Domínguez and Heredia, 1999). Higher water sorption was retrieved for *Araucaria bidwillii* leaf cuticles rather than angiosperms, mainly assigned to the lignin and polysaccharide fraction. The water sorption-desorption was defined as a hysteretic process (Reina et al., 2001). Moreover, a higher water sorption was detected in cutan-containing species comparing with cuticles absent of cutan on its polymer matrix (Vega et al., 2021). Indeed, the accumulation of cutan within cuticle has been proposed as an adaptative mechanism to overcome drought (Boom et al., 2005).

Although the involvement of waxes in non-stomata water loss was widely agreed, there have been some discrepancies on the role of epi and intracuticular waxes in this purpose (Jetter and Riederer, 2016; Zeisler-Diehl et al., 2018; Zhang et al., 2020). Vogg et al. (2004) reported that the water transpiration within tomato fruit cuticle was mainly influenced by the length of the aliphatic compounds present in the intracuticular waxes, also influenced by the triterpenoids on this fraction. Jetter and Riederer (2016) stressed that the water transport in species which included high percentages of alicyclic compounds, mainly in the intracuticular fraction, also included the action of the epicuticular waxes. The absence of implication of triterpenoids in cuticle transpiration was evidenced in the study of young tea leaves, mostly contained very long chain fatty acids (VLCFA) on its wax coverage, and matures tea leaves whose main wax coverage components were triterpenoids (Zhu et al., 2018), under drought stress. A general increase of the wax coverage as well as variations on wax composition was observed, without altering the triterpenoid amount (Chen et al., 2020). Water transpiration resulted to be also influenced by the side of the leaves. The adaxial transpiration was found to be controlled by intracuticular waxes while the abaxial was governed by the epicuticular fraction (Zhang et al., 2020; Chen et al., 2021). Moreover, around the 70% of the total leaf transpiration was ascribed to adaxial transpiration (Chen et al., 2021). Even transpiration varied among plant organs, for instance, the transpiration was lower in leaf than in tepal cuticle for lily flower (Cheng et al., 2021).

The transport of water within the plant cuticle has not been fully resolved. It was postulated to occur through randomly distributed aqueous pores within the cuticle (Kerstiens, 2006; Schreiber and Schönherr, 2009). Fernández et al. (2017)

proposed that the water transport in intact leaves may take place through hydrophilic domains within the cuticle related to polar functional groups of cuticular compounds. In wet conditions the amount of absorbed water from the environment enough increased and hydrophilic tortuous paths along the depth of the cuticle were established by water clustering, which could be used for the diffusion of hydrophilic solutes (Fernández et al., 2017). This model was supported by an increase of ion exchange at high environmental relative humidity (RH) conditions (Schönherr, 2000; Schönherr and Luber, 2001). Tredenick and Farquhar (2021) postulated, based on mathematical modelling, three separate routes as approach of water transport within the cuticle: aqueous pores, lipophilic pathways and cellulose. Additionally, Kamtsikakis et al. (2021) introduced that the water transport within cuticle membrane was asymmetrical. Surprisingly, the process was not governed by the region enriched in polysaccharides but by the outer side of the cuticle, which was plasticized in wet conditions to prevent water loss or to absorb moisture from the environment depending on plant demands. It is worth noting that cuticle isolation could generate artefacts or lead to misleading interpretations regarding water transport within the cuticle (Fernandez and Eichert, 2009; Fernández et al., 2016).

Thermal properties

Despite its importance related to plant adaptation to varying temperatures, scarce literature has been centered on studying thermal properties of plant cuticles.

Isolated leaf and fruit cuticles from different plant species experimented an enlargement in volume with increasing temperature (Schreiber and Schönherr, 1990). These cuticles showed second-order transition temperatures within physiological range (Schönherr et al., 1979; Eckl and Gruler, 1980; Schreiber and Schönherr, 1990). Two principal thermal transitions were detected: the first one was a first order transition ascribed to wax melting, and the second one corresponded to a second order or glass transition (T_g), which made that the plant cuticle turned from a rigid macromolecular polymer at low temperatures into a rubbery phase above T_g (Schreiber and Schönherr, 1990). The fact that the T_g fell within physiological temperature could imply changes in cutin structure related to the mass exchange

between the plant and the environment (Schreiber and Schönherr, 1990), modulation on the transport within the cuticle, and/or alteration of plant organ resistance against mechanical injuries (Domínguez et al., 2011). The study of thermal behavior of cutin revealed that the increase in volume was even higher than the observed for cuticles, suggesting that polysaccharides limited cuticle expansion (Schreiber and Schönherr, 1990).

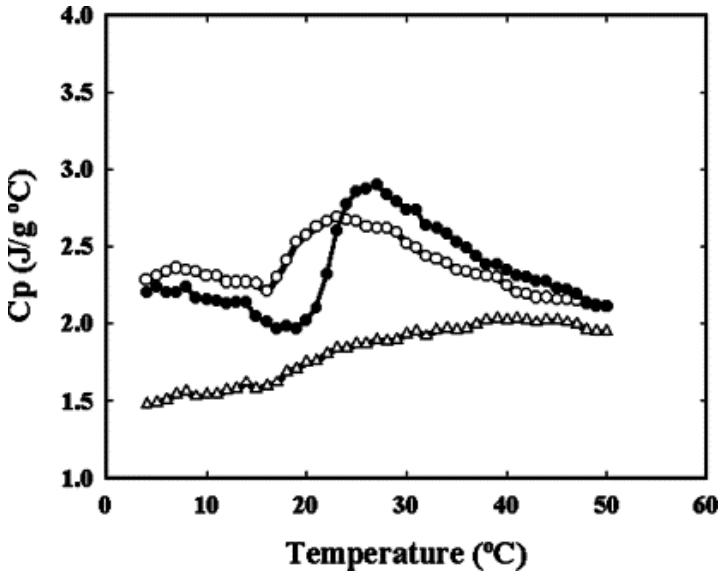

Figure 1.6. The temperature dependence of the C_p of a cutin from a young stage of development of tomato fruit cuticle (●), same cutin after absorbing water up to 5.5% of its dry weight (○) and cutin from a red ripe tomato (Δ). C_p values were estimated using differential scanning calorimetry (DSC). C_p: specific heat capacity. Reprinted with permission from (Matas et al., 2004b). Copyright 2004 *Thermochimica Acta* ©.

Matas et al. (2004b) registered the specific heat capacity (C_p), amount of heat that any substance needs to increase 1ºC its temperature per mass unit, of cutin and cuticles isolated from different stages of development of tomato fruit cuticles (Matas et al., 2004b). It revealed that their thermal behavior varied along fruit development. C_p values of red ripe tomato fruit cuticle and its isolated cutin lightly increased with temperature, not showing any evident T_g (Figure 1.6). It may be due to waxes could difficult the glass transition as well as the structural rearrangement

of the cutin matrix during the flavonoid incorporation (Matas et al., 2004b). Contrarily, samples isolated from young stages displayed a drastic positive slope characteristic of a T_g (Figure 1.6) (Matas et al., 2004b). The C_p value for cutin was 2-2.5 J/K·g, a high value in comparison with other plant components such as cellulose with a C_p of 1.5 J/K·g (Boraston, 2005). This preliminary study opened new insights to an in-depth exploration of the role of cuticle components in thermal properties.

The degree of hydration was reported to influence T_g of plant cuticles (Lendzian and Kerstiens, 1991). A dry cuticle is rigid whereas in wet conditions it turns into a softer conformation. The T_g of cutin from a young stage of development of tomato fruit was shifted towards lower temperature (16.3 ºC) after absorbing water up to 5.5 % of its dry weight (Figure 1.6) (Matas et al., 2004b).

Mechanical properties

During fruit development, the plant cuticle requires to combine extensibility and stiffness to sustain plant growth and overcome mechanical constraints (Reynoud et al., 2023). The standard mechanical curve of a plant cuticle (Figure 1.7) displayes a biphasic behaviour: at low strains, it behaves as an elastic material (high slope in the force–strain diagram) deforming itself immediately upon stress application and restoring its initial state after removing the stress. At higher strains, it acts as time-dependent plastic polymer (lower slope). Consequently, the plant cuticle can be considered as a viscoelastic material (Petracek and Bukovac, 1995).

Differences in mechanical properties of leaf and fruit cuticles were observed among different plant species. Changes in the proportion of cuticle compounds, cutin composition or content and cross-linking of phenolics were proposed as potential triggering of these differences (Wiedemann and Neinhuis, 1998; Marga et al., 2001; Matas et al., 2004a; Edelmann et al., 2005; Knoche and Peschel, 2006; Khanal and Knoche, 2014). The mechanical properties of the plant cuticle have been reported as adaptative mechanisms to overcome varying environmental conditions; for instance, the cuticle from *Yucca* grown in desserts showed a

pronounced elastic behaviour, contrary to the cuticle from *Hedera helix* cultivated in temperate climate which behaved as a viscoelastic and ductile polymer (Wiedemann and Neinhuis, 1998; Skrzydeł et al., 2021).

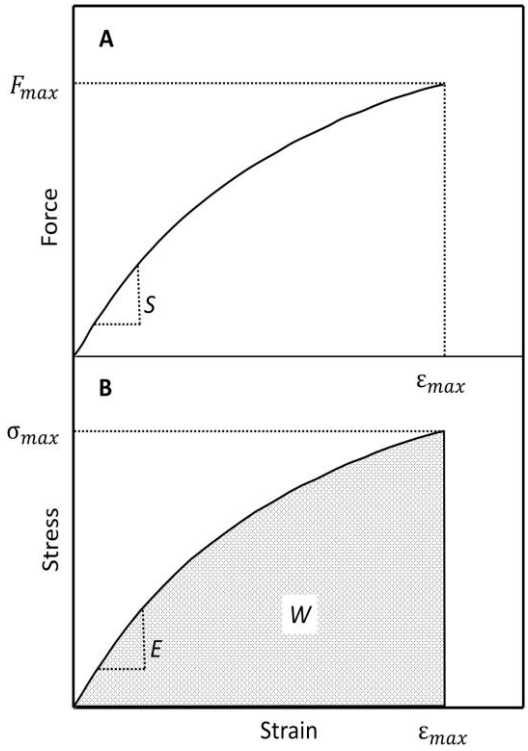

Figure 1.7. Classic (A) Force-Strain and (B) Stress-Strain curves obtained from a uniaxial tensile test of a plant cuticle used to calculate main mechanical parameters. The stiffness (*S*) and the modulus of elasticity (*E*) are the slopes of the Force-Strain and Stress-Strain plots, respectively; the maximum force (F_{max}), maximum strain (ε_{max}) and maximum stress (σ_{max}) represent the force, strain and stress at failure; the work of fracture (*W*) is the area under the stress–strain curve. Reprinted with permission from (Khanal and Knoche, 2017). Copyright 2017 *Journal of Experimental Botany* ©.

Effects of fruit development on mechanical properties have only been explored in tomato fruit cuticles. Bargel and Neinhuis (2005) studied exocarps and cuticles from different stages of development of tomato fruit. The modulus of elasticity, strength and failure strain tend to be generally higher for fruit peels than isolated cuticles, excepting for the red ripe stage. The modulus of elasticity reported for both tissues, exocarps and cuticles, usually increased during ripening while the

strength and strain to failure used to decrease along same period (Bargel and Neinhuis, 2005). Nonripening mutants (*nor*) displayed almost linear stress-strain curves during fruit development and ripening, which significatively differed from wild type fruits. Changes in composition and cross-linking of the cutin, alteration of ethylene production as well as impairment in phenolic compounds biosynthesis were postulated as potential triggering of these differences (Bargel and Neinhuis, 2004). The viscoelastic behaviour of the plant cuticle has been attributed to the cutin (López-Casado et al., 2007; Lopez-Casado et al., 2010; Takahashi et al., 2012; Khanal et al., 2013), whereas elasticity was related to polysaccharides in tomato fruit (López-Casado et al., 2007; Lopez-Casado et al., 2010) and to polysaccharides, waxes and cutan for mangrove leaves (Takahashi et al., 2012). Flavonoids gave stiffness, increased the breaking stress, decreased strain and extended the elastic component of the plant cuticle (Adato et al., 2009; Domínguez et al., 2009b; España et al., 2014a; Lara et al., 2019). The study of leaves from different plant species revealed that the role of wax amount linearly correlated with stiffness and maximum strain, hence waxes were suggested to translate reversible elastic into irreversible plastic strain (Khanal et al., 2013). In Fuyu Persimmon fruit cuticles, a nanocomposite formed by the interaction of cutin and triterpenoids, main component of its wax fraction, was suggested to function as nanofiller (Tsubaki et al., 2013). Regarding external agents, temperature and RH negatively correlated with plant cuticle stiffness and strength; while it positively correlated with cuticle extensibility (Khanal and Knoche, 2017).

Some relevant findings on mechanical properties have been recently reported studying different stages of development of tomato fruit cuticle. Dynamic mechanical analysis (DMA) revealed that the viscoelasticity of the cuticle raised while increasing the amount of phenolics even within the elastic phase. It could be explained ascribing to phenolics the compatibilizers role between cutin and polysaccharides. The major accumulation of phenolic compounds during ripening was responsible of the change from an elastic region to a more rigid one in the cuticle (Benítez et al., 2021). Besides, an in-depth nanomechanical analysis of tomato fruit cuticle revealed that the elastic modulus increased from the inner to the outer side of the cuticle from 15 to 40 days after anthesis (daa), yet including a cutin-enriched central furrow in the middle of pegs with the lowest elastic modulus

(Reynoud et al., 2023). It agreed with the reported potential role of the area above pegs as support for mechanical stresses in plants (Knoche and Lang, 2017).

Electrical properties

Schönherr and Bukovac (1973) reported for the first time that plant cuticle could exchange ions. This capacity was mainly ascribed to the presence of polysaccharides and to a minor extent to cutin. Two types of interplanar spaces were found among hydrophobic layers within the amorphous cutin matrix of tomato fruit cuticle. The largest one (around 1 nm of separation), region rich in hydroxyl groups from aromatics, is large enough to host ions within the cuticle (Luque et al., 1995b).

The plant cuticle, in an aqueous environment, displayed an electro-kinetic gradient along its depth (Heredia and Benavente, 1991; Tyree et al., 1991). Almost no charge was detected in the outer side of the cuticle; by contrast, a net negative charge was measured in the inner side (Heredia and Benavente, 1991). The homogenous dielectric properties of cutin isolated from tomato fruit cuticle pointed to polysaccharides as the main responsible of this negative charge (Benavente et al., 1998; Domínguez et al., 2011). The asymmetrical charge distribution within the cuticle could have multiple implications in ecotoxicology, transpiration or application of agrochemicals, among others (Kerstein, 1996; Domínguez et al., 2011).

Impedance measurements of modified (Na^+ and Ca^{+2} forms) and control tomato fruit cuticles in wet and dry conditions inferred that while dry cuticles poorly conducted electricity, wet cuticles increased their conductivity 10 times, almost independently of their modification. Moreover, the modified cuticles displayed that ionic hydration favoured protonic conductivity (Ramos-Barrado et al., 1993).

The plant cuticle together with the adjacent cellular tissues has been proposed as an integrated triboelectric generator conductor, which could transform mechanical stimuli into electricity (Meder et al., 2018).

Interconnection among biophysical properties

A connection among the thermal, mechanical and hydrodynamical properties has been observed (summarized in Figure 1.8). A wet cuticle had a lower T_g than a dry cuticle linking the hydrodynamical and thermal properties: more water, lower transition temperature from a rigid to a viscous material. Hydrodynamical and mechanical properties were also intimately linked: a higher RH induced viscoelasticity while in reverse a lower RH evoked stiffness. Finally, thermal was related to mechanical properties in the sense that cuticle performed as a stiff polymer at temperatures below the T_g while it was viscoelastic at higher temperatures than the T_g. Understanding these interactions could have applications for different purposes, for instance identification of the most appropriate post-harvest storage (Lara et al., 2019).

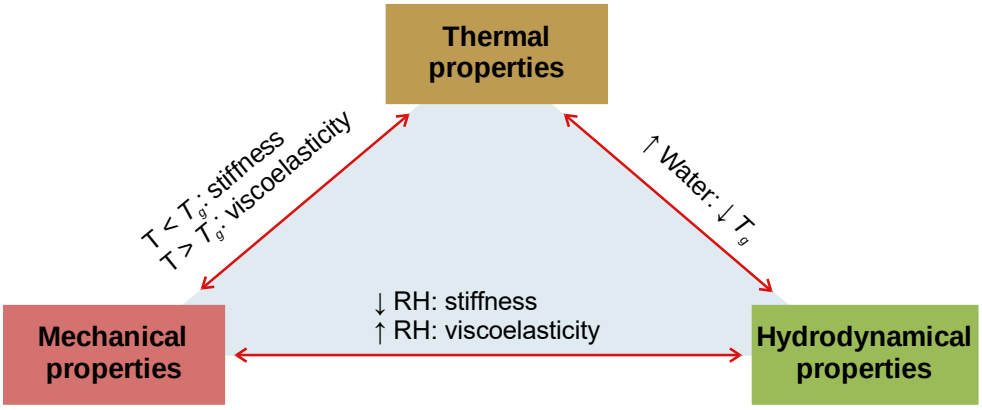

Figure 1.8. Reciprocal relationships between biophysical (mechanical, hydrodynamical and thermal) properties. RH: relative humidity; T_g: temperature of glass transition. Adapted with permission from (Domínguez et al., 2011). Copyright 2011 *New Phytologist* ©.

Photoprotection in plants: the key role of phenolic compounds

Between 7-9% of the total radiation that reaches the Earth corresponds to UVR (400-100 nm) (Solovchenko, 2010). This energetic radiation can be subdivided into three regions: UV-A (400–315 nm), UV-B (315-280 nm) and UV-C (280-100 nm). Thanks to the ozone layer only a small proportion of this UVR reaches the biosphere: the UV-C is almost completely blocked while around the 5 and 95 % of UV-B and UV-A respectively, reaches the Earth (Lacis and Hansen, 1974; Frederick et al., 1989). Plants are photoautotrophic organisms; hence the absorption of solar radiation, including UV-A and UV-B, is essential to efficiently carry out photosynthesis. Nevertheless, an overexposure to UVR could imply several deleterious effects in plant morphology, physiology and biochemistry (Bornman et al., 2019). Since plants are sessile organisms, they needed to develop some mechanisms to acclimatize to environmental changes including variations on incident radiation.

A first attempt to measure epidermal UV-B transmittance was carried out with peeled epidermises from different species. A relationship was observed between UV-B transmittance and latitude, with tropical species displaying lower epidermal transmittance than those from higher latitudes (Robberecht et al., 1980). The accumulation of UV-absorbing compounds, such as phenolics and flavonoids, within plant tissues was agreed to be the main responsible of this UVR attenuation and consequently, the primary mechanism involved in plant photoprotection (Caldwell et al., 1983; Tevini et al., 1991; Day, 1993; Awad et al., 2000; Bassman, 2004; Agati and Tattini, 2010; Neugart and Schreiner, 2018). Their accumulation also boosted the plant antioxidant capacity (Agati and Tattini, 2010; Neugart and Schreiner, 2018). Phenolic compounds are plant secondary metabolites which participate in multiple physiological roles acting as pigments, anti-inflammatory, anticarcinogenic, antioxidant, antibacterial and photoprotector, among others. Structurally, they consist of a hydroxylated aromatic ring which can be variedly substituted to derive in different groups including phenolic acids, flavonoids, tannins, lignans, and stilbenes (Zhang et al., 2022a). Phenolic compounds were defined as effective screening compounds due to UVR induced their biosynthesis, their accumulation implied photoprotection, they were long-term photostable and resulted to be

minimally influenced by environmental stresses (Cockell and Knowland, 1999; Munné-Bosch et al., 2001; Solovchenko, 2010). The absorption spectrum of a phenolic compound usually displays two bands: one centred around 280 nm assignable to their aromatic nature; and another one shifted towards higher wavelengths (within 300–360 nm range). Some variations could be observed depending on the environment. The molar absorption coefficient of phenolics involved in photoprotection and photodamage were ordinarily between 10 to 35 $mM^{-1}cm^{-1}$ (Solovchenko, 2010). The complementarity of the absorption spectra of phenolic compounds allowed to cover a wide range of the electromagnetic spectrum by combination of different classes of phenolics: for instance, hydroxycinnamic acids mainly screened UV-B radiation while flavonoids showed its maximum of absorption in the UV-A region (Agati and Tattini, 2010; Agati et al., 2013).

Beyond the accumulation of screening compounds, plants developed additional mechanisms to cope with radiation. Anatomical structures such as waxes or trichomes have been postulated as UVR cut-off filters in some plant tissues (Ward and Nussinovitch, 1996; Karabourniotis et al., 1999; Karabourniotis and Bornman, 1999) as well as chloroplast relocation under blue/UV-A enriched light has been described as an adaptative mechanism to light screening (Llorens et al., 2020).

Krauss et al. (1997) registered the transmittance spectra of isolated cuticles, mainly from leaves but also including some fruits. The plant cuticle blocked a big proportion of the incident UVR, especially the UV-B range. Further on, Solovchenko and Merzlyak (2003) reached similar conclusions in apple fruit cuticle also including reflectance measurements. Consequently, it was proved that a significant fraction of the incident UVR is filtered by plant cuticle and just a finely screened radiation was transmitted to inner tissues such as epidermal and hypodermal cells (Krauss et al., 1997; Solovchenko and Merzlyak, 2003). These underneath layers were not devoid of UV-shielding compounds. Indeed, flavonoids were detected not only in superficial tissues such as vacuoles and cell walls of epidermal cells or trichomes, but also in vacuoles of mesophyll cells and in chloroplasts (Agati et al., 2009; Agati and Tattini, 2010). Heterogeneity on UV filtering capability was observed among epidermis components (Barnes et al., 2015), leaf stages of development (Wagner et al., 2003);

sun and shade leaves (Barnes et al., 2013) or even comparing measurements of same plant tissue at different times of the day (Barnes et al., 2008).

An in-depth understanding of the influence of UV-B radiation on phenolics accumulation was successfully achieved since the identification of the UV RESISTANCE LOCUS 8 (UVR8) in *Arabidopsis thaliana* as photoreceptor of the UV-B radiation (Rizzini et al., 2011). It has been reported that UVR8 controlled the transcription of over a hundred genes involved in multiple functions (Jenkins, 2014); one of the main was the up-regulation of the phenylpropanoid synthetic route, promoting the biosynthesis and accumulation of UV-shielding compounds within plant tissues. UVR8 has also been detected in other plant species and within different plant tissues, not being exclusively confined to the epidermis, but also being present in the mesophyll tissues (Tossi et al., 2019). Recently, it has been proved that UVR8 was also involved in the perception of UV-A radiation, in conjunction with other proteins (Rai et al., 2020; Rai et al., 2021).

Apart from the promotion of phenolic biosynthesis, UV-B radiation has been related to DNA repair, development of beneficial plant morphological changes and promotion of the biosynthesis of secondary metabolites involved in plant protection against herbivores and pathogens (Bornman et al., 2019). UV-B could even favour the cross-tolerance to some abiotic factors such as drought (Robson et al., 2015) or extreme temperatures (Maja et al., 2016). Nevertheless, an overexposure to UV-B radiation may have fatal consequences for plants such as DNA disruption, impairment on the photosynthetic machinery, oxidative damage by the generation of ROS (reactive oxygen species), emergence of detrimental morphological changes (Neugart and Schreiner, 2018) and alteration of plant-pathogens interaction (Vanhaelewyn et al., 2020). UV-A radiation has been much less examined due to difficulties in adapting the experimental set up to this range. It has been reported that UV-A radiation affected the photosynthetic activity, plant morphology, plant growth and phenolic content (Verdaguer et al., 2017); nevertheless, additional studies are required to draw clear conclusions on this field (Neugart and Schreiner, 2018).

Further research on the implication of some plant tissues in photoprotection would provide highly useful information to better understand *planta* adaptations after

conquering land. Moreover, the mechanism by which phenolic compounds block much of the UV incident radiation is still a conundrum.

Shikimic acid pathway: synthesis of phenolic compounds

The shikimate pathway, which occurs in plastids, is the primary source of phenolic compounds present in plants. Concretely, this route produces aromatic amino acids among which L-phenylalanine (L-Phe) and L-tyrosine (L-Tyr) serve as precursors for different types of phenolic compounds: cinnamic acids, flavonoids, anthraquinones, coumarins, etc (Cheynier et al., 2013). It is a highly preserved biosynthetic route which can be found in fungi, bacteria, and plant (Tohge et al., 2013).

The shikimate pathway for L-Phe biosynthesis (precursor of a vast number of phenolics present in plants, see Figure 1.9a) starts with an aldol condensation between phosphoenolpyruvate (PEP) and D-erythrose 4-phosphate (E4P) enzymatically catalysed by 3-deoxy-D-arabinoheptulosonate 7-phosphate synthase (DAHPS). Then, the enzyme 3-dehydroquinate synthase (DHQS) carries out an internal rearrangement of the 3-deoxy-D-arabinoheptulosonate 7-phosphate (DAHP) ring resulting in 3-dehydroquinate. This molecule consecutively suffers processes of dehydration, reduction and phosphorylation catalysed by 3-dehydroquinate dehydratase (DHQD), shikimate dehydrogenase (SD) and shikimate kinase (SK) respectively. The outcoming shikimate 3-phospate (S3P) performs a condensation reaction with another molecule of PEP mediated by 5-enolypyruvylshikimate 3-phosphate synthase (EPSPS). Next, a trans-1,4 elimination of phosphate from 5-enolypyruvylshikimate 3-phosphate (EPSP) by chorismate synthase (CS) results in chorismate. From this molecule until L-Phe three more steps are required: a Claisen rearrangement by chorismate mutase followed by transamination of prephenate *via* prephenate aminotransferase (PAT) and finally the decarboxylation and dehydration of the arogenate catalysed by arogenate dehydratase (ADT) (Tohge et al., 2013; El-Azaz et al., 2020).

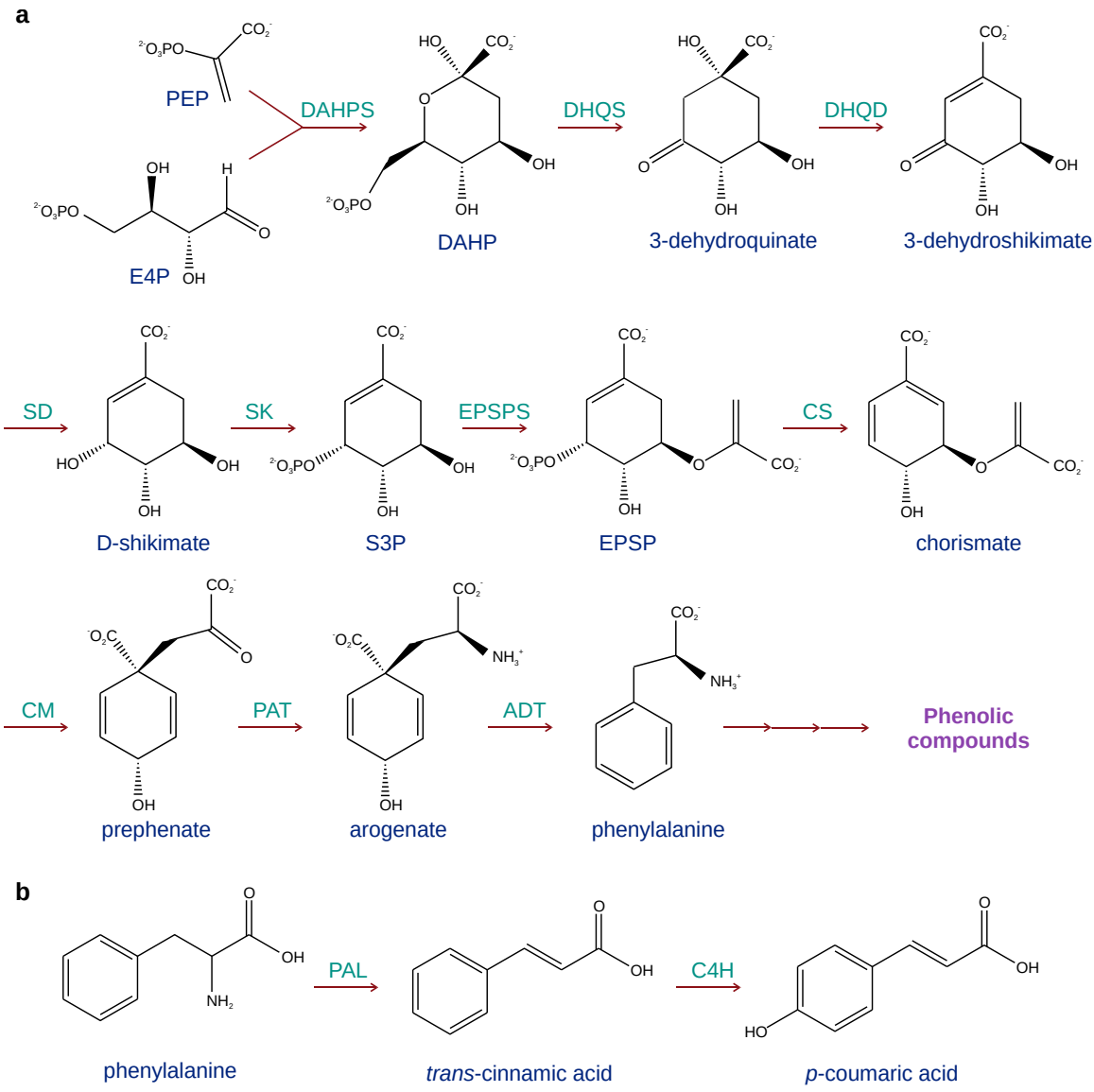

Figure 1.9. (a) Shikimate pathway responsible of phenolic compounds synthesis (derived from phenylalanine) *via* secondary metabolism in plants. (b) Biosynthesis pathway of *p*-coumaric acid from phenylalanine. The names of compounds and enzymes are shown in blue and green respectively. PEP: phosphoenolpyruvate; E4P: D-erythrose 4-phosphate; DAHPS: 3-deoxy-D-arabinoheptulosonate 7-phosphate synthase; DAHP: 3-deoxy-D-arabinoheptulosonate 7-phosphate; DHQS: 3- dehydroquinate synthase; DHQD: 3-dehydroquinate dehydratase; SD: shikimate dehydrogenase; SK: shikimate kinase; S3P: shikimate 3-phospate; EPSPS: 5-enolpyruvylshikimate-3-phosphate synthase; EPSP: 5-enolpyruvylshikimate-3-phosphate; CS: chorismate synthase; CM, chorismate mutase; PAT, prephenate aminotransferase; ADT, arogenate dehydratase; PAL, phenylalanine ammonia-lyase; C4H, cinnamate-4-hydroxylase. Adapted with permission from (Maeda and Dudareva, 2012; Li et al., 2018). Copyright 2012 *Annual Review of Plant Biology* © and Copyright 2018 *Molecules* ©.

One of the numerous metabolites derived from this route is *p*-coumaric acid. It may act as anti-oxidant, anti-inflammatory and antibacterial agent, having been employed in multiple fields such as pharmacy, nutrition or material science (Li et al., 2018). Further, it is a key molecule in the phenolic compounds synthetic route. Its modification allowed to obtain multiple derivatives such as alternative phenylpropanoids, anthocyanins, stilbenes and flavonoids. To synthetise *p*-coumaric acid from L-Phe (see Figure 1.9b) a first step based on the ammonium group loss *via* an E2 elimination catalysed by phenylalanine ammonia-lyase (PAL) is needed. The resulting *trans* cinnamic acid is hydroxylated at the *para* position by the *trans*-cinnamic acid 4-hydroxylase (C4H) bringing *p*-coumaric acid. Some PAL enzymes can also employ L-Tyr as starting substrate to reach *p*-coumaric acid (Maeda and Dudareva, 2012; Li et al., 2018).

Secondary metabolites such as phenolic compounds are synthesized by plants in response to multiple challenges. Phenolic compounds are rarely free molecules in living plant tissue; they are usually conjugated to other plant molecules (Harborne, 1979). At the concentration required to efficiently exert their role, these metabolites may be cytotoxic, interfering with the function of some cell proteins (Zhang et al., 2022b). Plants have employed different mechanism to reduce or remove this self-toxicity. They excrete these toxics to apoplast, sequester them into vacuoles or modify them into inactive less-toxic forms (Sirikantaramas et al., 2008; Shitan, 2016). Glycosylation, catalysed by glycosyltransferase, has been postulated as an efficient mechanism to reduce the toxicity of endogenous substances and xenobiotics as well as to improve the solubility of phenolics in water. These inactive less toxic glycosides could be stored in vacuoles (Li et al., 2021) until being released to perform their function as toxic aglycone (Morant et al., 2008; Zhang et al., 2022b). The vast majority of screening compounds are located in superficial tissues such as the plant cuticle, in some cases reported esterified to hydroxyl fatty acids of cutin (Cheng et al., 2013; Renault et al., 2017; Reynoud et al., 2021), epidermis and trichomes or pubescence if present (Solovchenko, 2010; Espinosa-Leal et al., 2022).

Flavonoids and *naringenin chalcone-naringenin isomerization*

Flavonoids are usually accumulated in vacuoles in form of glycosides soluble in water (Davies et al., 2020); yet, they can be also excreted to other plant tissues. The biosynthesis, conformation, specific location and transport of flavonoids located on the surface of plants are poorly understood. They have been mainly detected as aglycones, and frequently with high degree of substitution through the incorporation of methoxy groups. These modifications change the nature of the flavonoids turning them into a more hydrophobic molecules to be secreted to superficial tissues (Onyilagha, JC, Grotewold, 2004). Although their transport is still unclear, some ABC transporters have been reported as carrier of flavonoids to the vacuoles and among cells (Yazaki, 2006; Domínguez et al., 2015a). The use of vesicles, membrane transporters, glutathione S-transferase (GST), or even a conjunction of these three have been postulated as plausible mechanisms to explain the transport of flavonoids to plant surface (Zhao, 2015).

Naringenin chalcone has been the only flavonoid identified in tomato fruit cuticle, although some earlier reports suggested the presence of its isomer naringenin too (Baker et al., 1982). Nevertheless, phenolic compounds fraction only could be analysed after cutin depolymerization around 60 ºC and basic pH. These conditions could affect *in vivo* conformation of flavonoids even enable isomerisation from naringenin (at acid pH) to naringenin chalcone (at basic pH); consequently, it has been traditionally difficult to selectively distinguish them (Domínguez et al., 2015b). The *p*-coumaric acid requires to be converted into its corresponding CoA thiol ester *via* 4-coumarate:CoA ligase (4CL) (Ehlting et al., 1999). CHALCONE SYNTHASE (CHS), belonging to type III of polyketide synthases, is the first enzyme in flavonoid biosynthetic pathway (Figure 1.10). Its mechanism action has been studied in detail by (Ferrer et al., 1999). Briefly, it sequentially carries out the iterative condensation of one molecule of *p*-coumaroyl-CoA with three molecules of malonyl-CoA. The initial step of each condensation consists in the decarboxylation of malonyl-CoA generating an anion which acts as nucleophile to elongate the carbon skeleton. The reached tetraketide intermediate is transformed to naringenin chalcone *via* Claisen condensation, which means intramolecular cyclization

followed by aromatization (Ferrer et al., 1999). A large number of flavonoids derived from naringenin (Austin and Noel, 2003).

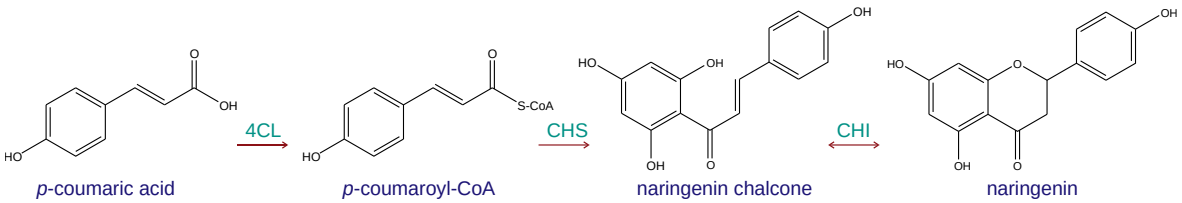

Figure 1.10. Biosynthesis pathway for the flavonoid isomers naringenin and naringenin chalcone from *p*-coumaric acid. The names of compounds and enzymes are shown in blue and green respectively. 4CL: 4 coumarate:coenzyme A ligase; CHS: chalcone synthase; CHI: chalcone isomerase.

The slow non-stereospecific spontaneous cyclization of naringenin chalcone to naringenin in solution has been mentioned by some authors (Jez and Noel, 2002). In solution an enantiomeric mixture of both R and S isomers was obtained by spontaneous isomerization; nevertheless, the stereospecific conversion mediated by the CHI synthesized almost exclusively the biologically active *(2S)*-naringenin isomer with a ratio preference of 100,000:1 against the R-isomer (Noel et al., 2000).

Two approaches have been postulated to elucidate the catalytic mechanism of the CHI. The first one was based on a nucleophilic catalysis where a residue from the active site generated a covalent intermediate to be liberated after a bimolecular nucleophilic substitution in the hydroxyl group involved in the ring closure of the naringenin chalcone (Hahlbrock et al., 1970; Noel et al., 2000); the second postulation, backed by the structure of the CHI, supported an acid-base catalysis through an enol intermediate (Boland and Wong, 1979; Jez and Noel, 2001). In this second model, two solid interaction networks are required. One is initiated by an H bonding between the carbonyl group of the flavonoid and a water molecule interacting at the same time with Tyr106. This network was completed by additional H bonding stabilizations involving another molecule of water and four additional amino acids (Thr48, Ala49, Lys97 and Tyr152). The other interaction network employs Asn113 and Thr190 interacting with the hydroxyl group of the chalcone which performs the ring closure (2´-OH). The deprotonation of this 2´-OH is required to form an oxyanion which intramolecularly attack the α,β-unsaturated double bond of the naringenin chalcone following a Michael addition reaction. At this point a water

molecule plays the role of acid stabilizing the enolate intermediate which achieves the structure of the *(2S)*-naringenin after its tautomerisation (Jez and Noel, 2001).

References

Adato A, Mandel T, Mintz-Oron S, Venger I, Levy D, Yativ M, Domínguez E, Wang Z, De Vos RCH, Jetter R, et al (2009) Fruit-surface flavonoid accumulation in tomato is controlled by a SlMYB12-regulated transcriptional network. *PLOS Genet* **5**: e1000777

Agati G, Brunetti C, Di Ferdinando M, Ferrini F, Pollastri S, Tattini M (2013) Functional roles of flavonoids in photoprotection: new evidence, lessons from the past. *Plant Physiol Biochem* **72**: 35–45

Agati G, Stefano G, Biricolti S, Tattini M (2009) Mesophyll distribution of antioxidant flavonoid glycosides in Ligustrum vulgare leaves under contrasting sunlight irradiance. *Ann Bot* **104**: 853–861

Agati G, Tattini M (2010) Multiple functional roles of flavonoids in photoprotection. *New Phytol* **186**: 786–793

Austin MB, Noel JP (2003) The chalcone synthase superfamily of type III polyketide synthases. *Nat Prod Rep* **20**: 79–110

Awad MA, De Jager A, Van Westing LM (2000) Flavonoid and chlorogenic acid levels in apple fruit: Characterisation of variation. *Sci Hortic* **83**: 249–263

Baker EA, Bukovac MJ, Hunt GM (1982) Composition of tomato fruit cuticle as related to fruit growth and development. *In* D. Cutler, KL Alvin, C. Price, eds, *The plant cuticle*. Academic Press, pp 33–44

Bargel H, Neinhuis C (2004) Altered tomato (*Lycopersicon esculentum* Mill.) fruit cuticle biomechanics of a pleiotropic non ripening mutant. *J Plant Growth Regul* **23**: 61–75

Bargel H, Neinhuis C (2005) Tomato (*Lycopersicon esculentum* Mill.) fruit growth and ripening as related to the biomechanical properties of fruit skin and isolated cuticle. *J Exp Bot* **56**: 1049–1060

Barnes PW, Flint SD, Ryel RJ, Tobler MA, Barkley AE, Wargent JJ (2015) Rediscovering leaf optical properties: New insights into plant acclimation to solar UV radiation. *Plant Physiol Biochem* **93**: 94–100

Barnes PW, Flint SD, Slusser JR, Gao W, Ryel RJ (2008) Diurnal changes in epidermal UV transmittance of plants in naturally high UV environments. *Physiol Plant* **133**: 363–372

Barnes PW, Kersting AR, Flint SD, Beyschlag W, Ryel RJ (2013) Adjustments in epidermal UV-transmittance of leaves in sun-shade transitions. *Physiol Plant* **149**: 200–213

Bassman JH (2004) Ecosystem consequences of enhanced solar ultraviolet radiation: Secondary plant metabolites as mediators of multiple trophic interactions in terrestrial plant communities. *Photochem Photobiol* **79**: 382–398

Benavente J, Ramos-Barrado JR, Heredia A (1998) A study of the electrical behaviour of isolated tomato cuticular membranes and cutin by impedance spectroscopy measurements. *Colloids Surfaces A Physicochem. Eng. Asp*. **140**: 333–338

Benítez JJ, Guzmán-Puyol S, Vilaplana F, Heredia-Guerrero JA, Domínguez E, Heredia A (2021) Mechanical performances of isolated cuticles along tomato fruit growth and ripening. *Front Plant Sci* **12**: 787839

Berhin A, de Bellis D, Franke RB, Buono RA, Nowack MK, Nawrath C (2019) The root cap cuticle: A cell wall structure for seedling establishment and lateral root formation. *Cell* **176**: 1367–1378

Berry ZC, Emery NC, Gotsch SG, Goldsmith GR (2019) Foliar water uptake: Processes, pathways, and integration into plant water budgets. *Plant Cell Environ* **42**: 410–423

Bhanot V, Fadanavis SV, Panwar J (2021) Revisiting the architecture, biosynthesis and functional aspects of the plant cuticle: There is more scope. *Environ Exp Bot* **183**: 104364

Bianchi G (1995) Plant waxes. *In* Richard John Hamilton, ed, *Waxes: chemistry, molecular biology and functions*. The Oily Press, pp 175–222

Boland MJ, Wong E (1979) Mechanism of action of chalcone isomerase. *Bioorg Chem* **8**: 1–8

Boom A, Sinninge Damsté JS, De Leeuw JW (2005) Cutan, a common aliphatic biopolymer in cuticles of drought-adapted plants. *Org Geochem* **36**: 595–601

Boraston AB (2005) The interaction of carbohydrate-binding modules with insoluble non-crystalline cellulose is enthalpically driven. *Biochem J* **385**: 479–484

Bornman JF, Barnes PW, Robson TM, Robinson SA, Jansen MAK, Ballare CL, Flint SD (2019) Linkages between stratospheric ozone, UV radiation and climate change and their implications for terrestrial ecosystems. *Photochem Photobiol Sci* **18**: 681–716

Brongniart A (1830) Recherches sur la structure et sur les fonctions des feuilles. *Ann des Sci Nat 1st Ser* **21**: 420–457

Brongniart A (1834) Sur l´épiderme des plantes. Nouvelles recherches sur la structure de l´épiderme des vegetaux. *Ann des Sci Nat 2nd Ser* **1**: 65–71

Bruck DK, Walker DB (1985) Cell Determination During Embryogenesis in Citrus jambhiri. I. Ontogeny of the Epidermis. *Bot Gaz* **146**: 188–195

Burkhardt J (2010) Hygroscopic particles on leaves: Nutrients or desiccants? *Ecol Monogr* **80**: 369–399

Buschhaus C, Jetter R (2011) Composition differences between epicuticular and intracuticular wax substructures: How do plants seal their epidermal surfaces? *J Exp Bot* **62**: 841–853

Caldwell MM, Robberecht R, Flint SD (1983) Internal filters: Prospects for UV-acclimation in higher plants. *Physiol Plant* **58**: 445–450

Casado CG, Heredia A (1999) Structure and dynamics of reconstituted cuticular waxes of grape berry cuticle (*Vitis vinifera* L.). *J Exp Bot* **50**: 175–182

Casado CG, Heredia A (2001) Self-association of plant wax components: A thermodynamic analysis. *Biomacromolecules* **2**: 407–409

Chamel A, Pineri M, Escoubes M (1991) Quantitative determination of water sorption by plant cuticles. *Plant Cell Environ* **14**: 87–95

Chen M, Zhang Y, Kong X, Du Z, Zhou H, Yu Z, Qin J, Chen C (2021) Leaf cuticular transpiration barrier organization in tea tree under normal growth conditions. *Front Plant Sci* **12**: 655799

Chen M, Zhu X, Zhang Y, Du Z, Chen X, Kong X, Sun W, Chen C (2020) Drought stress modify cuticle of tender tea leaf and mature leaf for transpiration barrier enhancement through common and distinct modes. *Sci Rep* **10**: 6696

Cheng AX, Gou JY, Yu XH, Yang H, Fang X, Chen XY, Liu CJ (2013) Characterization and ectopic expression of a populus hydroxyacid hydroxycinnamoyltransferase. *Mol Plant* **6**: 1889–1903

Cheng G, Wang L, Wu H, Yu X, Zhang N, Wan X, He L, Huang H (2021) Variation in petal and leaf wax deposition affects cuticular transpiration in cut lily flowers. *Front Plant Sci* **12**: 781987

Cheynier V, Comte G, Davies KM, Lattanzio V, Martens S (2013) Plant phenolics: Recent advances on their biosynthesis, genetics, andecophysiology. *Plant Physiol Biochem* **72**: 1–20

Cockell CS, Knowland J (1999) Ultraviolet radiation screening compounds. *Biol Rev* **74**: 311–345

Croteau R, Kolattukudy PE (1974) Biosynthesis of hydroxyfatty acid polymers. Enzymatic synthesis of cutin from monomer acids by cell-free preparations from the epidermis of *Vicia faba* leaves. *Biochemistry* **13**: 3193–3202

Davies KM, Jibran R, Zhou Y, Albert NW, Brummell DA, Jordan BR, Bowman JL, Schwinn KE (2020) The evolution of flavonoid biosynthesis: A bryophyte perspective. *Front Plant Sci* **11**: 7

Dawson TE, Goldsmith GR (2018) The value of wet leaves. *New Phytol* **219**: 1156–1169

Day TA (1993) Relating UV-B radiation screening effectiveness of foliage to absorbing-compound concentration and anatomical characteristics in a diverse group of plants. *Oecologia* **95**: 542–550

De Giorgi J, Piskurewicz U, Loubery S, Utz-Pugin A, Bailly C, Mène-Saffrané L, Lopez-Molina L (2015) An endosperm-associated cuticle is required for Arabidopsis seed viability, dormancy and early control of germination. *PLoS Genet* **11**: e1005708

Diarte C, Lai PH, Huang H, Romero A, Casero T, Gatius F, Graell J, Medina V, East A, Riederer M, et al (2019) Insights into olive fruit surface functions: A comparison of cuticular composition, water permeability, and surface topography in nine cultivars during maturation. *Front Plant Sci* **10**: 1484

Domínguez E, España L, López-Casado G, Cuartero J, Heredia A (2009b) Biomechanics of isolated tomato (*Solanum lycopersicum*) fruit cuticles during ripening: The role of flavonoids. *Funct Plant Biol* **36**: 613–620

Domínguez E, Heredia-Guerrero JA, Heredia A (2011) The biophysical design of plant cuticles: An overview. *New Phytol* **189**: 938–949

Domínguez E, Heredia-Guerrero JA, Heredia A (2015a) Plant cutin genesis: Unanswered questions. *Trends Plant Sci* **20**: 551–558

Domínguez E, Heredia-Guerrero JA, Heredia A (2017) The plant cuticle: old challenges, new perspectives. *J Exp Bot* **68**: 5251–5255

Domínguez E, Heredia A (1999) Water hydration in cutinized cell walls: A physico-chemical analysis. *Biochim Biophys Acta - Gen Subj* **1426**: 168–176

Domínguez, E., López-Casado, G., Heredia A (2015b) Role of flavonoids in the cuticle of tomato fruit (*Solanum lycopersicum*). *In* T Higashide, ed, *Solanum lycopersicum: Production, biochemistry and health benefits*. Nova Publishers, pp 151–178

Domínguez E, Luque P, Heredia A (2009a) Sorption and interaction of the flavonoid naringenin on tomato fruit cuticles. *J Agric Food Chem* **57**: 7560–7564

Eckl K, Gruler H (1980) Phase transitions in plant cuticles. *Planta* **150**: 102–113

Edelmann HG, Neinhuis C, Bargel H (2005) Influence of hydration and temperature on the rheological properties of plant cuticles and their impact on plant organ integrity. *J Plant Growth Regul* **24**: 116–126

Ehlting J, Büttner D, Wang Q, Douglas CJ, Somssich IE, Kombrink E (1999) Three 4-coumarate:coenzyme A ligases in *Arabidopsis thaliana* represent two evolutionarily divergent classes in angiosperms. *Plant J* **19(1)**: 9–20

Eigenbrode SD, Jetter R (2002) Attachment to plant surface waxes by an insect predator. *Integr. Comp. Biol*. **42**: 1091–1099

El-Azaz J, De La Torre F, Pascual MB, Debille S, Canlet F, Harvengt L, Trontin JF, Ávila C, Cánovas FM, Turner S (2020) Transcriptional analysis of arogenate dehydratase genes identifies a link between phenylalanine biosynthesis and lignin biosynthesis. *J Exp Bot* **71**: 3080–3093

España L, Heredia-Guerrero JA, Reina-Pinto JJ, Fernández-Muñoz R, Heredia A, Domínguez E (2014a) Transient silencing of CHALCONE SYNTHASE during fruit ripening modifies tomato epidermal cells and cuticle properties. *Plant Physiol* **166**: 1371–1386

España L, Heredia-Guerrero JA, Segado P, Benítez JJ, Heredia A, Domínguez E (2014b) Biomechanical properties of the tomato (*Solanum lycopersicum*) fruit cuticle during development are modulated by changes in the relative amounts of its components. *New Phytol* **202**: 790–802

Espinosa-Leal CA, Mora-Vásquez S, Puente-Garza CA, Alvarez-Sosa DS, García-Lara S (2022) Recent advances on the use of abiotic stress (water, UV radiation, atmospheric gases, and temperature stress) for the enhanced production of secondary metabolites on in vitro plant tissue culture*. Plant Growth Regul* **97**: 1–20

FAOSTAT (2020) Datos sobre alimentación y agricultura. https://www.fao.org/faostat/es/

Fernández V, Bahamonde HA, Peguero-Pina JJ, Gil-Pelegrín E, Sancho-Knapik D, Gil L, Goldbach HE, Eichert T (2017) Physico-chemical properties of plant cuticles and their functional and ecological significance. *J Exp Bot* **68**: 5293–5306

Fernandez V, Eichert T (2009) Uptake of hydrophilic solutes through plant leaves: Current state of knowledge and perspectives of foliar fertilization. *Crit Rev Plant Sci* **28**: 36–68

Fernández V, Gil-Pelegrín E, Eichert T (2021) Foliar water and solute absorption: an update. *Plant J* **105**: 870–883

Fernández V, Guzmán-Delgado P, Graça J, Santos S, Gil L (2016) Cuticle structure in relation to chemical composition: Re-assessing the prevailing model. *Front Plant Sci* **7**: 427

Fernández V, Khayet M, Montero-Prado P, Heredia-Guerrero J, Liakopoulos G, Karabourniotis G, del Río V, Domínguez E, Tacchini I, Nerín C, et al (2011) New insights into the properties of pubescent surfaces: Peach fruit as a model. *Plant Physiol* **156**: 2098–2108

Ferrer JL, Jez JM, Bowman ME, Dixon RA, Noel JP (1999) Structure of chalcone synthase and the molecular basis of plant polyketide biosynthesis. *Nat Struct Biol* **6**: 775–784

Franke R, Briesen I, Wojciechowski T, Faust A, Yephremov A, Nawrath C, Schreiber L (2005) Apoplastic polyesters in *Arabidopsis* surface tissues - A typical suberin and a particular cutin. *Phytochemistry* **66**: 2643–2658

Frederick JE, Snell HE, Haywood EK (1989) Solar ultraviolet radiation at the Earth's surface. *Photochem Photobiol* **50**: 443–450

Gorb E, Kastner V, Peressadko A, Arzt E, Gaume L, Rowe N, Gorb S (2004) Structure and properties of the glandular surface in the digestive zone of the pitcher in the carnivorous plant *Nepenthes ventrata* and its role in insect trapping and retention. *J Exp Biol* **207(17)**: 2947–2963

Graça J, Schreiber L, Rodrigues J, Pereira H (2002) Glycerol and glyceryl esters of omega-hydroxyacids in cutins. *Phytochemistry* **61(2)**: 205–215

Grant RH, Jenks MA, Rich PJ, Peters PJ, Ashworth EN (1995) Scattering of ultraviolet and

photosynthetically active radiation by *Sorghum bicolor*: influence of epicuticular wax. *Agric For Meteorol* **75(4)**: 263–281

Grew N (1672) The anatomy of vegetables begun. With a general account of vegetation founded thereon, 1st Edn. Spencer Hickman, London

Guzmán P, Fernández V, García ML, Khayet M, Fernández A, Gil L (2014) Localization of polysaccharides in isolated and intact cuticles of eucalypt, poplar and pear leaves by enzyme-gold labelling. *Plant Physiol Biochem* **76**: 1–6

Hahlbrock K, Wong E, Schill L, Grisebach H (1970) Comparison of chalcone-flavanone isomerase heteroenzymes and isoenzymes. *Phytochemistry* **9**: 949–958

Harborne JB (1979) Variation in and functional significance of phenolic conjugation in plants. *In* T Swain, J Harborne, C Van Sumere, eds, *Biochemistry of Plant Phenolics*. Plenum Press, pp 457–474

Henslow, J.S (1831) On the examination of a hybrid Digitalis. *Trans Cambridge Philos Soc* **4**: 257–278

Heredia-Guerrero JA, Benítez JJ, Heredia A (2008) Self-assembled polyhydroxy fatty acids vesicles: A mechanism for plant cutin synthesis. *BioEssays* **30**: 273–277

Heredia A (2003) Biophysical and biochemical characteristics of cutin, a plant barrier biopolymer. *Biochim Biophys Acta* **1620**: 1–7

Heredia A, Benavente J (1991) A study of membrane potential across isolated fruit cuticles for NaCl and $CaCl_2$ solutions. *BBA - Biomembr* **1062(2)**: 239–244

Hong L, Qian Q, Tang D, Wang K, Li M, Cheng Z (2012) A mutation in the rice chalcone isomerase gene causes the *golden hull and internode 1* phenotype. *Planta* **236(1)**: 141–151

Hosmani PS, Flores-Gonzalez M, Geest H van de, Maumus F, Bakker L V, Schijlen E, Haarst J van, Cordewener J, Sanchez-Perez G, Peters S, et al (2019) An improved *de novo* assembly and annotation of the tomato reference genome using single-molecule sequencing, Hi-C proximity ligation and optical maps. bioRxiv. doi: 10.1101/767764

Hunt GM, Baker EA (1980) Phenolic constituents of tomato fruit cuticles. *Phytochemistry* **19(7)**: 1415–1419

Jeffree CE (2006) The fine structure of the plant cuticle. *In* M Riederer, C Müller, eds, *Biology of the Plant Cuticle*. Wiley Blackwell, pp 11–125

Jenkins GI (2014) Structure and function of the UV-B photoreceptor UVR8. *Curr Opin Struct Biol* **29**: 52–57

Jetter R, Riederer M (2016) Localization of the transpiration barrier in the epi- and intracuticular waxes of eight plant species: Water transport resistances are associated with fatty acyl rather than alicyclic components. *Plant Physiol* **170**: 921–934

Jez JM, Noel JP (2001) Reaction mechanism of chalcone isomerase. pH Dependence, diffusion control, and product binding differences. *J Biol Chem* **277**: 1361–1369

Jez JM, Noel JP (2002) Reaction mechanism of chalcone isomerase. *J Biol Chem* **277**: 1361–1369

Jiang W, Yin Q, Wu R, Zheng G, Liu J, Dixon RA, Pang Y (2015) Role of a chalcone isomerase-like protein in flavonoid biosynthesis in *Arabidopsis thaliana*. *J Exp Bot* **66**: 7165–7179

Ju Z, Bramlage WJ (1999) Phenolics and lipid-soluble antioxidants in fruit cuticle of apples and their antioxidant activities in model systems. *Postharvest Biol Technol* **16**: 107–118

Kamtsikakis A, Baales J, Zeisler-Diehl V V., Vanhecke D, Zoppe JO, Schreiber L, Weder C (2021) Asymmetric water transport in dense leaf cuticles and cuticle-inspired compositionally graded membranes. *Nat Commun* **12**: 1267

Kannan S (1986) Foliar absorption and transport of inorganic nutrients. *Crit Rev Plant Sci* **4**: 341–375

Karabourniotis G, Bornman JF (1999) Penetration of UV-A, UV-B and blue light through the leaf trichome layers of two xeromorphic plants, olive and oak, measured by optical fibre microprobes. *Physiol Plant* **105**: 655–661

Karabourniotis G, Bornman JF, Liakoura V (1999) Different leaf surface characteristics of three grape cultivars affect leaf optical properties as measured with fibre optics: Possible implication in stress tolerance. *Aust J Plant Physiol* **26**: 47–53

Kerstein G (1996) Plant cuticles: an integrated functional approach. BIOS Scientific Publishers, Oxford, UK

Kerstiens G (2006) Parameterization, comparison, and validation of models quantifying relative change of cuticular permeability with physicochemical properties of diffusants. *J. Exp. Bot.* **57**: 2525–2533

Khanal BP, Knoche M (2014) Mechanical properties of apple skin are determined by epidermis and hypodermis. *J Am Soc Hortic Sci* **139**: 1–9

Khanal BP, Knoche M (2017) Mechanical properties of cuticles and their primary determinants. *J Exp Bot* **68**: 5351–5367

Khanal BP, Grimm E, Finger S, Blume A, Knoche M (2013) Intracuticular wax fixes and restricts strain in leaf and fruit cuticles. *New Phytol* **200**: 134–143

Knoche M, Lang A (2017) Ongoing growth challenges fruit skin integrity. *Crit Rev Plant Sci* **36**: 190–215

Knoche M, Peschel S (2006) Water on the surface aggravates microscopic cracking of the sweet cherry fruit cuticle. *J Am Soc Hortic Sci* **131**: 192–200

Kögel-Knabner I, de Leeuw JW, Tegelaar EW, Hatcher PG, Kerp H (1994) A lignin-like polymer in the cuticle of spruce needles: implications for the humification of spruce litter. *Org Geochem* **21**: 1219–1228

Kolattukudy PE (2001) Polyesters in Higher Plants. *In* T Scheper, ed, *Biopolyesters*. Springer, pp 1–49

Kolattukudy PE (2002) Cutin from Plants. *In* A. Steinbüchel, ed, *Biopolymers Online*. John Wiley and Sons, pp 1–12

Kosma DK, Parsons EP, Isaacson T, Lü S, Rose JKC, Jenks MA (2010) Fruit cuticle lipid composition during development in tomato ripening mutants. *Physiol Plant* **139**: 107–117

Krauss P, Markstädter C, Riederer M (1997) Attenuation of UV radiation by plant cuticles from woody species. *Plant, Cell Environ* **20**: 1079–1085

Kunst L, Samuels AL (2003) Biosynthesis and secretion of plant cuticular wax. *Prog Lipid Res* **42**: 51–80

Lacis AA, Hansen JE (1974) Parameterization for the absorption of solar radiation in the Earth's atmosphere. *J Atmos Sci* **31**: 118–133

Lara I, Heredia A, Domínguez E (2019) Shelf life potential and the fruit cuticle: The unexpected player. *Front Plant Sci* **10**: 770

Lee DD, Seung HS (1999) Learning the parts of objects by non-negative matrix factorization. *Nature* **401**: 788–791

Leide J, Hildebrandt U, Reussing K, Riederer M, Vogg G (2007) The developmental pattern of tomato fruit wax accumulation and its impact on cuticular transpiration barrier properties: Effects of a deficiency in a *β*-ketoacyl-coenzyme A synthase (LeCER6). *Plant Physiol* **144**: 1667–1679

Leide J, Xavier de Souza A, Papp I, Riederer M (2018) Specific characteristics of the apple fruit cuticle: Investigation of early and late season cultivars 'Prima' and 'Florina' (*Malus domestica* Borkh.). *Sci Hortic* **229**: 137–147

Lendzian KJ, Kerstiens G (1991) Sorption and transport of gases and vapors in plant cuticles. *Rev. Environ. Contam. Toxicol.* pp 65–128

Lendzian KJ, Kerstiens, G (1991). Sorption and Transport of Gases and Vapors in Plant Cuticles. *In* GW Ware, ed, *Reviews of Environmental Contamination and Toxicology*. Springer, pp 65–128

Li J, Halitschke R, Li D, Paetz C, Su H, Heiling S, Xu S, Baldwin IT (2021) Controlled hydroxylations of diterpenoids allow for plant chemical defense without autotoxicity. *Science* **371**: 255–260

Li Y, Beisson F (2009) The biosynthesis of cutin and suberin as an alternative source of enzymes for the production of bio-based chemicals and materials. *Biochimie* **91**: 685–691

Li Y, Li J, Qian B, Cheng L, Xu S, Wang R (2018) De novo biosynthesis of *p*-coumaric acid in *E. coli* with a *trans*-cinnamic acid 4-hydroxylase from the Amaryllidaceae plant *Lycoris aurea*. Molecules **23**: 3185

Llorens L, Neugart S, Vandenbussche F, Castagna A (2020) Ultraviolet radiation: friend or foe for plants? *Front Plant Sci* **11**: 541

Lolle SJ, Berlyn GP, Engstrom EM, Krolikowski KA, Reiter WD, Pruitt RE (1997) Developmental regulation of cell interactions in the *Arabidopsis fiddlehead-1* mutant: A role for the epidermal cell wall and cuticle. *Dev Biol* **189**: 311–321

López-Casado G, Matas AJ, Domínguez E, Cuartero J, Heredia A (2007) Biomechanics of isolated tomato (*Solanum lycopersicum* L.) fruit cuticles: The role of the cutin matrix and polysaccharides. *J Exp Bot* **58**: 3875–3883

Lopez-Casado G, Salamanca A, Heredia A (2010) Viscoelastic nature of isolated tomato (*Solanum lycopersicum*) fruit cuticles: A mathematical model. *Physiol Plant* **140**: 79–88

Luque P, Bruque S, Heredia A (1995b) Water permeability of isolated cuticular membranes: A structural analysis. *Arch Biochem Biophys* **317**: 417–422

Luque P, Gavara R, Heredia A (1995a) A study of the hydration process of isolated cuticular membranes. *New Phytol* **129**: 283–288

Maeda H, Dudareva N (2012) The shikimate pathway and aromatic amino acid biosynthesis in plants. *Annu Rev Plant Biol* **63**: 73–105

Maja MM, Kasurinen A, Holopainen T, Julkunen-Tiitto R, Holopainen JK (2016) The effect of warming and enhanced ultraviolet radiation on gender-specific emissions of volatile organic compounds from European aspen. *Sci Total Environ* **547**: 39–47

Malpighi M (1675) *Anatome Plantarum. Cui fubjungitur Appendix, Iteratas & Aucta Ejufdem Authoris de ovo Incubato Obfervationes Continens*. Johannis Martyn

Marga F, Pesacreta TC, Hasenstein KH (2001) Biochemical analysis of elastic and rigid cuticles

of *Cirsium horridulum*. *Planta* **213**: 841–848

Martens P (1933) Recherches sur la cuticule - III. Structure, origine et signification du relief cuticulaire. *Protoplasma* **20**: 483–515

Martin LBB, Rose JKC (2014) There's more than one way to skin a fruit: Formation and functions of fruit cuticles. *J Exp Bot* **65**: 4639–4651

Matas AJ, Cobb ED, Bartsch JA, Paolillo DJ, Niklas KJ (2004a) Biomechanics and anatomy of *Lycopersicon esculentum* fruit peels and enzyme-treated samples. *Am J Bot* **91**: 352–360

Matas AJ, Cuartero J, Heredia A (2004b) Phase transitions in the biopolyester cutin isolated from tomato fruit cuticles. *Thermochim Acta* **409**: 165–168

Meder F, Must I, Sadeghi A, Mondini A, Filippeschi C, Beccai L, Mattoli V, Pingue P, Mazzolai B (2018) Energy conversion at the cuticle of living plants. *Adv Funct Mater* **28**: 1806689

Meyer M (1938) Die submikroskopische Struktur der kutinisierten Zellmembranen. *Protoplasma* **29**: 552–586

Molina I, Kosma D (2015) Role of HXXXD-motif/BAHD acyltransferases in the biosynthesis of extracellular lipids. *Plant Cell Rep* **34**: 587–601

Molina I, Ohlrogge JB, Pollard M (2008) Deposition and localization of lipid polyester in developing seeds of *Brassica napus* and *Arabidopsis thaliana*. *Plant J* **53**: 437–449

Morant AV, Jørgensen K, Jørgensen C, Paquette SM, Sánchez-Pérez R, Møller BL, Bak S (2008) β-Glucosidases as detonators of plant chemical defense. *Phytochemistry* **69**: 1795–1813

Munné-Bosch S, Jubany-Marí T, Alegre L (2001) Drought-induced senescence is characterized by a loss of antioxidant defences in chloroplasts. *Plant, Cell Environ* **24**: 1319–1327

Neinhuis C, Barthlott W (1997) Characterization and distribution of water-repellent, self-cleaning plant surfaces. *Ann Bot* **79**: 667–677

Neugart S, Schreiner M (2018) UVB and UVA as eustressors in horticultural and agricultural crops. *Sci Hortic* **234**: 370–381

Nip M, Tegelaar EW, Brinkhuis H, De Leeuw JW, Schenck PA, Holloway PJ (1986a) Analysis of modern and fossil plant cuticles by Curie point Py-GC and Curie point Py-GC-MS: Recognition of a new, highly aliphatic and resistant biopolymer. *Org Geochem* **10**: 769–778

Nip M, Tegelaar EW, de Leeuw JW, Schenck PA, Holloway PJ (1986b) A new non-saponifiable highly aliphatic and resistant biopolymer in plant cuticles - Evidence from pyrolysis and ^{13}C-NMR analysis of present-day and fossil plants. *Naturwissenschaften* **73**: 579–585

Nobusawa T, Okushima Y, Nagata N, Kojima M, Sakakibara H, Umeda M (2013) Synthesis of very-long-chain fatty acids in the epidermis controls plant organ growth by restricting cell proliferation. *PLoS Biol* **11**: e1001531

Noel JP, Jez JM, Bowman ME, Dixon RA (2000) Structure and mechanism of the evolutionarily unique plant enzyme chalcone isomerase. *Nat Struct Biol* **7**: 786–791

Onyilagha, JC, Grotewold E (2004) The biology and structural distribution of surface flavonoids. *Recent Res Dev Plant Sci* **2**: 53–71

Panikashvili D, Shi JX, Schreiber L, Aharoni A (2009) The Arabidopsis *DCR* encoding a soluble BAHD acyltransferase is required for cutin polyester formation and seed hydration properties. *Plant Physiol* **151**: 1773–1789

Pati YC, Rezaiifar R, Krishnaprasad PS (1993) Orthogonal matching pursuit: recursive function

approximation with applications to wavelet decomposition. *Proceedings of 27th asilomar conference on signals, systems and computers* **1**: 40–44

Peschel S, Franke R, Schreiber L, Knoche M (2007) Composition of the cuticle of developing sweet cherry fruit. *Phytochemistry* **68**: 1017–1025

Petit J, Bres C, Just D, Garcia V, Mauxion JP, Marion D, Bakan B, Joubès J, Domergue F, Rothan C (2014) Analyses of tomato fruit brightness mutants uncover both cutin-deficient and cutin-abundant mutants and a new hypomorphic allele of *GDSL Lipase*. *Plant Physiol* **164**: 888–906

Petit J, Bres C, Reynoud N, Lahaye M, Marion D, Bakan B, Rothan C (2021) Unraveling cuticle formation, structure, and properties by using tomato genetic diversity. *Front Plant Sci* **12**: 778131

Petracek PD, Bukovac MJ (1995) Rheological properties of enzymatically isolated tomato fruit cuticle. *Plant Physiol* **109**: 675–679

Qin YM, Hu CY, Pang Y, Kastaniotis AJ, Hiltunen JK, Zhu YX (2007) Saturated very-long-chain fatty acids promote cotton fiber and *Arabidopsis* cell elongation by activating ethylene biosynthesis. *Plant Cell* **19**: 3692–3704

Raffaele S, Leger A, Roby D (2009) Very long chain fatty acid and lipid signaling in the response of plants to pathogens. *Plant Signal Behav* **4**: 94–99

Rai N, Morales LO, Aphalo PJ (2021) Perception of solar UV radiation by plants: photoreceptors and mechanisms. *Plant Physiol* **186**: 1382–1396

Rai N, O'Hara A, Farkas D, Safronov O, Ratanasopa K, Wang F, Lindfors A V., Jenkins GI, Lehto T, Salojärvi J, et al (2020) The photoreceptor UVR8 mediates the perception of both UV-B and UV-A wavelengths up to 350 nm of sunlight with responsivity moderated by cryptochromes. *Plant Cell Environ* **43**: 1513–1527

Ramos-Barrado J, Benavente J, Heredia A (1993) Electrical conductivity of differently treated isolated cuticular membranes by impedance spectroscopy. *Arch Biochem Biophys* **306**: 337–341

Reina JJ, Domínguez E, Heredia A (2001) Water sorption-desorption in conifer cuticles: The role of lignin. *Physiol Plant* **112**: 372–378

Renault H, Alber A, Horst NA, Basilio Lopes A, Fich EA, Kriegshauser L, Wiedemann G, Ullmann P, Herrgott L, Erhardt M, et al (2017) A phenol-enriched cuticle is ancestral to lignin evolution in land plants. *Nat Commun* **8**: 14713

Reynoud N, Geneix N, D´Orlando A, Petit J, Mathurin J, Deniset-Besseau A, Marion D, Rothan C, Lahaye M, Bakan B (2023) Cuticle architecture and mechanical properties: a functional relationship delineated through correlated multimodal imaging. *New Phytol* **238**: 2033-2046

Reynoud N, Petit J, Bres C, Lahaye M, Rothan C, Marion D, Bakan B (2021) The complex architecture of plant cuticles and its relation to multiple biological functions. *Front Plant Sci* **12**: 2907

Riederer M (2006) Introduction: Biology of the Plant Cuticle. *In* C Müller, ed, *Annual Plant Reviews*. Blackwell Publishing, pp 1–10

Rizzini L, Favory JJ, Cloix C, Faggionato D, O'Hara A, Kaiserli E, Baumeister R, Schäfer E, Nagy F, Jenkins GI, et al (2011) Perception of UV-B by the *Arabidopsis* UVR8 protein. *Science* **332**: 103–106

Robberecht R, Caldwell MM, Billings WD (1980) Leaf ultraviolet optical properties along a

latitudinal gradient in the Aarctic-alpine life zone. *Ecology* **61**: 612–619

Robson TM, Hartikainen SM, Aphalo PJ (2015) How does solar ultraviolet-B radiation improve drought tolerance of silver birch (*Betula pendula* Roth.) seedlings? *Plant Cell Environ* **38**: 953–67

Roudier F, Gissot L, Beaudoin F, Haslam R, Michaelson L, Marion J, Molino D, Lima A, Bach L, Morin H, et al (2010) Very-long-chain fatty acids are involved in polar auxin transport and developmental patterning in *Arabidopsis*. *Plant Cell* **22**: 364–375

Sargent C (1976) The occurrence of a secondary cuticle in *Libertia elegans* (Iridaceae). *Ann Bot* **40**: 355–359

Schönherr J (2000) Calcium chloride penetrates plant cuticles via aqueous pores. *Planta* **212**: 112–118

Schönherr J, Bukovac MJ (1973) Ion exchange properties of isolated tomato fruit cuticular membrane: Exchange capacity, nature of fixed charges and cation selectivity. *Planta* **109**: 73–93

Schönherr J, Eckl K, Gruler H (1979) Water permeability of plant cuticles: The effect of temperature on diffusion of water. *Planta* **147**: 21–26

Schönherr J, Luber M (2001) Cuticular penetration of potassium salts: Effects of humidity, anions, and temperature. *Plant Soil* **236**: 117–122

Schreel JDM, Steppe K (2020) Foliar water uptake in trees: Negligible or necessary? *Trends Plant Sci* **25**: 590–603

Schreiber L, Schönherr J (1990) Phase transitions and thermal expansion coefficients of plant cuticles - The effects of temperature on structure and function. *Planta* **182**: 186–193

Schreiber L, Schönherr J (2009) Water and solute permeability of plant cuticles: Measurement and data analysis. Springer Verlag

Shitan N (2016) Secondary metabolites in plants: Transport and self-tolerance mechanisms. *Biosci Biotechnol Biochem* **80**: 1283–1293

Sirikantaramas S, Yamazaki M, Saito K (2008) Mechanisms of resistance to self-produced toxic secondary metabolites in plants. *Phytochem Rev* **7**: 467–477

Skrzydeł J, Borowska-wykręt D, Kwiatkowska D (2021) Structure, assembly and function of cuticle from mechanical perspective with special focus on perianth. *Int J Mol Sci* **22**: 4160

Solovchenko A (2010) *Photoprotection in Plants*. Springer

Solovchenko A, Merzlyak M (2003) Optical properties and contribution of cuticle to UV protection in plants: Experiments with apple fruit. *Photochem Photobiol Sci* **2**: 861–866

Steinmüller D, Tevini M (1985) Action of ultraviolet radiation (UV-B) upon cuticular waxes in some crop plants. *Planta* **164**: 557–564

Steinmüller D, Tevini M (1986) UV-B-induced effects upon cuticular waxes of cucumber, bean, and barley leaves. *In* RC Worrest, MM Caldwell, eds, *Stratospheric ozone reduction, solar ultraviolet radiation and plant life*. Springer, pp 261–269

Tafolla-Arellano JC, Báez-Sañudo R, Tiznado-Hernández ME (2018) The cuticle as a key factor in the quality of horticultural crops. *Sci Hortic* **232**: 145–152

Takahashi Y, Tsubaki S, Sakamoto M, Watanabe S, Azuma JI (2012) Growth-dependent chemical and mechanical properties of cuticular membranes from leaves of *Sonneratia alba*. *Plant, Cell Environ* **35**: 1201–1210

Tanaka T, Tanaka H, Machida C, Watanabe M, Machida Y (2004) A new method for rapid visualization of defects in leaf cuticle reveals five intrinsic patterns of surface defects in *Arabidopsis*. *Plant J* **37**: 139–146

Tevini M, Braun J, Fieser G (1991) The protective function of the epidermal layer of rye seedlings against ultraviolet-B radiation. *Photochem Photobiol* **53**: 329–333

The tomato Genome Consortium (2012) The tomato genome sequence provides insights into fleshy fruit evolution. *Nature* **485**: 635–641

Thimmappa R, Geisler K, Louveau T, O'Maille P, Osbourn A (2014) Triterpene biosynthesis in plants. *Annu Rev Plant Biol* **65**: 225–257

Tohge T, Watanabe M, Hoefgen R, Fernie AR (2013) Shikimate and phenylalanine biosynthesis in the green lineage. *Front Plant Sci* **4**: 62

Tossi VE, Regalado JJ, Iannicelli J, Laino LE, Burrieza HP, Escandón AS, Pitta-Álvarez SI (2019) Beyond Arabidopsis: Differential UV-B response mediated by UVR8 in diverse species. *Front Plant Sci* **10**: 780

Tredenick EC, Farquhar GD (2021) Dynamics of moisture diffusion and adsorption in plant cuticles including the role of cellulose. *Nat Commun* **12**: 5042

Tsubaki S, Sugimura K, Teramoto Y, Yonemori K, Azuma J ichi (2013) Cuticular membrane of *Fuyu* persimmon fruit is strengthened by triterpenoid nano-fillers. *PLoS One* **8**: e75275

Tyree MT, Wescott CR, Tabor CA (1991) Diffusion and electric mobility of ions within isolated cuticles of *Citrus aurantium* steady-state and equilibrium values. *Plant Physiol* **97**: 273–279

Vanhaelewyn L, Van Der Straeten D, De Coninck B, Vandenbussche F (2020) Ultraviolet radiation from a plant perspective: The plant-microorganism context. *Front Plant Sci* **11**: 597642

Vega C, Valbuena-Carabaña M, Gil L, Fernández V (2021) Water sorption and desorption of isolated cuticles from three woody species with focus on *Ilex aquifolium*. *Front Plant Sci* **12**: 728627

Verdaguer D, Jansen MAK, Llorens L, Morales LO, Neugart S (2017) UV-A radiation effects on higher plants: Exploring the known unknown. *Plant Sci* **255**: 72–81

Villena JF, Domínguez E, Stewart D, Heredia A (1999) Characterization and biosynthesis of non-degradable polymers in plant cuticles. *Planta* **208**: 181–187

Vogg G, Fischer S, Leide J, Emmanuel E, Jetter R, Levy AA, Riederer M (2004) Tomato fruit cuticular waxes and their effects on transpiration barrier properties: Functional characterization of a mutant deficient in a very-long-chain fatty acid β-ketoacyl-CoA synthase. *J Exp Bot* **55**: 1401–1410

von Mohl H (1847) Untersuchungen der Frage: bildet die cellulose die grundlage sammtlicher vegetabilischen membranen. *Bot Zeitung* **5**: 497–505

Wagner H, Gilbert M, Wilhelm C (2003) Longitudinal leaf gradients of UV-absorbing screening pigments in barley (*Hordeum vulgare*). *Physiol Plant* **117**: 383–391

Ward G, Nussinovitch A (1996) Gloss properties and surface morphology relationships of fruits. *J Food Sci* **61**: 973–977

Wiedemann P, Neinhuis C (1998) Biomechanics of isolated plant cuticles. *Bot Acta* **111**: 28–34

Yang S, Johnston N, Talideh E, Mitchell S, Jeffree C, Goodrich J, Ingram G (2008) The endosperm-specific *ZHOUPI* gene of *Arabidopsis thaliana* regulates endosperm breakdown

and embryonicepidermal development. *Development* **135**: 3501–3509

Yang W, Pollard M, Li-Beisson Y, Ohlrogge J (2016) Quantitative analysis of glycerol in dicarboxylic acid-rich cutins provides insights into Arabidopsis cutin structure. *Phytochemistry* **130**: 159–169

Yazaki K (2006) ABC transporters involved in the transport of plant secondary metabolites. *FEBS Lett* **580**: 1183–1191

Yeats TH, Rose JKC (2013) The formation and function of plant cuticles. *Plant Physiol* **163**: 5–20

Zeisler-Diehl V, Müller Y, Schreiber L (2018) Epicuticular wax on leaf cuticles does not establish the transpiration barrier, which is essentially formed by intracuticular wax. *J Plant Physiol* **227**: 66–74

Zhang W, Wang S, Yang J, Kang C, Huang L, Guo L (2022b) Glycosylation of plant secondary metabolites: Regulating from chaos to harmony. *Environ Exp Bot* **194**: 104703

Zhang Y, Cai P, Cheng G, Zhang Y (2022a) A brief review of phenolic compounds identified from plants: their extraction, analysis, and biological activity. *Nat Prod Commun* **17**: 1–14

Zhang Y, Chen X, Du Z, Zhang W, Devkota AR, Chen Z, Chen C, Sun W, Chen M (2020) A proposed method for simultaneous measurement of cuticular transpiration from different leaf surfaces in *Camellia sinensis*. *Front Plant Sci* **11**: 420

Zhao J (2015) Flavonoid transport mechanisms: How to go, and with whom. *Trends Plant Sci* **20**: 576–585

Zhu X, Zhang Y, Du Z, Chen X, Zhou X, Kong X, Sun W, Chen Z, Chen C, Chen M (2018) Tender leaf and fully-expanded leaf exhibited distinct cuticle structure and wax lipid composition in *Camellia sinensis cv Fuyun 6*. *Sci Rep* **8**: 14944

2. OBJECTIVES

Objectives

The present doctoral thesis is focussed on the study of phenolic compounds present in the plant cuticle, specifically their location and interaction within the plant cuticle as well as their contribution to plant photoprotection. The main objectives are:

1. Locate and identify the main cuticle components throughout tomato fruit development.

2. Study the spontaneous isomerization between naringenin chalcone and naringenin as well as flavonoid clustering within the tomato fruit cuticle using quantum calculations.

3. Investigate the optical properties of tomato fruit cuticles along development.

4. Analyse the individual and combined photochemistry of naringenin chalcone and *p*-coumaric acid, the main phenolic compounds accumulated in ripe tomato fruit cuticles.

5. Elucidate the mechanism of UV-B photoprotection performed by plant cuticle phenolics, specifically *p*-coumaric acid, a phenolic compound present in all plant cuticles studied.

3. CHAPTERS

Chapter 1. Structure, isomerization and dimerization processes of naringenin flavonoids

PCCP

ROYAL SOCIETY OF CHEMISTRY

PAPER

View Article Online
View Journal | View Issue

Cite this: *Phys. Chem. Chem. Phys.*, 2021, **23**, 18068

Structure, isomerization and dimerization processes of naringenin flavonoids†

Ana González Moreno, *[a] Pilar Prieto, [b] M. Carmen Ruiz Delgado, [c] Eva Domínguez, [d] Antonio Heredia *[a] and Abel de Cózar *[ef]

In this study, the theoretical and experimental results on the molecular structure and reactivity of the plant flavonoids naringenin chalcone and naringenin are reported. UV-vis and Raman spectra were recorded and their main bands have been assigned theoretically. Moreover, the analysis of the naringenin chalcone–naringenin cyclization–isomerization reaction and the formation of homodimers and heterodimers have been performed within a DFT framework. The presence of H-bonded water networks is mandatory to make the cyclization energetically suitable, suggesting that this equilibrium will occur in an aqueous intracellular environment rather than in the extracellular and hydrophobic plant cuticles. Additionally, the preferential formation of homodimers stabilized by π–π stacking that will interact with other dimers by H-bonding over the formation of naringenin chalcone–naringenin heterodimers is also proposed in a hydrophobic environment. These results give a plausible model to explain how flavonoids are located within the cuticle molecular arrangement.

Received 15th March 2021,
Accepted 23rd July 2021

DOI: 10.1039/d1cp01161h

rsc.li/pccp

1. Introduction

Flavonoids are one of the most important families of phenolic compounds. From a structural point of view, they are phenylpropanoid or cinnamic acid derivatives based on a C6–C3–C6 flavan nucleus (Fig. 1), which consists of two benzene rings (rings A and B) joined by a tetrahydro-2*H*-pyran ring (ring C).[1] Flavonoids are ubiquitously present in plants, where they have been found in the fruits, leaves, roots, and various flower organs such as petals, stigmas, styles and pollen. According to the saturation and oxidation degrees of their central C-ring, flavonoids can be divided into different subclasses: flavanones, flavones, isoflavones, flavonols, flavanols and anthocyanins.[2]

Flavonoids are involved in a broad spectrum of pivotal functions in the plant kingdom. They have been widely reported as pigments that colour the flowers, seeds and leaves,[3] but they also participate in several protective and developmental roles. Among them are the contribution to seed-coat development, pollen viability, participation in plant hormone signalling and reduction of reactive oxygen species (ROS). Regarding the interaction with the environment, flavonoids protect the plant against UV-B radiation, pathogen attack and some stresses such as salinity.[4,5] Flavonoids are present in the human diet, and over the past few years they have been regarded as nutraceuticals due to their impact in several chronic conditions such as diabetes, osteoporosis, inflammatory processes, cardiovascular diseases or some types of cancer.[6]

Flavonoids are synthesized in the cytoplasm of cells and are typically stored in vacuoles, transported to other cells or tissues or secreted to the cuticle.[7,8] The cuticle is the outermost membrane that covers the surface of leaves, fruits and non-lignified stems of plants. It is composed of an amorphous and hydrophobic

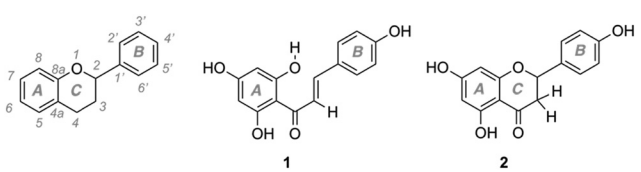

Fig. 1 General structure of the flavan nucleus, naringenin chalcone (**1**) and naringenin (**2**).

[a] *IHSM-UMA-CSIC La Mayora, Departamento de Biología Molecular y Bioquímica, Universidad de Málaga (UMA), 29071, Málaga, Spain. E-mail: gonzalezana@uma.es, heredia@uma.es*
[b] *Departamento de Química Inorgánica, Orgánica y Bioquímica, Facultad de Ciencias y Tecnologías Químicas-IRICA, Universidad de Castilla la Mancha. (UCLM), 13071, Ciudad Real, Spain*
[c] *Departamento de Química Física, Universidad de Málaga (UMA), 29071, Málaga, Spain*
[d] *IHSM-UMA-CSIC La Mayora, Plant breeding and Biotechnology, CSIC, 29750 Algarrobo-Costa, Málaga, Spain*
[e] *Departamento de Química Orgánica I, Facultad de Química, Universidad del País EHU) and Donostia International Physics/EHU) and Donostia International Physics Center (DIPC), 1072, E-20018, San Sebastián-Donostia, Spain. E-mail: abel.decozar@ehu.es*
[f] *IKERBASQUE, Basque Foundation for Science, 48009, Bilbao, Spain*

† Electronic supplementary information (ESI) available: Level of theory benchmarks, Raman band assignments, Cartesian coordinates, energies and thermal corrections of optimized structures discussed in the main text. See DOI: 10.1039/d1cp01161h

Chapter 2. 3D (x-y-t) Raman imaging of tomato fruit cuticle: Microchemistry during development

https://doi.org/10.1093/plphys/kiac369 PLANT PHYSIOLOGY 2023: 191: 219–232

Plant Physiology®

3D (x-y-t) Raman imaging of tomato fruit cuticle: Microchemistry during development

Ana González Moreno [1,*] Eva Domínguez [2] Konrad Mayer [3] Nannan Xiao [3] Peter Bock [3] Antonio Heredia [1] and Notburga Gierlinger [3,*]

1 IHSM-UMA-CSIC La Mayora, Departamento de Biología Molecular y Bioquímica, Universidad de Málaga, 29071, Málaga, Spain
2 IHSM-UMA-CSIC La Mayora, Plant breeding and Biotechnology, CSIC, 29750 Algarrobo-Costa, Málaga, Spain
3 Department of Nanobiotechnology, BOKU-University of Natural Resources and Life Science, Vienna, Muthgasse 11, 1190 Vienna, Austria

*Author for correspondence: burgi.gierlinger@boku.ac.at (N.G.), gonzalezana@uma.es (A.G.M.)

A.G.M. performed DFT calculations and confocal Raman microscopy measurements of the different stages of development of isolated tomato fruit cuticles, contributed to the nonnegative matrix factorization (NMF), basis analysis, and data interpretation. A.G.M. wrote the first draft of the manuscript. E.D. isolated tomato fruit cuticles and participated in data analysis and discussion. K.M. contributed to mixture analysis. N.X. took part in sample preparation and carried out technical support and P.B. recorded all reference spectra. A.H. participated in data analysis and interpretation and N.G. supervised Raman experiments, spectral data analysis, and paper writing.
The author responsible for distribution of materials integral to the findings presented in this article in accordance with the policy described in the Instructions for Authors (https://academic.oup.com/plphys/pages/general-instructions) is: Notburga Gierlinger (burgi.gierlinger@boku.ac.at).

Abstract

The cuticle is a protective extracellular matrix that covers the above-ground epidermis of land plants. Here, we studied the cuticle of tomato (*Solanum lycopersicum* L.) fruits in situ using confocal Raman microscopy. Microsections from cuticles isolated at different developmental stages were scanned to visualize cuticle components with a spatial resolution of 342 nm by univariate and multivariate data analysis. Three main components, cutin, polysaccharides, and aromatics, were identified, with the latter exhibiting the strongest Raman scattering intensity. Phenolic acids and flavonoids were differentiated within the cuticle, and three schematic cuticle models were identified during development. Phenolic acids were found across the entire cuticle at the earliest stage of development, i.e. during the formation of the procuticle layer. Based on a mixture analysis with reference component spectra, the phenolic acids were identified as mainly esterified *p*-coumaric acid together with free *p*-hydroxybenzoic acid. During the cell expansion period of growth, phenolic acids accumulated in an outermost layer of the cuticle and in the middle region of the pegs. In these stages of development, cellulose and pectin were detected next to the inner cuticle region, close to the epidermal cell where flavonoid impregnation started during ripening. In the first ripening stage, chalconaringenin was observed, while methoxylated chalcones were chosen by the algorithm to fit the mature cuticle spectra. The colocation of carbohydrates, esterified *p*-coumaric acid, and methoxylated chalconaringenin suggests that the latter two link polysaccharide and cutin domains. Elucidating the different distribution of aromatics within the cuticle, suggests important functions: (1) overall impregnation conferring mechanical and thermal functions (2) the outermost phenolic acid layer displaying UV-B protection of the plant tissue.

Introduction

The plant cuticle is the outermost barrier, which covers the surface of aerial nonlignified organs (leaves, stems, flowers, and fruits) of land plants. This outer layer is responsible for some critical functions in the plant kingdom, such as

Received June 01, 2022. Accepted July 15, 2022. Advance access publication August 16, 2022

Chapter 3. The response of tomato fruit cuticle membranes against heat and light

frontiers in Plant Science

ORIGINAL RESEARCH
published: 07 January 2022
doi: 10.3389/fpls.2021.807723

The Response of Tomato Fruit Cuticle Membranes Against Heat and Light

José J. Benítez[1], Ana González Moreno[2], Susana Guzmán-Puyol[3], José A. Heredia-Guerrero[3], Antonio Heredia[2] and Eva Domínguez[3]*

[1] Instituto de Ciencia de Materiales de Sevilla, Centro Mixto Consejo Superior de Investigaciones Científicas-Universidad de Sevilla, Seville, Spain, [2] Departamento de Biología Molecular y Bioquímica, Instituto de Hortofruticultura Subtropical y Mediterránea "La Mayora", Universidad de Málaga-Consejo Superior de Investigaciones Científicas, Universidad de Málaga, Málaga, Spain, [3] Departamento de Mejora Genética y Biotecnología, Instituto de Hortofruticultura Subtropical y Mediterránea "La Mayora", Universidad de Málaga-Consejo Superior de Investigaciones Científicas, Estación Experimental La Mayora, Málaga, Spain

Two important biophysical properties, the thermal and UV-Vis screening capacity, of isolated tomato fruit cuticle membranes (CM) have been studied by differential scanning calorimetry (DSC) and UV-Vis spectrometry, respectively. A first order melting, corresponding to waxes, and a second order glass transition (T_g) thermal events have been observed. The glass transition was less defined and displaced toward higher temperatures along the fruit ripening. In immature and mature green fruits, the CM was always in the viscous and more fluid state but, in ripe fruits, daily and seasonal temperature fluctuations may cause the transition between the glassy and viscous states altering the mass transfer between the epidermal plant cells and the environment. CM dewaxing reduced the T_g value, as derived from the role of waxes as fillers. T_g reduction was more intense after polysaccharide removal due to their highly interwoven distribution within the cutin matrix that restricts the chain mobility. Such effect was amplified by the presence of phenolic compounds in ripe cuticle membranes. The structural rigidity induced by phenolics in tomato CMs was directly reflected in their mechanical elastic modulus. The heat capacity (Cp_{rev}) of cuticle membranes was found to depend on the developmental stage of the fruits and was higher in immature and green stages. The average Cp_{rev} value was above the one of air, which confers heat regulation capacity to CM. Cuticle membranes screened the UV-B light by 99% irrespectively the developmental stage of the fruit. As intra and epicuticular waxes contributed very little to the UV screening, this protection capacity is attributed to the absorption by cinnamic acid derivatives. However, the blocking capacity toward UV-A is mainly due to the CM thickness increment during growth and to the absorption by flavone chalconaringenin accumulated during ripening. The build-up of phenolic compounds was found to be an efficient mechanism to regulate both the thermal and UV screening properties of cuticle membranes.

Keywords: tomato fruit cuticle membrane, thermal characterization, UV-Vis screening, heat capacity, glass transition, fruit growth and ripening

OPEN ACCESS

Edited by:
Eduardo A. Ceccarelli, CONICET Instituto de Biología Molecular y Celular de Rosario (IBR), Argentina

Reviewed by:
Moritz Knoche, Leibniz University Hannover, Germany
Nikolai Borisjuk, Huaiyin Normal University, China

****Correspondence:***
José J. Benítez
benitez@icmse.csic.es

Specialty section:
This article was submitted to Plant Physiology, a section of the journal Frontiers in Plant Science

Received: *02 November 2021*
Accepted: *16 December 2021*
Published: *07 January 2022*

Citation:
Benítez JJ, González Moreno A, Guzmán-Puyol S, Heredia-Guerrero JA, Heredia A and Domínguez E (2022) The Response of Tomato Fruit Cuticle Membranes Against Heat and Light. Front. Plant Sci. 12:807723. doi: 10.3389/fpls.2021.807723

Chapter 4. Radiationless mechanism of UV deactivation by cuticle phenolics in plants

nature COMMUNICATIONS

ARTICLE

https://doi.org/10.1038/s41467-022-29460-9 OPEN

Radiationless mechanism of UV deactivation by cuticle phenolics in plants

Ana González Moreno [1], Abel de Cózar [2,3]✉, Pilar Prieto [4], Eva Domínguez [5] & Antonio Heredia [1]✉

Hydroxycinnamic acids present in plant cuticles, the interphase and the main protective barrier between the plant and the environment, exhibit singular photochemical properties that could allow them to act as a UV shield. Here, we employ transient absorption spectroscopy on isolated cuticles and leaf epidermises to study in situ the photodynamics of these molecules in the excited state. Based on quantum chemical calculations on *p*-coumaric acid, the main phenolic acid present in the cuticle, we propose a model in which cuticle phenolics display a photoprotective mechanism based in an ultrafast and non-radiative excited state deactivation combined with fluorescence emission. As such, the cuticle can be regarded as the first and foremost protective barrier against UV radiation. This photostable and photodynamic mechanism seems to be universal in land plants giving a special role and function to the presence of different aromatic domains in plant cuticles and epidermises.

[1] Instituto de Hortofruticultura Subtropical y Mediterránea La Mayora, Universidad de Málaga - Consejo Superior de Investigaciones Científicas Departamento de Biología Molecular y Bioquímica, Universidad de Málaga, E-29071 Málaga, Spain. [2] Departamento de Química Orgánica I / Kimika Organikoa I Saila, Facultad de Química / Kimika Fakultatea, Universidad del País Vasco / Euskal Herriko Unibertsitatea (UPV/EHU) and Donostia International Physics Center (DIPC), P. K, 1072, 20018 San Sebastián – Donostia, Spain. [3] Ikerbasque, Basque Foundation for Science, Plaza Euskadi 5, 48009 Bilbao, Spain. [4] Departamento de Inorgánica, Orgánica y Bioquímica. Facultad de Ciencias y Tecnología Química-IRICA, Universidad de Castilla-La Mancha, 13071 Ciudad Real, Spain. [5] Instituto de Hortofruticultura Subtropical y Mediterránea La Mayora, Universidad de Málaga - Consejo Superior de Investigaciones Científicas, Departamento de Mejora Genética y Biotecnología, Estación Experimental La Mayora, Algarrobo-Costa, E-29750 Málaga, Spain. ✉email: abel.decozar@ehu.es; heredia@uma.es

Chapter 5. Synergic photoprotection of phenolic compounds present in tomato fruit cuticle: a spectroscopic investigation in solution

PCCP

ROYAL SOCIETY OF CHEMISTRY

PAPER

View Article Online
View Journal | View Issue

Check for updates

Cite this: *Phys. Chem. Chem. Phys.*, 2023, **25**, 12791

Synergic photoprotection of phenolic compounds present in tomato fruit cuticle: a spectroscopic investigation in solution†

Ana González Moreno, *[a] Jack M. Woolley, [b] Eva Domínguez,[c] Abel de Cózar, [de] Antonio Heredia[a] and Vasilios G. Stavros *[b]

Received 8th February 2023,
Accepted 6th April 2023

DOI: 10.1039/d3cp00630a

rsc.li/pccp

Coumaric acids and flavonoids play pivotal roles in protecting plants against ultraviolet radiation (UVR) exposure. In this work, we focus our photoprotection studies on *p*-coumaric acid and the flavonoid naringenin chalcone. Photoprotection is well-understood in *p*-coumaric acid; in contrast, information surrounding photoprotection in naringenin chalcone is lacking. Additionally, and vitally, how these two species work in unison to provide photoprotection across the UV-B and UV-A is unknown. Herein, we employ transient absorption spectroscopy together with steady-state irradiation studies to unravel the photoprotection mechanism of a solution of *p*-coumaric acid and naringenin chalcone. We find that the excited state dynamics of *p*-coumaric acid are significantly altered in the presence of naringenin chalcone. This finding concurs with quenching of the *p*-coumaric acid fluorescence with increasing concentration of naringenin chalcone. We propose a Förster energy transfer mechanism is operative *via* the formation of dipole–dipole interactions between *p*-coumaric acid and naringenin chalcone. To our knowledge, this is the first demonstration in plants of a synergic effect between two classes of phenolics to bypass the potentially damaging effects of UVR.

1. Introduction

Around 450 million years ago, plants started to migrate from water to dry land. This necessitated plants to develop mechanisms to protect them against new stresses, including harmful radiation.[1] The most energetic radiation that reaches the Earth is ultraviolet radiation (UVR). It can be subdivided into UV-A (400–315 nm), UV-B (315–280 nm) and UV-C (280–100 nm). Since the ozone layer absorbs much of this radiation, notably UV-C and UV-B, only 5% of UVB and 95% of UV-A reach the Earth's surface.[2]

UVR is required for plant survival and it is involved in photosynthesis and gene signalling, among other functions.[3] Nevertheless, a strict balance is needed as excessive exposure to this radiation has deleterious effects such as DNA damage, protein and lipid damage, formation of reactive oxygen species (ROS), plant growth and development disruption.[4] Plants respond to UVR exposure by accumulating aromatic 'screening' compounds, known henceforth as UV-filters.

UV-filters have a broad absorption within the UV-A and UV-B radiation range, often with critical wavelengths greater than 370 nm,[5] typically dissipating this gained (usually electronic excitation) energy into non-harmful vibrational energy (or heat). Furthermore, these UV-filters are photostable even after prolonged periods of irradiation. Indeed, there is a growing library of such UV-filters being explored as potential plant-based sunscreens including sinapoyl malate. sinapic acid,[6] sinapate ester derivates[7,8] and symmetrical esterification of sinapic acid.[9,10]

The plant cuticle which covers the aerial parts of plants has been recently reported as a very efficient filter against UVR. Phenolic compounds accumulated within the cuticle, specifically

[a] *IHSM-UMA-CSIC La Mayora, Departamento de Biología Molecular y Bioquímica, Universidad de Málaga (UMA), 29071, Málaga, Spain. E-mail: gonzalezana@uma.es*
[b] *Department of Chemistry, University of Warwick, Coventry, UK. E-mail: v.stavros@warwick.ac.uk*
[c] *IHSM-UMA-CSIC La Mayora, Plant breeding and Biotechnology, CSIC, 29750 Algarrobo-Costa, Málaga, Spain*
[d] *Departamento de Química Orgánica I/Kimika Organikoa I Saila, Facultad de Química/Kimika Fakultatea, Universidad del País Vasco/Euskal Herriko Unibertsitatea (UPV/EHU) and Donostia International Physics Center (DIPC), P. K, 1072, 20018 San Sebastián – Donostia, Spain*
[e] *Ikerbasque, Basque Foundation for Science, Plaza Euskadi 5, 48009, Bilbao, Spain*

† Electronic supplementary information (ESI) available: Excited state lifetimes and EADS after excitation at 365 nm, solvent only scans, residuals' data and power measurements for the TAS; cartesian coordinates, energy details and frontier orbitals related to the **nch** isomerization profile calculations; further UV-Vis spectra and photostability tests; cartesian coordinates, structural information, computed orbitals and assignments of UV-Vis spectra bands for **pca** and **nch**; quantum calculations on **pca–nch** heterodimers and their cartesian coordinates; ^{1}H-NMR spectra; and Stern–Volmer plot. See DOI: **https://doi.org/10.1039/d3cp00630a**

4. OVERALL SUMMARY OF RESULTS AND DISCUSSION

Overall Summary of Results and Discussion

Main results of the present doctoral thesis are summarized and discussed hereunder.

Would it be plausible the interconversion between naringenin chalcone and naringenin within the tomato fruit cuticle scenario?

Naringenin chalcone has been the unique flavonoid identified in tomato fruit cuticle, albeit some earlier research has also suggested the presence of its isomer naringenin. The drastic conditions of pH and temperature required to phenolics extraction hampered their selective isolation. A slow non-stereospecific spontaneous naringenin chalcone-naringenin conversion has been observed in solution. Nevertheless, the stereospecific isomerisation must be mediated by the CHI to reach mostly the biologically active *(2S)*-naringenin isomer with a ratio preference of 100.000:1 against the R-isomer. To my knowledge, the viability of the naringenin chalcone-naringenin chemical isomerization in different environments simulating different plant tissues has not been previously studied.

Firstly, a preliminary study of the molecular structures of naringenin chalcone and naringenin as well as the assignment of their absorption and Raman features were carried out by combining Density Functional Theory (DFT) calculations and experimental evidence (see Chapter 1 for further information). From these optimized structures, the spontaneous naringenin chalcone-naringenin isomerization pathway was predicted in two different environments: water, to simulate the conversion in the cytoplasm, and *n*-octanol, to mimic the lipophilic plant cuticle matrix.

The energy barriers in both environments, using implicit solvent, were high (33.6 and 31.8 kcal/mol for water and *n*-octanol, respectively) similar to the value of conversion in vacuum (31.5 kcal/mol); thus, the spontaneous isomerisation would not be plausible in these scenarios. In water, the potential stabilizer force of H bonding must be taken into consideration due to it highly influences on proton transfer process and, hence, in the flavonoid isomerization. Consequently, additional explicit water molecules were included in the solvation model to explore

the pathway using the hybrid model named microsolvation or cluster continuum model (CCM). Molecular dynamics were performed to optimize the geometry of a given number of explicit water molecules (*n*, from none to seven). These conformations were later optimized using DFT calculations. Four molecules of explicit water resulted to be the optimum coordination number.

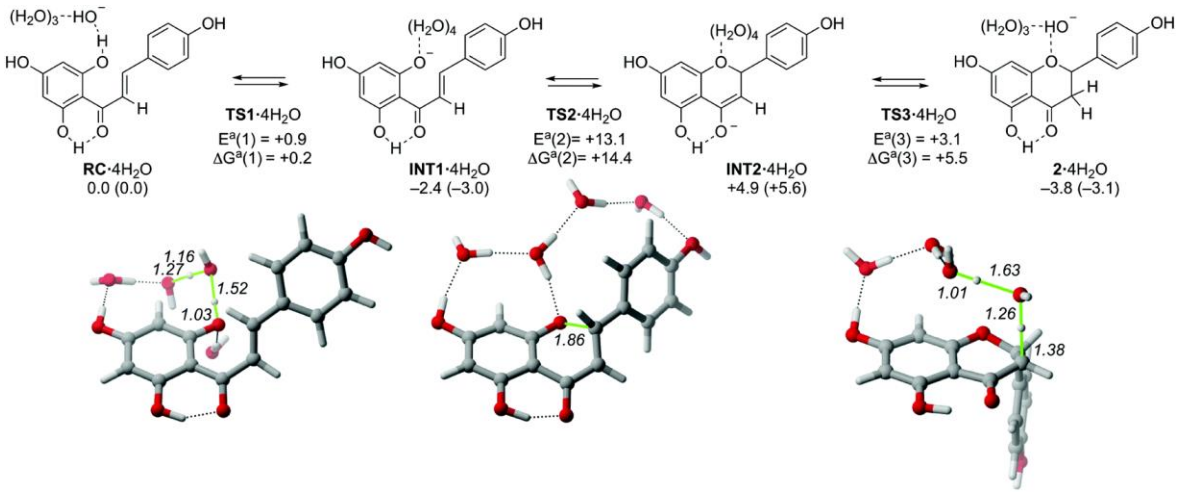

Figure 4.1. Proposed three-step naringenin chalcone-naringenin isomerization profile. This model includes explicit water molecules (n=4). Relative energies are shown under their respective geometries in kcal/mol (and relative Gibbs free energies in parentheses) calculated at B3LYP/D3(PCM)/6-31+G(d,p). E^a and ΔG^a values of each step computed at the same level are also shown in kcal/mol. Numbers displayed in transition states geometries (**TS1**·4H_2O, **TS2**·4H_2O and **TS3**·4H_2O) represent H bonding distances in Å. **RC**: reactive complex; **TS1**: transition state 1; **INT1**: Intermediate 1; **TS2**: transition state 2; **INT2**: Intermediate 2; **TS3**: transition state 3; E^a: activation energy; ΔG^a: Gibbs free energy. Reproduced with permission from (González Moreno et al., 2021). Copyright 2021 *Physical Chemistry Chemical Physics* ©.

The predicted isomerization profile is summarised in Figure 4.1. Firstly, a solvated hydroxide anion carried out the deprotonation of the naringenin chalcone to form solvated **INT1** (**INT1**·4H_2O). This intermediate performed the cyclization, which was the rate-determining step (ΔG^a=14.4 kcal/mol). The formation of this **INT2**·4H_2O was a thermodynamically unfavoured process (relative Gibbs free

energy of +5.6 kcal/mol), pointing towards the protonation of **INT2**·4H_2O as the driving force of the reaction (relative Gibbs free energy of -3.1 kcal/mol).

In light of the foregoing, the naringenin chalcone-naringenin isomerization would be more likely to occur in an aqueous environment than in *n*-octanol favoured by its dielectric constant and the formation of H-bonding networks. Thereupon and extrapolating these results to the plant scenario, the chemical isomerization of the flavonoid should take place within the hydrophilic cytoplasm and be later transported to the hydrophobic plant cuticle, rather than the *in situ* interconversion within the cuticle.

An approach to in vivo conformation of flavonoids within tomato fruit cuticle

From above, the coexistence of naringenin chalcone and naringenin within the cuticle scenario might be plausible. The potential formation of naringenin *clusters* within tomato fruit cuticle at high concentration of flavonoids has been previously postulated. In the present doctoral thesis, the aggregation process of both flavonoid isomers, naringenin and naringenin chalcone, has been explored by DFT calculations mimicking the cuticle environment.

Six naringenin homodimers **(2,2)** (structures shown in Chapter 1) derived from its X-ray structure were examined in *n*-octanol by calculating their binding energy ($E_{binding}$(X,Y)) and Gibbs free energy of formation (ΔG_f^0(X,Y)) (see data in Chapter 1). A negative value of $E_{binding}$(X,Y) or ΔG_f^0(X,Y) was indicative of a energetically favoured aggregation process. Only the dimers stabilized by H-bonding or π-π stacking existed as minima; the others advanced to π-π stacked arrangements. The research was expanded to additional **(2,2)** π-π stacked conformers (schematic representation shown in Figure 4.2a). Similarly, analogous conformers of naringenin chalcone homodimers **(1,1)** and naringenin chalcone-naringenin heterodimers **(1,2)** were also explored (Figure 4.2a). The $E_{binding}$(X,Y) were negative for all the studied dimers (see Chapter 1), pointing towards flavonoids had tendency to aggregate among them. Moreover, π-π stacking resulted to be, in most cases, more significant interactions than H-bonding.

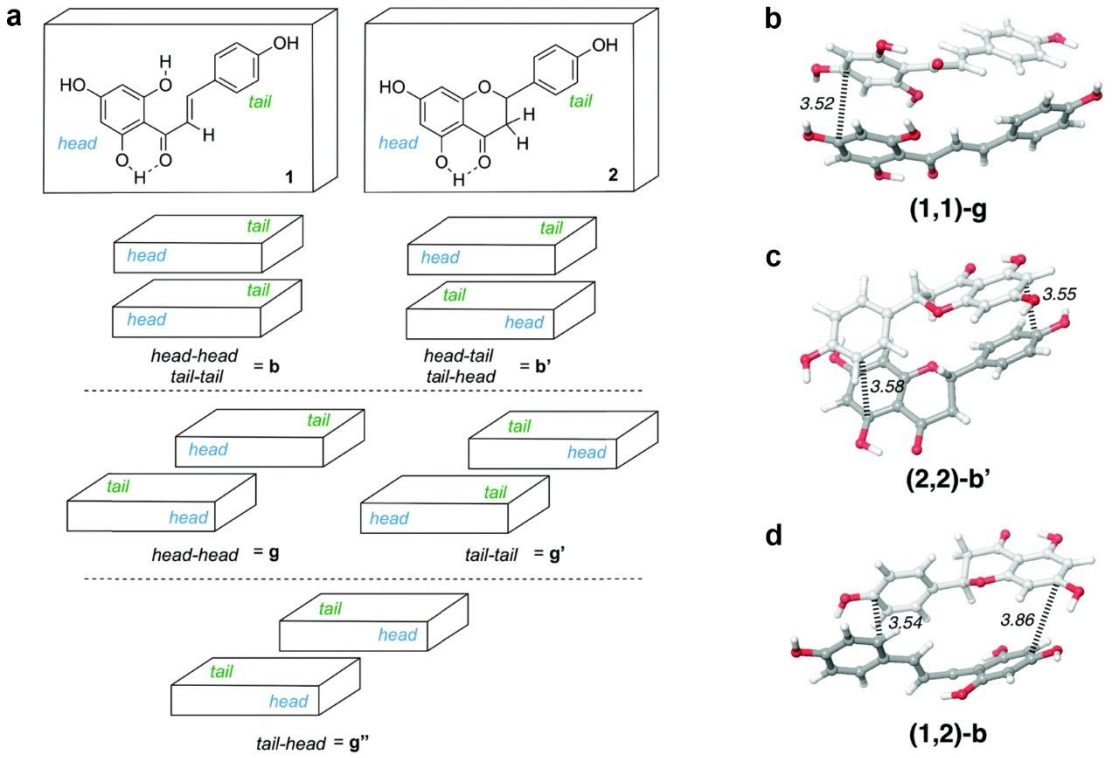

Figure 4.2. (a) Schematic representation of the explored π-π stacked dimers of naringenin chalcone (**1**) and naringenin (**2**). Optimized geometries of the most stable (b) **(1,1)** homodimer, (c) **(2,2)** homodimer and (d) **(1,2)** heterodimer computed at ωB97XD(PCM, *n*-octanol)/6-31+G(d,p) level. Numbers in (b-d) show interaction distances in Å. Adapted with permission from (González Moreno et al., 2021). Copyright 2021 *Physical Chemistry Chemical Physics* ©.

Considering thermal corrections (values of ΔG_f^0(X,Y) in Chapter 1), the aggregation process resulted to be thermodynamically favourable only for **(1,1)-g** (ΔG_f^0(X,Y)= -3.6 kcal/mol, see optimized geometry in Fig. 4.2b). Differences in ΔG_f^0(X,Y) of around 2 kcal/mol indicated an effective thermal equilibrium among those conformers. For **(2,2)** homodimers only a slight thermodynamic priority to aggregate was observed for **(2,2)-b´** (ΔG_f^0(X,Y)= -1 kcal/mol, see optimized geometry in Fig. 4.2c). For **(1,2)** heterodimers, no preference among dimers was noticed due to the low differences among their calculated ΔG_f^0(X,Y). In brief, it was hypothesized that naringenin chalcone and naringenin mainly dimerized through π-π stacking, and that the formation of homodimers was slightly favoured in

comparison to heterodimers. This potential aggregation might have an influence on the biophysical properties of the plant cuticle.

In-depth location and microchemistry of tomato fruit cuticle along fruit development

The spatial location of cuticle components and their changes during development have not been successfully achieved yet (see *General Introduction* for more details*)*. Confocal Raman Microscopy (CRM) combined with multivariate approaches intended to fill this knowledge gap in the present doctoral thesis.

Average Raman spectra of cross sections of tomato fruit cuticles isolated from different stages of development revealed an overall increase in band intensity along fruit development and a slight band shift towards lower wavenumbers during ripening. The integration of the purest bands assigned to main cuticle components (cutin, phenolics and flavonoids, see Chapter 2 for assignment details) allowed to get a semi-quantitative general view of changes in cuticle composition through fruit development and ripening. Briefly, the total phenolics band was constant during fruit growth, while a harsh increase was detected during ripening. The cutin sign increased from 8 to 15 daa and it was almost constant until red ripe stage. Band assigned to flavonoids, only detected during ripening, experimented a steep increase from 40 to 55 daa. The flavonoid/phenolics ratio suggested that the increase in total phenolics during ripening was mainly associated to the emergence of flavonoids. Neither polysaccharides nor waxes could be selectively resolved due to the masking effect of other cuticle components.

Univariate analysis by the integration of the above-mentioned bands, was employed as first approach to track the location of main cuticle components. Although this analysis unveiled significant novel information about depth profiling of cuticle from unripe fruits, it showed limitations regarding the selective location of hydroxycinnamic acid derivates (mainly *p*-coumaric acid) and *p*-hydroxybenzoic acid.

To overcome the limitations of univariate analysis, nonnegative matrix factorization (NMF) was employed to selectively calculate basis spectra sharing

Raman features. Despite the complex nature of the plant cuticle, the analysis of multiple stages of development of tomato fruit provided the opportunity to find some pixels where one or another cuticle component was exclusively present. From 12 daa, an almost pure basis spectrum for phenolics (with minor contribution of water and cutin) was extracted (turquoise in Fig 4.3a and 4.3d), which was mainly located as a thin superficial layer close to the environment. The purest basis spectrum for cutin, homogenously distributed along the depth of the cuticle, was found at 25 daa (blue in Fig. 4.3b and 4.3e), yet including few signals from polysaccharides and waxes. Selective distinction of the flavonoid fraction could not be achieved even at 40 daa. The richest spectrum in flavonoids was found in 40 daa (yellow in Fig. 4.3c and 4.3f) as a layer underneath phenolics, also including some features from phenolics and cutin.

The three representative basis spectra of main cuticle components were verified by the Orthogonal Matching Pursuit (OMP) algorithm in conjunction with a reference library of 149 entities including water, cutin from a recombinant inbred line (RIL115) and a large set of aromatics, lipids, minerals and carbohydrates. Interestingly, esterified *p*-coumaric acid (ethyl *p*-methoxycinnamate) was selected from the library instead of free *p*-coumaric acid in both, phenolics and flavonoids basis spectra, in agreement with previously reported esterification evidence between phenolics and cutin monomers. This suggested the potential role of phenolics as esterified wax component and as linkers between cutin and polysaccharides or as non-lipid monomers of cutin. Free naringenin chalcone was neither identified, being methoxylated and glycosylated modifications of this molecule (hesperidin methyl chalcone and flavokavain C) which explained the flavonoids basis spectrum. Aglycones often methoxylated has been reported to be present in superficial flavonoids in plants. It is worth mentioning that the structural isomer naringenin was not selected by the algorithm in any stage of development. Linear combination at each pixel of these three verified basis together with an extra water basis, *via* basis analysis, generated false colour maps of the location of main cuticle components along the thickness of the cuticle of all the studied stages of development (see Chapter 2 for more details).

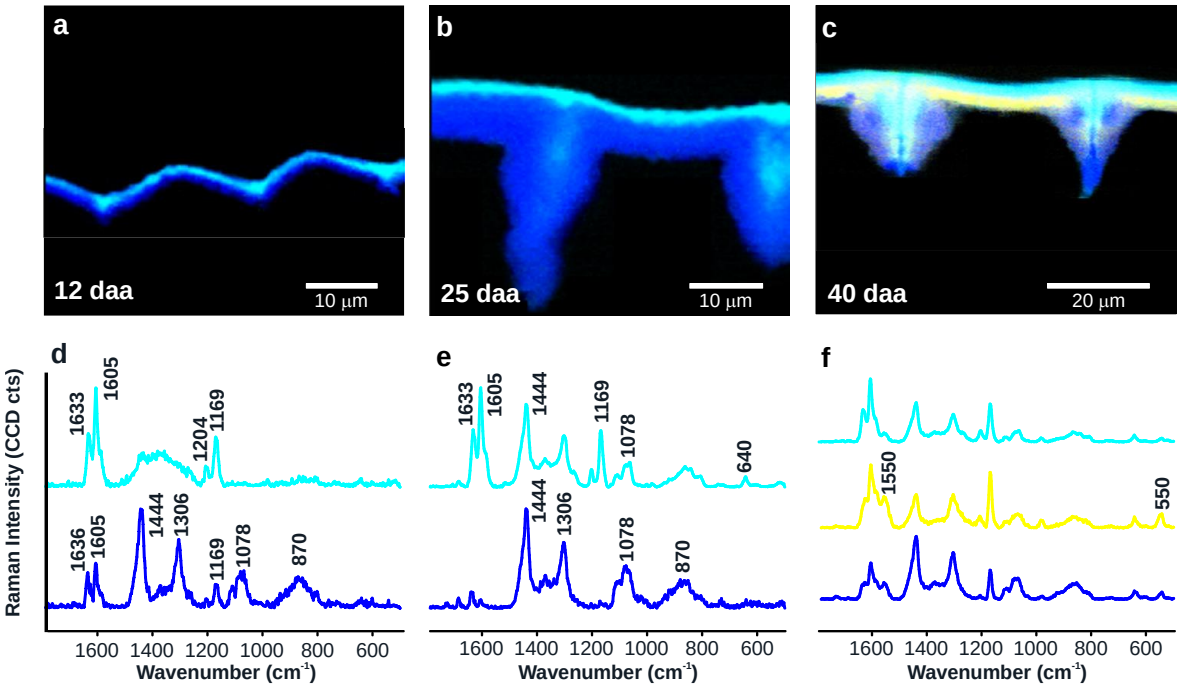

Figure 4.3. Component distribution maps of cross sections of isolated tomato fruit cuticles at (a) 12, (b) 25 and (c) 40 daa. Basis spectra calculated from unmixing analysis (NMF) for (d) 12, (e) 25 and (f) 40 daa stages of development. Adapted with permission from (González Moreno et al., 2023a). Copyright 2023 *Plant Physiology* ©.

Similarly, OMP algorithm in combination with the above-described reference library was directly applied to the hyperspectral dataset of the different stages of development of tomato fruit cuticle. This analysis allowed to selectively locate specific compounds of the library at every pixel of the images. Regarding phenolics, in early stages of development *p*-coumaric acid (mainly as an ester) and *p*-hydroxybenzoic acid co-located forming a superficial layer close to the environment as well as in the middle area of the pegs (cutinized anticlinal epidermal wall). Nevertheless, in mature stages the ester of *p*-coumaric acid (ethyl *p*-methoxycinnamate) was present throughout the cuticle. Cutin and carbohydrates could only be successfully tracked in unripe stages due to band overlapping and/or weak Raman scattering. Cutin displayed a homogenous distribution within the cuticle for all the stages; while polysaccharides were mainly accumulated underneath phenolics layer, coinciding with the location of flavonoids in ripe stages. Surprisingly, naringenin chalcone was only detected in small proportion in 40 daa.

Flavonoids features were mainly assigned to hesperidin methyl chalcone and flavokavain C as it was suggested from the verification of the basis. It should be noted that in ripe stages the error of the fit was higher which pointed towards the emergence of interactions among cuticle components in ripe stages (see Chapter 2 for more details). Figure 4.4 summarizes the three different scenarios which could be distinguished along fruit development, based on the microdistribution of the main cuticle components.

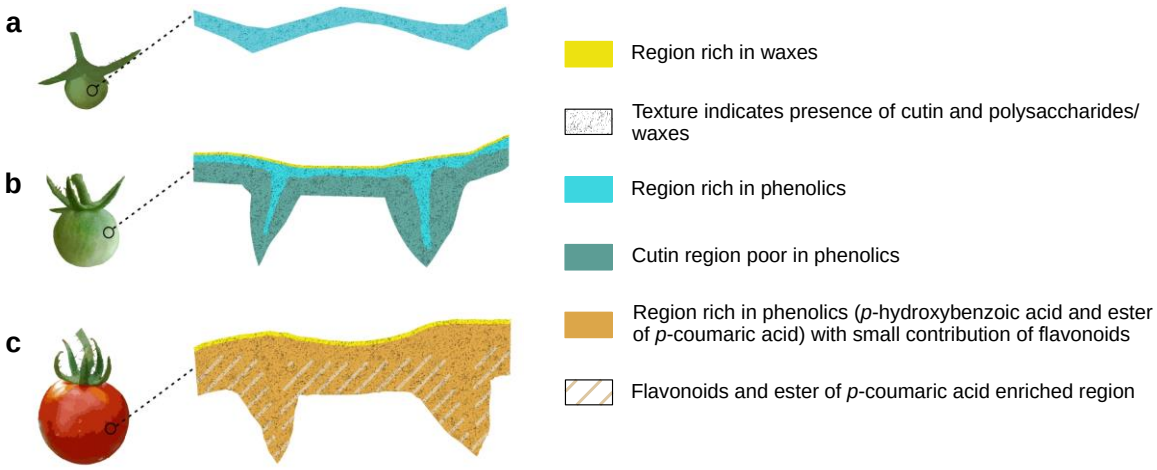

Figure 4.4. Schematic models of the distribution of main cuticle components in cross sections of tomato fruit cuticle in (a) the earliest stages of development, (b) remaining growing period and (c) ripening. Adapted with permission from (González Moreno et al., 2023a). Copyright 2023 *Plant Physiology* ©.

Thermal and optical behaviour of tomato fruit cuticle along fruit development

The essential role of the plant cuticle in protecting plant tissues from excessive heat and/or radiation has been widely agreed. Nevertheless, thermal and optical properties of plant cuticles have been meagerly studied to date and many questions remain still uncertain. Especially, changes that these biophysical properties need to undergo throughout the growth and ripening of fruits have not been explored in detail.

Differential scanning calorimetry (DSC) thermograms of isolated cuticles membranes (CMs), dewaxed (DW) cuticles and cuticles after waxes and polysaccharides removal (cutin matrixes) from different stages of development of tomato fruit were registered (Chapter 3). A second-order event, a glass transition (T_g), was clearly observed in green fruit stages (15-35 daa) delimiting a temperature where the cuticle behaved as a rigid glassy material (below T_g) and where it changed into a rubbery polymer (over T_g). The T_g became more blurred and shifted toward higher temperature during ripening. For green fruit stages the T_g was below 0ºC (Figure 4.5a); consequently, at usual environmental temperatures, the cuticle behaved as a viscous and more fluidized polymer. Nevertheless, the T_g increased up to 20-35ºC (Figure 4.5a) during ripening, a range of temperature where plants usually grow and live. It implied that cuticle could be changing from a rigid to a viscous state depending on daily or seasonal temperature fluctuations. Additionally, a slight endothermic process around 55 ºC was solely evidenced in thermograms of CMs, which was assigned to epi and intracuticular wax melting.

Intracuticular waxes were considered to behave as fillers, slightly reducing the molecular mobility within the tomato fruit cuticle framework, and consequently, shifting the T_g towards higher temperatures. Nevertheless, a very subtle reduction was observed when the T_g of CMs and DW cuticles at same stage of development were compared (Figure 4.5a). Moreover, the T_g of the cutin matrixes were significantly lower than their respective CMs, yet maintaining the harsh increase in T_g from 35 daa (Figure 4.5a). The reduction was more notable during ripening which suggested that phenolics could play as potential linkers between cutin and polysaccharides. This hypothesis was backed up by ATR-FTIR (see Chapter 3 for more details). The T_g values of different stages of development (Figure 4.5a) were positively correlated to both, phenolic content for CMs and cutin matrixes, and mechanical parameters (young and storage modulus) for CMs. This correlation was stemmed from phenolics filled nanometric cavities within tomato fruit cuticle as well as they acted as linkers and cross-linkers among cuticle polymeric chains.

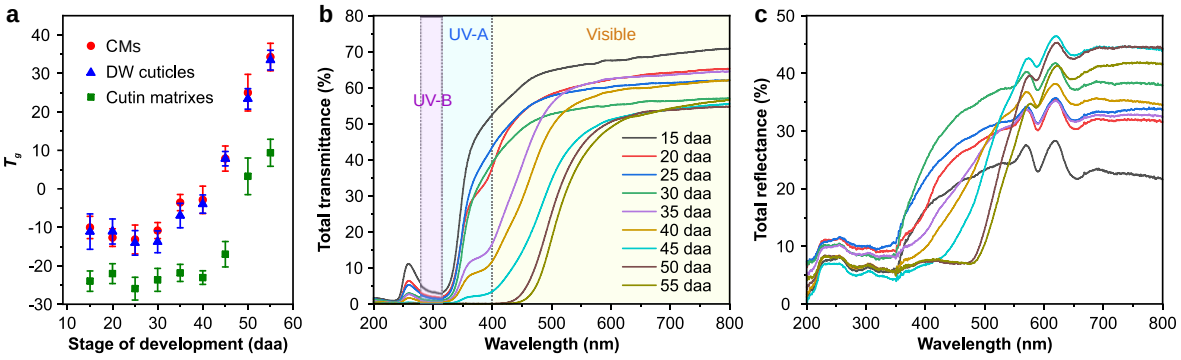

Figure 4.5. (a) Glass transition (T_g) for isolated cuticles membranes (CMs), dewaxed (DW) cuticles and cutin matrixes from different stages of development of tomato fruit. (b) Total transmittance and (c) reflectance spectra of different stages of development of tomato fruit CMs. Values in (a) are shown as mean ± standard error. Adapted with permission from (Benítez et al., 2022). Copyright 2022 *Frontiers in Plant Science* ©.

A more detailed thermal analysis of cuticles was reached calculating the reversible specific heat capacity (Cp_{rev}) by non-isothermal modulated DSC (M-DSC). An almost linear tendency between Cp_{rev} and temperature was observed, excepting for the stages of development where the T_g fell within the studied range of temperature and/or stages where the transitions were acute. The melting of waxes in CMs increased the Cp_{rev}. Generally, Cp_{rev} plots were shifted towards lower values and displayed a higher slope along fruit development. The increment of the Cp_{rev} with temperature was higher for ripe stages, which equated the protection against heat of cuticles from green and red stages of development. The Cp_{rev} for all stages of development were higher than the atmospheric air (around 1J/g^{o}C); therefore, the cuticle contributes to overcoming changes in environmental temperatures avoiding abrupt variations within plant tissues. The average Cp_{rev} (calculated within 0-50^{o}C range) were lower for CMs than for cutin matrixes attributable to lower reported Cp_{rev} of polysaccharides.

The above-mentioned superficial location of phenolic compounds within tomato fruit cuticle from early stages of development, pointed to phenolics as key compounds for photoprotection in plants. Esters of *p*-coumaric acid displayed an optimal location to cope with the incident radiation. Moreover, their chemical structure contained a double bond which has the potentiality to carry out a

photochemical *trans-cis* isomerization. The combined register of transmittance and reflectance spectra at different stages of development of tomato fruit cuticle (Figure 4.5b-c) revealed noticeable findings.

Transmittance spectra of tomato fruit cuticles showed their maximum in the visible region. A harsh decrease within UV-A range was observed until reaching an almost complete blockage in the UV-B region. The position of this strong decrease depended on the stage of development. Along fruit ripening, this harsh negative slope was progressively shifted towards higher wavelength, until reaching a cut-off wavelength of 525 nm for red ripe. A weak peak of transmittance around 260 nm was present from first stages of development, which slightly decreased along fruit development (Figure 4.5b). Transmittance in the visible region decreased along fruit development, from 70% in young stages to 53% in red ripe. Complete blockage of UV-A radiation was only detected in red ripe stage. This could be due to the incorporation of the flavonoid naringenin chalcone to the cuticle of ripe tomatoes, which shifted the maximum of absorbance of plant cuticles towards red. Additionally, a small increase in UV-A blockage was also observed during fruit growth, from 15 to 30 daa, and it was positively correlated with cuticle thickness. This suggested that, at low content of phenolics, cuticle thickness participated in reducing UV-A transmittance. The UV-B blockage was almost complete from very early stages of development, without showing significant changes along fruit growth and ripening. This blockage has been assigned to the strong absorption of the UV-B radiation by phenolics. Generally, the reflectance of tomato CMs in the UV-B and UV-A region was very low, reaching their maximum, between 20 and 45%, in the visible region for the different stages of development (Figure 4.5c). No clear relation was found between reflectance and stage of development.

DW cuticles showed comparable UV-B blockage and very similar UV-B and UV-A reflectance than CMs from same stages of development. A very minor decrease in the UV-A blockage, especially in cuticles from green stages was observed comparing CMs and their corresponding DW cuticles. Thus, it could be inferred that waxes were not involved in the UV-B reflectance, and they had a very minor contribution in the UV-A reflectance. Nevertheless, removal of waxes significatively increased the transmittance in the visible region and decreased

around 35% the reflectance in comparison to their respective CMs. Thus, waxes actively participated in filtering the visible light.

Analysis of cuticle optical properties in different plant species: unravelling the mechanism of photoprotection in plants

The previous study about optical properties of tomato fruit cuticle was expanded to fruits and leaves from additional plant species. Isolated cuticles from *Brassica oleracea* L., *Beta vulgaris* L., *Hedera helix* L., *Iris germanica* L., *Agave americana* L. and *Clivia miniata* (Lindl.) Regel leaves as well as from *Capsicum annuum* L. and *Vitis vinifera* L. fruits were selected to explore if there was a common photoprotection mechanism in plants.

In general, the plant cuticle notably filtered the UV-B and UV-C radiation. The UV-B transmittance of most of species varied between 0.3-12%, except for *I. germanica, B. vulgaris* and *B. oleracea* whose average UV-B transmittance were 28, 40 and 48 % respectively (see Chapter 4). The low amount of cuticle in *B. vulgaris* and *B. oleracea* could explain this limited blockage. The UV-A transmittance was more variable, although all the species experimented a harsh increase in this region. The maximum of transmittance, between 60-90 % depending on the species, was reached in the visible range.

Low UVR reflectance was registered for all species and increased until reaching its maximum, between 10-35%, in the visible region. The reflectance variations among species were assigned to changes in content, composition, morphology and crystallization of the epicuticular waxes. Absorbance spectra of most of cuticles showed an energetic broad band with two maxima around 220-240 and 280-310 nm respectively. Slight differences were observed for *B. oleracea, B. vulgaris* and *I. germanica* which showed a broad band apparently centred below 200 nm with a shoulder around 280-300 nm. For all species, the absorbance in the visible range, and more precisely from 500 nm, was near to zero (see Chapter 4 for more details).

The strong attenuation of the UVR was mainly ascribed to phenolics, concretely to *p*-coumaric acid, ubiquitously detected in all the studied species. Nevertheless, the mechanism by which the *p*-coumaric dissipated most of the UVR is still a conundrum. To unravel this photoprotection mechanism transient absorption spectroscopy (TAS) was employed. TAS is a pump-probe spectroscopy technique which employs two laser pulses to gain information about ultrafast dynamics of a sample of interest. The pump pulse excites a portion of molecules from the electronic ground state (S_0) to an accessible electronic excited state (S_n). A probe pulse at different time delays (Δt) monitors the population of the excite state. Tracking changes in absorbance intensity within a few nanoseconds window, in small pump-probe delay steps, enables one to garner information about relaxation pathways of excited-state molecules.

As first approach, TAS maps of a methanolic solution, powder, and an alkylcoumarate oligomer of *p*-coumaric acid were registered (Figure 4.6a-c) to study the influence of the environment on their excited state (S_1) dynamics. Additionally, a detailed kinetic decay analysis of their main TAS bands was executed to compute their evolution associated difference spectra (EADS) and their related lifetimes (τ_n). For the *p*-coumaric acid methanolic solution (Figure 4.6a), an excited state absorption (ESA) around 340-450 nm and a weak stimulated emission (SE) around 400-500 nm were detected, which very fast decayed. For solid samples, powder and oligomer of *p*-coumaric acid (Figure 4.6 b-c), a unique very broad positive band (350-550 nm) was registered, which decayed in hundreds of picoseconds (ps).

From the global analysis three main processes were distinguished in S_1 (Table 4.1). One of them, τ_4, was a very long lifetime (>ns) assigned to photoproducts that persisted beyond the measurement time, such as the formation of the *cis* isomer or radicals. Two main lifetimes were calculated to define the *trans-cis* isomerisation pathway of *p*-coumaric acid in different environments. τ_2 was referred to vibrational cooling of the molecule in the excited state, while τ_3 represented the internal conversion to recover the S_0. A first very fast lifetime (τ_1) assigned to the relaxation associated to the Franck-Condon principle was unresolved since the instrument response function (IRF) might fall within same temporal range.

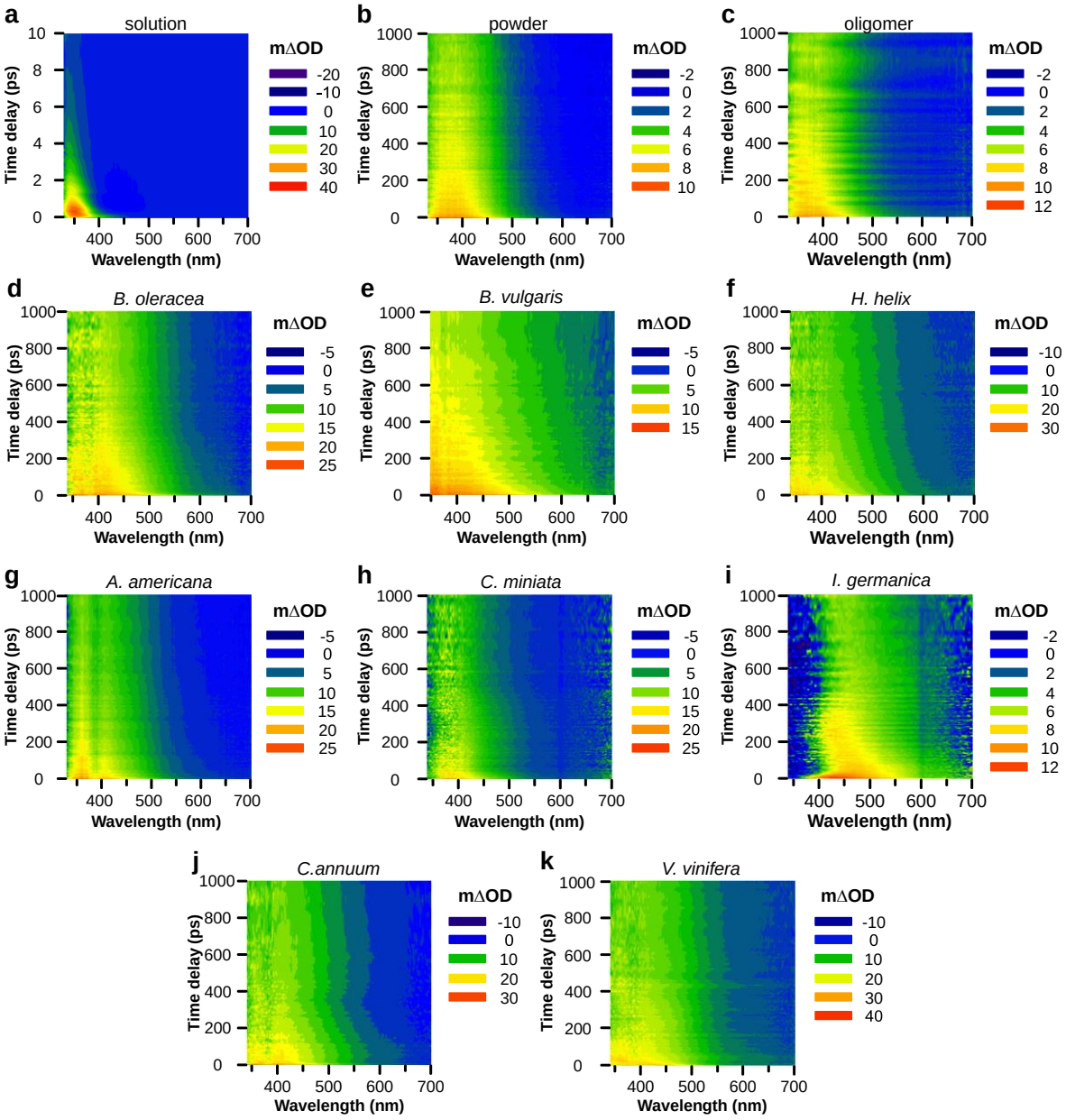

Figure 4.6. Transient absorption spectra (TAS) maps of (a) a methanolic solution of *p*-coumaric acid, (b) *p*-coumaric acid powder, (c) an oligomer of *p*-coumaric acid, isolated cuticles from (d) *B. oleracea*, (e) *B. vulgaris*, (f) *H. helix*, (g) *A. americana*, (h) *C. miniata*, (i) *I. germanica* leaves and (j) *C. annuum* and (k) *V. vinifera* fruits (excitation at 300 nm). Colour scales indicate changes in optical density (mΔOD). Adapted with permission from (González Moreno et al., 2022). Copyright 2022 *Nature Communications* ©.

The lifetimes associated to the solution of *p*-coumaric acid (see Table 4.1) revealed a fast isomerisation process, less than 2 ps. Contrary, the lifetimes for both

solid environments, powder and oligomer, were considerably higher. It might be caused by a notable decrease of degrees of freedom in solid phase. The comparison of ^{1}H-NMR spectra of a solution and powder of *p*-coumaric acid before and after irradiation revealed that the *cis* isomer was only present in solution (see Chapter 4).

Table 4.1. Summary of excited state lifetimes of *p*-coumaric acid samples, plant cuticles and fresh leaves from different plant species after excitation at 300 nm from a sequential fit. Errors are shown as twice the standard error extracted from the Global fitting. Adapted with permission from (González Moreno et al., 2022). Copyright 2022 *Nature Communications* ©.

Sample	**τ_2 (ps)**	**τ_3 (ps)**	**τ_4 (ns)**
p-coumaric acid solution	0.25 ± 0.11	1.55 ± 0.11	> ns
p-coumaric acid powder	8.98 ± 0.20	367.11 ± 5.03	> ns
p-coumaric acid oligomer	42.07 ± 1.11	438.57 ± 18.21	> ns
Brassica oleracea	4.52 ± 0.13	249.33 ± 4.16	> ns
Beta vulgaris	46.55 ± 0.93	689.70 ± 16.36	> ns
Hedera helix	6.55 ± 0.29	260.00 ± 3.42	> ns
Agave americana	10.93 ± 0.22	284.65 ± 3.39	> ns
Clivia miniata	15.92 ± 0.78	365.47 ± 10.14	> ns
Iris germanica	17.26 ± 0.74	407.33 ± 12.18	> ns
Capsicum annuum	5.02 ± 0.17	249.31 ± 3.15	> ns
Vitis vinifera	9.61 ± 0.33	207.08 ± 3.06	> ns
Adiantum raddianum	7.48 ± 0.26	319.38 ± 3.60	> ns
Cycas revoluta	3.23 ± 0.12	97.13 ± 4.69	> ns
Araucaria bidwillii	6.31 ± 0.11	362.20 ± 6.44	> ns

These two solid environments have been employed as approaches to simulate potential conformations of *p*-coumaric acid (free or esterified to cutin monomers) within a restricted environment, such as the plant cuticle. TAS maps of isolated cuticles (Figure 4.6d-k) were similar to those from *p*-coumaric in solid environments. A broad band around 340-450 nm was identified as unique band for most of species, excepting for *B. vulgaris* which displayed a broader signal (up to 500 nm) and *I. germanica* whose signal was shifted towards red (400-550 nm). Although maps from all species were fitted to three lifetimes, their values were varied (see Table 4.1). The τ_2 was in general comparable or lower than that calculated for the powder of *p*-coumaric acid. Exceptionally, *I. germanica* and *C. miniata* showed lifetimes between the powder and the oligomer, and *B. vulgaris* similar to the oligomer. The trend of the τ_3 was similar to the explained for τ_2, except for a longer lifetime for *B. vulgaris.* Cutan was detected as main polymer in *B. vulgaris* cuticle. The higher rigidity of this polymer could explain the longer lifetimes calculated for this species in comparison to the rest.

TAS maps of fresh leaves from *Adiantum raddianum*, *Cycas revoluta* and *Araucaria bidwilli* were also registered. A broad band around 350-450 nm was observed for these species (see Chapter 4), which was in consonance with data from isolated cuticles. Their associated lifetimes were also within same range (Table 4.1), being even lower for *C. revoluta*. This proved the superficial nature of TAS measurements.

Despite the difference among species a common process against radiation could be surmised. To inspected it, a computational study of the *trans-cis* photoisomerization pathway of *p*-coumaric acid in two environments, mimicking a methanolic and a solid environment respectively, was carried out combining Time-Dependent Density Functional Theory (TD-DFT), Complete Active Space Self-Consistent Field (CASSCF) and Complete Active Space Second Order Perturbation Theory (CASPT2). Significance differences were observed between the isomerization pathway in both environments (summarized in Figure 4.7).

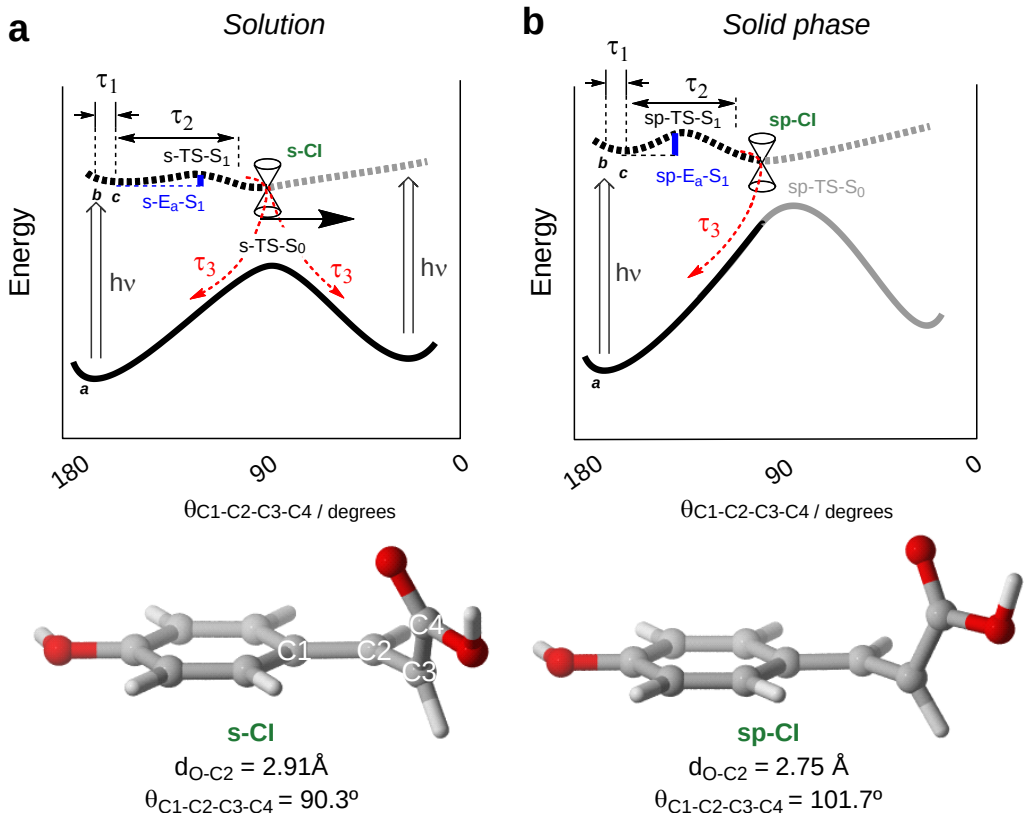

Figure 4.7. Postulated photoprotection mechanism *via trans-cis* isomerization profile of *p*-coumaric acid in (a) a solvated and (b) a solid environment computed at ωB97XD(PCM,methanol)/6-31+g(d,p) and ωB97XD/6-31+g(d,p), respectively. In the bottom, conical intersections (CI), computed at CASSCF(12,11)/PCM,methanol/6-31+G(d) and CASSCF(12,11)/6-31+G(d), associated to both mechanisms are shown. Adapted with permission from (González Moreno et al., 2022). Copyright 2022 *Nature Communications* ©.

After UV excitation, the *p*-coumaric acid experimented a very fast vertical excitation to reach the S_1 preserving the geometry of the molecule in the ground state (S_0). The relaxation time of this geometry in the excited state associated to the Franck-Condon principle corresponded to τ_1 (See Figure 4.7). Subsequently, the molecule performed changes in its geometry along τ_2 approaching towards a conical intersection (CI), molecular geometries where S_0 and S_1 potential energy surfaces crossed. For solution, these conformational changes were barrierless according to CASPT2 results, while a free energy activation barrier of around 9 kcal/mol was predicted for solid environment. Lastly, within τ_3 the molecule crossed the CI and returned to the ground state. The difference between solvated and solid phase largely lied in the position of the CI. In solution, the CI was located at the C1-

C2-C3-C4 dihedral ($\theta_{C1-C2-C3-C4}$, see Figure 4.7 for atom labels) of 90.3º (Figure 4.7a), which was over the transition state (TS) geometry, $\theta_{C1-C2-C3-C4}$= 94.5º. This meaned that after crossing the CI the molecule could continue the isomerization until reaching the *cis* isomer or recovering the *trans* conformer in the S_0. Nevertheless, in solid environment the CI was detected sooner, $\theta_{C1-C2-C3-C4}$= 101.7º; consequently, additional energy would be required to reach the TS and to complete the isomerisation towards the *cis* isomer. Therefore, in solid phase the τ_3 represented the recovering of the *trans* isomer of *p*-coumaric acid in S_0.

From above, it could be inferred that plant cuticle dissipated a great fraction of the UVR which reached the plant through an ultrafast non-radiative mechanism. A non-radiative deactivation mechanism by an early CI for *p*-coumaric acid bypassed the isomerization to *cis*. This attenuation of the incident radiation could be complemented by other minor channels of energy dissipation, such as cuticle fluorescence or reflection, which varied from 3 to 10% among the studied species. These complementary and cooperative mechanisms of photoprotection are summarized in Figure 4.8.

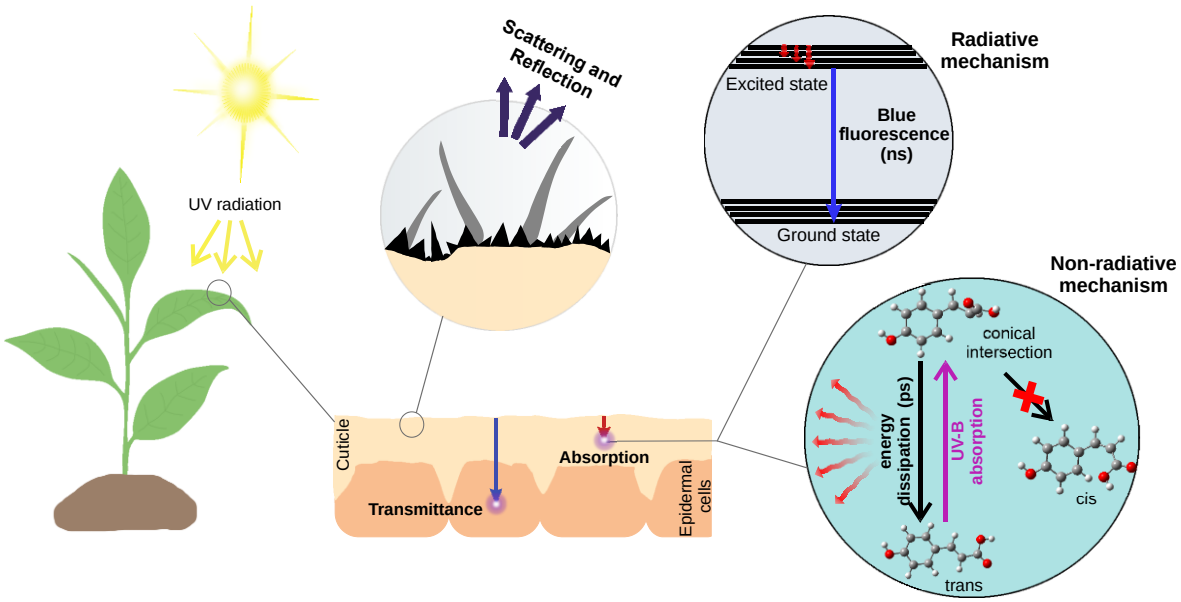

Figure 4.8. Schematic representation of different mechanisms involved in plant photoprotection. Reproduced with permission from (González Moreno et al., 2022). Copyright 2022 *Nature Communications* ©.

Additionally, underneath layers such as outer epidermal cell wall, also contained phenolic compounds which could screen the remaining UVR, via isomerization or CI depending on the environment. This secondary protection was especially important in species with high transmittance percentage in this range. This photoprotection mechanism seemed to be shared among different plant species and preserved from ancient plants, indeed *p*-coumaric acid has been detected even in fossil plant cuticles.

Synergic effect of phenolic compounds in plant photoprotection

Different types of phenolic compounds are present within the plant cuticle. For instance, in tomato fruit, naringenin chalcone appears within the plant cuticle during ripening. As it was pointed in Chapter 2, phenolic compounds, mainly the ester of *p*-coumaric acid, was detected throughout the cuticle in ripe fruits, collocating with flavonoids mainly in the inner side of the cuticle. In the present doctoral thesis, the naringenin chalcone photodynamics as well as the influence of the presence of naringenin chalcone on *p*-coumaric acid excited state dynamics were explored through molecular spectroscopy in solution.

The photodegradation profile of *p*-coumaric acid in ethanol revealed a decrease of around 29% in its main absorption band, centred at 312 nm, after two hours of solar irradiation. Moreover, signs of the formation of the *cis* isomer were detected through comparing the absorption spectra of *p*-coumaric acid pre- and post-solar irradiation (see Chapter 5). In contrast, the naringenin chalcone-only experiments showed a mild decreased around 2% of its maximum of absorption at 365 nm following solar irradiation. ^{1}H-NMR spectra of a solution of naringenin chalcone pre- and post-irradiation at 365 nm showed no *trans-cis* isomerization. The absorbance spectrum of an equimolar mixture of both compounds returned (essentially) the sum of the individual absorbance spectra, showing two bands centred at 312 and 365 nm, respectively. The first band associated to the *p*-coumaric acid decreased approximately 20% after 2 hours of solar irradiation; while the band related to naringenin chalcone experienced a similar mild decrease in absorption, akin to that observed in a solution of naringenin chalcone.

The deactivation of *p*-coumaric acid was mainly non-radiative facilitated by a CI geometrically similar to the TS in S_0 as reported in Chapter 4. Consequently, both *trans* and *cis* isomers could be reached after vibrational cooling. Complementary, *p*-coumaric acid after UV excitation displayed a very weak blue fluorescence around 380 nm. Mixtures with increasing amount of naringenin chalcone quenched this fluorescence until almost being extinguished for the 50 μM of *p*-coumaric acid: 60 μM of naringenin chalcone mixture. This quenching was asymmetrical due to a higher light attenuation in the maximum absorption range of naringenin chalcone. The formation of a complex between *p*-coumaric acid and naringenin chalcone mixtures was proposed to be unlikely due to the absence of additional absorption bands nor broadening of the existing ones, even at equimolar mixtures of 10 mM. Consequently, the possibility of static quenching was discarded. A Stern-Volmer plot of the quenching mixtures positively deviated from linearity at concentrations higher than 25 μM of naringenin chalcone with the concentration of *p*-coumaric acid kept constant at 50 μM. This behaviour has been previously related to dynamic quenching, characterized by the deactivation of the S_1 of the fluorophore by collision with the quencher. In this way, Förster resonance energy transfer appeared to be the most plausible explanation for the quenching observed in the mixtures. This type of dynamic quenching requires a separation between partner fluorophore and quencher of 10-100 Å as well as spectral overlap of the emission spectrum of fluorophore and the absorption spectrum of the quencher. Extrapolating these conclusions to the cuticle scenario, the establishment of dipole-dipole interactions could imply a cotransport of *p*-coumaric acid and flavonoid from the cytoplasm to the plant cuticle. A latter approach inside the cuticle would be more unlikely due to the restrictive mobility within the matrix. The potential biological implications of this quenching in ripe stages deserves further investigation.

TAS spectra of ethanolic solutions of *p*-coumaric acid, naringenin chalcone and an equimolar mixture of both phenolics (excitation at 312 nm) were recorded (Figure 4.9 *left*). It should be mentioned that both phenolic compounds absorbed some portion of radiation at this wavelength (see absorption spectra in Chapter 5). For the solution of *p*-coumaric acid, a strong ESA around 375 nm was detected as well as additional lower absorptions around 330, 390 and 600 nm, respectively

(Figure 4.9a). Three lifetimes were computed from a sequential kinetics analysis. A very fast τ_1 (~180 fs) was defined as the time of the relaxation profile in the S_1 while approaching the CI. Based on data from its isomerization pathway (Chapter 4), this CI would be slightly over the TS. Consecutively, the τ_2 (~1.5 ps) included traversing the CI and then non-radiative recovering to the ground state of both *cis* and *trans* isomers. The signatures from the τ_3 (>> 2 ns, blue in Figure 4.9a *right*) have been ascribed to the formation of the *cis* isomer (at 330 nm), phenoxyl radicals (at 390 nm) and solvated electrons (at 600 nm).

For the solution of naringenin chalcone, a strong ESA around 420 nm and a ground state bleaching (GSB) around 360 nm were detected after exciting at 312 nm (Figure 4.9b). As noted above, naringenin chalcone did not isomerize post irradiation. Therefore, a different mechanism of deactivation was proposed. A fast τ_1 (~580 fs) was defined as the time of the relaxation profile in the S_1 while approaching to the CI. DFT/CASSCF calculations were employed to explore the S_0 and S_1 energetic surfaces of naringenin chalcone and to potentially locate a CI. An "early" CI was computed, meaning the molecule deactivated non-radiatively, returning to its *trans* isomer. These results agreed with NMR data which revealed a lack of isomerization for this molecule post irradiation. Therefore, τ_2 for naringenin chalcone (~3 ps) was ascribed to traversing the CI and subsequent vibrational cooling of the *trans* isomer. A long τ_3 (~1 ns) suggested the presence of some molecules trapped in excited states. For naringenin chalcone, TAS experiments were additionally performed exciting the solution at 365 nm, showing similar values of τ_1 and τ_2, but a shorter τ_3 (see Chapter 5 for more details).

TAS was also carried out on an equimolar mixture of *p*-coumaric acid and naringenin chalcone after exciting at 312 nm (Figure 4.9c). The TAS of the mixture did not result in the sum of the TAS from the individual compounds; instead, it showed strong similarities with the TAS maps and EADS of the solution of naringenin chalcone. τ_1 for the mixture (~540 fs) was comparable to that observed for the naringenin chalcone solution. However, τ_2 and τ_3 were longer, ~4 ps and >2 ns respectively. It could be due to the formation of interactions between naringenin chalcone and *p*-coumaric acid in the mixture, as suggested by the quenching experiment. A detailed inspection of the τ_3 revealed features from both molecules.

From *p*-coumaric acid, a very weak band was detected at 330 nm as well as a broad band around 600 nm; and from naringenin chalcone the GSB was observed around 360 nm. TAS map of the mixture exciting at 365 nm was similar to the solution of naringenin chalcone but their associated lifetimes were shorter (see Chapter 5 for more details).

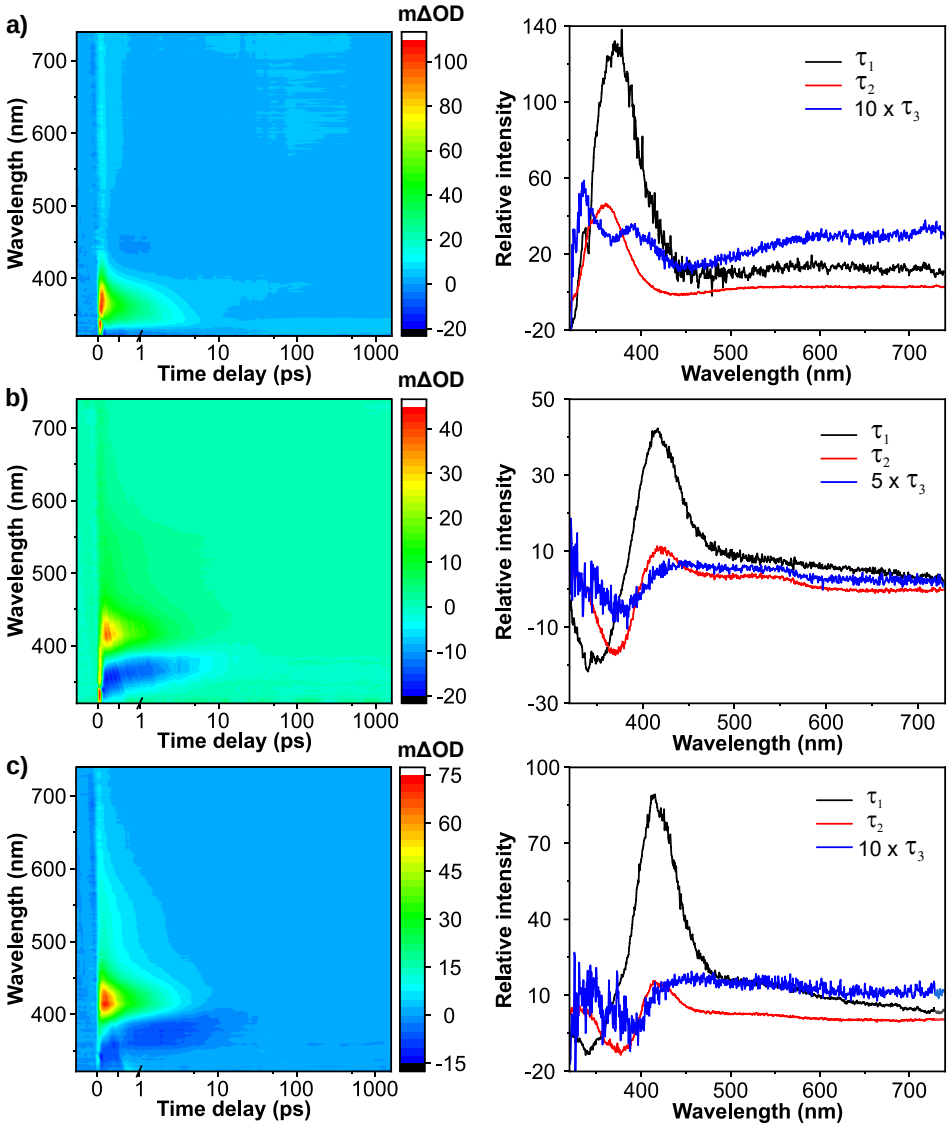

Figure 4.9. Transient absorption spectra (TAS) maps (*left*) and evolution associated difference spectra (EADS) computed by sequential fit (*right*) of an ethanolic solution of (a) *p*-coumaric acid, (b) naringenin chalcone and (c) an equimolar mixture of *p*-coumaric acid and naringenin chalcone after excitation at 312 nm. Colour scales indicate changes in optical density (mΔOD). Reproduced with permission from (González Moreno et al., 2023b). Copyright 2023 Physical Chemistry Chemical Physics ©.

In summary, extrapolating data obtained in solution to the plant cuticle, a potential dipole-dipole interaction between collocating *p*-coumaric acid and naringenin chalcone within the tomato fruit cuticle is proposed, implying a synergic effect of both compounds in photoprotection against UVR. Further studies are necessary to understand the biological implications of these interactions.

References

Benítez JJ, González Moreno A, Guzmán-Puyol S, Heredia-Guerrero JA, Heredia A, Domínguez E (2022) The response of tomato fruit cuticles against heat and light. *Front Plant Sci* **12**: 807723

González Moreno A, de Cózar A, Prieto P, Domínguez E, Heredia A (2022) Radiationless mechanism of UV deactivation by cuticle phenolics in plants. *Nat Commun* **13**: 1786

González Moreno A, Domínguez E, Mayer K, Xiao N, Bock P, Heredia A, Gierlinger N (2023a) 3D (x-y-t) Raman imaging of tomato fruit cuticle: Microchemistry during development. *Plant Phisiology* **191**: 219–232

González Moreno A, Prieto P, Ruiz Delgado MC, Domínguez E, Heredia A, De Cózar A (2021) Structure, isomerization and dimerization processes of naringenin flavonoids. *Phys Chem Chem Phys* **23**: 18068–18077

González Moreno A, Woolley JM, Domínguez E, De Cózar A, Heredia A, Stavros VG (2023b) Synergic photoprotection of phenolic compounds present in tomato fruit cuticle: a spectroscopic investigation in solution. *Phys Chem Chem Phys* **25**: 12791-12799

5. CONCLUSIONS

Conclusions

The main conclusions derived from this doctoral thesis are:

1. The isomerization barrier of naringenin chalcone-naringenin conversion shows that the cyclization of naringenin chalcone only occurs in a water environment, thus highlighting the relevance of the H bonding network in this mechanism. Additionally, naringenin chalcone tends to aggregate by π-π stacking interactions in an *n*-octanol environment.

2. The micro-distribution of phenolic compounds across the tomato fruit cuticle changes with development. While phenolic acids incorporated during growth locate to the outermost region, *p*-coumaric acid and naringenin chalcone accumulated during ripening are present throughout the entire cuticle.

3. A synergic photoprotection effect based on dipole-dipole interactions is detected in a solution of naringenin chalcone and *p*-coumaric acid, the main phenolic compounds present in tomato fruit cuticle. Förster energy transfer may explain the quenching of the fluorescence from *p*-coumaric acid by naringenin chalcone.

4. The optical properties of tomato fruit cuticle are mainly ascribed to phenolic compounds and waxes. Phenolic acids provide UV-B blockage from early stages of development and naringenin chalcone accumulation during ripening expands photoprotection to the UV-A region. Waxes only participate in visible light reflection.

5. Identification of a conserved photoprotective mechanism based in an ultrafast and non-radiative excited state deactivation of *p*-coumaric acid, in combination with fluorescence emission, reveals that the cuticle can be considered the first and most important barrier against UV-B radiation.

ANNEXE

Licenses

Published papers

Structure, isomerization and dimerization processes of naringenin flavonoids

3D (x-y-t) Raman imaging of tomato fruit cuticle: microchemistry during development

The response of tomato fruit cuticle membranes against heat and light

Radiationless mechanism of UV deactivation by cuticle phenolics in plants

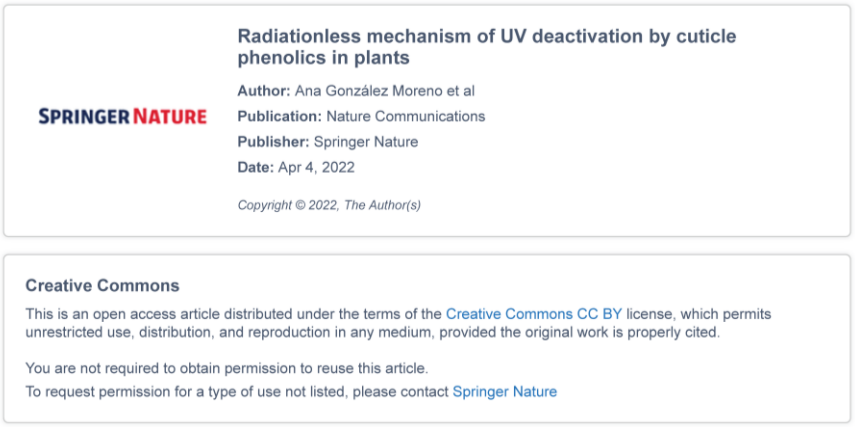

SPRINGER NATURE

Radiationless mechanism of UV deactivation by cuticle phenolics in plants

Author: Ana González Moreno et al
Publication: Nature Communications
Publisher: Springer Nature
Date: Apr 4, 2022

Copyright © 2022, The Author(s)

Creative Commons

This is an open access article distributed under the terms of the Creative Commons CC BY license, which permits unrestricted use, distribution, and reproduction in any medium, provided the original work is properly cited.

You are not required to obtain permission to reuse this article.
To request permission for a type of use not listed, please contact Springer Nature

Synergic photoprotection of phenolic compounds present in tomato fruit cuticle: a spectroscopic investigation in solution

Synergic photoprotection of phenolic compounds present in tomato fruit cuticle: a spectroscopic investigation in solution

A. González Moreno, J. M. Woolley, E. Domínguez, A. de Cózar, A. Heredia and V. G. Stavros, *Phys. Chem. Chem. Phys.*, 2023, **25**, 12791 **DOI:** 10.1039/D3CP00630A

Figures

Figure 1.1

Figure 1.2

ELSEVIER LICENSE
TERMS AND CONDITIONS

Apr 06, 2023

This Agreement between Mrs. Ana González Moreno ("You") and Elsevier ("Elsevier") consists of your license details and the terms and conditions provided by Elsevier and Copyright Clearance Center.

License Number	5523001054641
License date	Apr 06, 2023
Licensed Content Publisher	Elsevier
Licensed Content Publication	Environmental and Experimental Botany
Licensed Content Title	Revisiting the architecture, biosynthesis and functional aspects of the plant cuticle: There is more scope
Licensed Content Author	Vishalakshi Bhanot,Shreya Vivek Fadanavis,Jitendra Panwar
Licensed Content Date	Mar 1, 2021
Licensed Content Volume	183
Licensed Content Issue	n/a
Licensed Content Pages	1
Start Page	104364
End Page	0
Type of Use	reuse in a thesis/dissertation
Portion	figures/tables/illustrations
Number of figures/tables/illustrations	1
Format	both print and electronic
Are you the author of this Elsevier article?	No
Will you be translating?	No
Title	Optical properties and location of phenolic compounds in plant cuticles
Institution name	Universidad de Málaga
Expected presentation date	Apr 2023
Order reference number	figuure1-2
Portions	Fig. 3

Figure 1.5

ACS Publications
Most Trusted. Most Cited. Most Read.

Sorption and Interaction of the Flavonoid Naringenin on Tomato Fruit Cuticles

Author: Eva Domínguez, Patricia Luque, Antonio Heredia
Publication: Journal of Agricultural and Food Chemistry
Publisher: American Chemical Society
Date: Aug 1, 2009

Copyright © 2009, American Chemical Society

PERMISSION/LICENSE IS GRANTED FOR YOUR ORDER AT NO CHARGE

This type of permission/license, instead of the standard Terms and Conditions, is sent to you because no fee is being charged for your order. Please note the following:

- Permission is granted for your request in both print and electronic formats, and translations.
- If figures and/or tables were requested, they may be adapted or used in part.
- Please print this page for your records and send a copy of it to your publisher/graduate school.
- Appropriate credit for the requested material should be given as follows: "Reprinted (adapted) with permission from {COMPLETE REFERENCE CITATION}. Copyright {YEAR} American Chemical Society." Insert appropriate information in place of the capitalized words.
- One-time permission is granted only for the use specified in your RightsLink request. No additional uses are granted (such as derivative works or other editions). For any uses, please submit a new request.

If credit is given to another source for the material you requested from RightsLink, permission must be obtained from that source.

BACK CLOSE WINDOW

Figure 1.6

ELSEVIER LICENSE
TERMS AND CONDITIONS

Apr 06, 2023

This Agreement between Mrs. Ana González Moreno ("You") and Elsevier ("Elsevier") consists of your license details and the terms and conditions provided by Elsevier and Copyright Clearance Center.

License Number	5523020112591
License date	Apr 06, 2023
Licensed Content Publisher	Elsevier
Licensed Content Publication	Thermochimica Acta
Licensed Content Title	Phase transitions in the biopolyester cutin isolated from tomato fruit cuticles
Licensed Content Author	Antonio J. Matas,Jesús Cuartero,Antonio Heredia
Licensed Content Date	Jan 30, 2004
Licensed Content Volume	409
Licensed Content Issue	2
Licensed Content Pages	4
Start Page	165
End Page	168
Type of Use	reuse in a thesis/dissertation
Portion	figures/tables/illustrations
Number of figures/tables/illustrations	1
Format	both print and electronic
Are you the author of this Elsevier article?	No
Will you be translating?	No
Title	Optical properties and location of phenolic compounds in plant cuticles
Institution name	Universidad de Málaga
Expected presentation date	Apr 2023
Order reference number	Figure 1-6
Portions	Fig. 1

Figure 1.7

OXFORD UNIVERSITY PRESS LICENSE TERMS AND CONDITIONS

Apr 06, 2023

This Agreement between Mrs. Ana González Moreno ("You") and Oxford University Press ("Oxford University Press") consists of your license details and the terms and conditions provided by Oxford University Press and Copyright Clearance Center.

License Number	5523020502873
License date	Apr 06, 2023
Licensed Content Publisher	Oxford University Press
Licensed Content Publication	Journal of Experimental Botany
Licensed Content Title	Mechanical properties of cuticles and their primary determinants
Licensed Content Author	Khanal, Bishnu P; Knoche, Moritz
Licensed Content Date	Sep 13, 2017
Type of Use	Thesis/Dissertation
Institution name	
Title of your work	Optical properties and location of phenolic compounds in plant cuticles
Publisher of your work	Universidad de Málaga
Expected publication date	Apr 2023
Permissions cost	0.00 EUR
Value added tax	0.00 EUR
Total	**0.00 EUR**
Title	Optical properties and location of phenolic compounds in plant cuticles
Institution name	Universidad de Málaga
Expected presentation date	Apr 2023
Order reference number	Figure 1-7
Portions	Fig. 1.

Figure 1.8

JOHN WILEY AND SONS LICENSE TERMS AND CONDITIONS

Apr 06, 2023

This Agreement between Mrs. Ana González Moreno ("You") and John Wiley and Sons ("John Wiley and Sons") consists of your license details and the terms and conditions provided by John Wiley and Sons and Copyright Clearance Center.

License Number	5523021104045
License date	Apr 06, 2023
Licensed Content Publisher	John Wiley and Sons
Licensed Content Publication	New Phytologist
Licensed Content Title	The biophysical design of plant cuticles: an overview
Licensed Content Author	Antonio Heredia, José Alejandro Heredia-Guerrero, Eva Domínguez
Licensed Content Date	Nov 25, 2010
Licensed Content Volume	189
Licensed Content Issue	4
Licensed Content Pages	12
Type of Use	Dissertation/Thesis
Requestor type	University/Academic
Format	Print and electronic
Portion	Figure/table
Number of figures/tables	1
Will you be translating?	No
Title	Optical properties and location of phenolic compounds in plant cuticles
Institution name	Universidad de Málaga
Expected presentation date	Apr 2023
Order reference number	Fig 1-8
Portions	Figure 6

Figure 1.9

CCC Marketplace

This is a License Agreement between Ana González Moreno ("User") and Copyright Clearance Center, Inc. ("CCC") on behalf of the Rightsholder identified in the order details below. The license consists of the order details, the Marketplace Permissions General Terms and Conditions below, and any Rightsholder Terms and Conditions which are included below.

All payments must be made in full to CCC in accordance with the Marketplace Permissions General Terms and Conditions below.

Order Date	06-Apr-2023	Type of Use	Republish in a thesis/dissertation
Order License ID	1342389-1		
ISSN	1545-2123	Publisher	ANNUAL REVIEWS
		Portion	Image/photo/illustration

LICENSED CONTENT

Publication Title	Annual review of plant biology	Country	United States of America
		Rightsholder	Annual Reviews, Inc.
Author/Editor	Annual Reviews, Inc.	Publication Type	e-Journal
Date	01/01/2002	URL	http://arjournals.annualreviews.org/loi/arplant.1
Language	English		

REQUEST DETAILS

Portion Type	Image/photo/illustration	Distribution	Worldwide
Number of Images / Photos / Illustrations	1	Translation	Original language of publication
Format (select all that apply)	Print, Electronic	Copies for the Disabled?	No
		Minor Editing Privileges?	Yes
Who Will Republish the Content?	Academic institution	Incidental Promotional Use?	No
Duration of Use	Life of current edition	Currency	EUR
Lifetime Unit Quantity	Up to 499		
Rights Requested	Main product		

NEW WORK DETAILS

Title	Optical properties and location of phenolic compounds in plant cuticles	Institution Name	Universidad de Málaga
		Expected Presentation Date	2023-04-13
Instructor Name	Ana González Moreno		

ADDITIONAL DETAILS

Order Reference Number	Figure 1-9	The Requesting Person/Organization to Appear on the License	Ana González Moreno

REQUESTED CONTENT DETAILS

Title, Description or Numeric Reference of the Portion(s)	Figure 2	Title of the Article/Chapter the Portion Is From	The Shikimate Pathway and Aromatic Amino Acid Biosynthesis in Plants
Editor of Portion(s)	Ana González Moreno	Author of Portion(s)	Annual Reviews, Inc.

Volume of Serial or Monograph	N/A	Issue, if Republishing an Article From a Serial	N/A
Page or Page Range of Portion	77	Publication Date of Portion	2012-06-01

Copyright and Licensing

Ana González Moreno

Tesis Doctoral por compendio de publicaciones

UNIVERSIDAD DE MÁLAGA
IHSM La Mayora
Instituto de Hortofruticultura Subtropical y Mediterránea
UNIVERSIDAD DE MÁLAGA
CSIC
Consejo Superior de Investigaciones Científicas

Málaga 2023